

Maritime Vehicle Routing under Uncertainty: Liquefied
Natural Gas Shipping and Offshore Pipeline Damage
Assessment Problems

A Dissertation

Presented to

the Faculty of the Department of Industrial Engineering
University of Houston

In Partial Fulfillment

of the Requirements for the Degree

Doctor of Philosophy

in Industrial Engineering

by

Jaeyoung Cho

August 2016

Maritime Vehicle Routing under Uncertainty: Liquefied
Natural Gas Shipping and Offshore Pipeline Damage
Assessment Problems

Jaeyoung Cho

Approved:

Chair of the Committee
Gino Lim, Associate Professor,
Industrial Engineering

Committee Members:

Jiming Peng, Associate Professor,
Industrial Engineering

Eylem Tekin, Instructional Associate
Professor, Industrial Engineering

Cumaraswamy Vipulanandan, Professor,
Civil and Environmental Engineering

Michael Nikolaou, Professor,
Chemical and Biomolecular Engineering

Suresh K. Khator, Associate Dean,
Cullen College of Engineering

Gino Lim, Associate Professor and
Chairman, Industrial Engineering

Maritime Vehicle Routing under Uncertainty: Liquefied
Natural Gas Shipping and Offshore Pipeline Damage
Assessment Problems

An Abstract
of a
Dissertation
Presented to
the Faculty of the Department of Industrial Engineering
University of Houston

In Partial Fulfillment
of the Requirements for the Degree
Doctor of Philosophy
in Industrial Engineering

by
Jaeyoung Cho
August 2016

Abstract

Maritime vehicle routing and scheduling problem has been studied extensively in the context of risk mitigation. This dissertation addresses three maritime vehicle routing problems and its mathematical frameworks considering environmental uncertainty.

First, LNG shipping problem is investigated considering LNG market change, ship construction technology advances and random boil-off gas (BOG) generation. This is formulated as a two-stage stochastic mixed integer program. In the initial stage, a single production-inventory plan and routing schedule is determined before the realization of the random BOG generation. For every possible realization of the random BOG, the second-stage variables are represented by the amount of LNG surplus or shortage when an LNG carrier arrives at a regasification plant. This model provides a flexible transportation strategy reflecting LNG market trend and diversified LNG carrier specifications.

Second, LNG production-inventory planning and ship routing under random weather disruptions is discussed. This problem is formulated to two optimization models: a two-stage stochastic mixed integer programming model and a parametric optimization model. The first one maximizes the overall expected revenue while minimizing disruption cost which results from extreme weathers. The second one, a parametric optimization model, attempts to reflect the decision maker's preference on risks by varying the ratio of revenue to on-time delivery. Therefore, a decision maker can have a 'what-if analysis' to compare multiple options for the final planning decision. Stochastic production-inventory control constraints set is also developed which synchronizes production-inventory plan and LNG carrier routing schedule under weather disruption.

Lastly, offshore pipeline networks damage assessment problem is discussed. In order to collect how/what might have caused pipeline damages by a weather disruption, multiple AUVs are pre-positioned at some selected underwater locations before the beginning of the extreme weather. Once the weather clears up, the pre-deployed AUVs start pipeline damage assessment. This problem is formulated as a two-phased multiple AUVs pre-positioning and routing model. The first phase problem is to determine optimum AUVs' pre-positioning locations considering maximum AUV operating distance and random weather impact. In the second phase, AUV paths are generated to scan the designated offshore pipeline networks while minimizing operating cost proportional to the number of pre-deployed AUVs.

Table of Contents

Abstract	v
Table of Contents	vii
List of Figures	x
List of Tables	xiii
Chapter 1 Introduction	1
1.1 Background	1
1.1.1 LNG Value Chain	3
1.1.2 Offshore Pipeline Damage Assessment	8
1.2 Optimization Problems	12
1.2.1 LNG Production-Inventory Planning and Vessel Routing Problem	12
1.2.2 AUV-aided Offshore Pipeline Damage Assessment Problem . .	13
1.2.3 Contributions	14
1.2.4 List of Publications	17
1.3 Organization	20
Chapter 2 Literature Review	21
2.1 LNG Inventory Routing Problem	21
2.2 AUV Deployment and Path Planning Problem	23

Chapter 3	A New Deterministic Framework for LNG IRP	27
3.1	Introduction	27
3.2	Problem Statement and Model Overview	27
3.3	Mathematical Formulation	29
3.3.1	Sets, Elements, Data and Variables	29
3.3.2	Objective Function	32
3.3.3	Constraints	32
Chapter 4	LNG IRP under BOG Uncertainty	36
4.1	Introduction	36
4.2	Problem Description	36
4.3	A Stochastic Extension of BOG Impact to LNG IRP	37
4.4	Computational Result	41
4.4.1	Numerical Example	41
4.4.2	Result	42
4.5	Conclusion	45
Chapter 5	LNG IRP under Weather Disruptions	48
5.1	Introduction	48
5.2	Problem Description	51
5.3	Mathematical Formulation	53
5.3.1	Sets, Elements, Data and Variables	55
5.3.2	A Two-Stage Stochastic Approach to LNG IRP	59
5.3.3	Generalization of Production-Inventory Constraints	65

5.3.4	Decision Maker's Preference Model (DMP)	69
5.3.5	Computational Considerations	71
5.4	Computational Result	74
5.5	Conclusion	83
Chapter 6	Multiple Autonomous Underwater Vehicle Pre-positioning and Routing for Offshore Pipeline Damage Assessment .	85
6.1	Introduction	85
6.2	Problem Statement and Model Outline	90
6.3	Mathematical Formulation	93
6.3.1	Sets, Elements, Data and Variables	93
6.3.2	Phase 1: AUV Pre-positioning (MAUV-ph1)	95
6.3.3	Phase 2: AUV Path Generation (MAUV-ph2)	97
6.3.4	Computational Considerations	99
6.4	Simulation Result	102
6.5	Conclusion	111
Chapter 7	Summary and Future Work	113
References	117

List of Figures

Figure 1.1	World GDP, merchandise trade and seaborne shipments (1975-2014) [1]	2
Figure 1.2	International seaborne trade (millions of tons loaded) [1]	2
Figure 1.3	LNG trade volumes (1990-2013)	4
Figure 1.4	Total, contracted and spot & short-term LNG trade [2]	5
Figure 1.5	LNG value chain [3]	6
Figure 1.6	Instantaneous pressure distribution at the moment of sloshing impacts in high and low-filling level conditions[4]	6
Figure 1.7	LNG stratification inside tank	7
Figure 1.8	A dust storm in the Persian Gulf [5]	9
Figure 1.9	Saffir-Simpson hurricane scale [6]	11
Figure 1.10	The scope of the study	15
Figure 4.1	LNG ship routing plan from D+1 to D+192	44
Figure 4.2	Optimal solutions of WS, RP and EEV	44
Figure 4.3	Sensitivity analysis: SA#1-5	45
Figure 4.4	Sensitivity analysis #6-#10	46
Figure 5.1	A random extreme weather impacts to LNG production & storage plan and vessel departure time	54
Figure 5.2	Three types of transportation routes connecting terminals	55

Figure 5.3	Two-stage production-inventory planning strategy	67
Figure 5.4	An illustrative example of DMP solutions with two extreme weather scenarios: 1) inventory schedule, 2) production schedule and 3) departure time of an LNG vessel	70
Figure 5.5	Five routing cases	71
Figure 5.6	An illustrative example of routing options serving two regasifi- cation plants	72
Figure 5.7	Historical records of dust storm in the Persian Gulf (1990-1999)	77
Figure 5.8	A shipping schedule	78
Figure 5.9	Production and inventory schedule considering random weather scenario changes	79
Figure 5.10	Production-inventory schedule by varying the risk preference ratio based on risk preference ratio	80
Figure 5.11	Profit and number of delay days changing with preference ratio	81
Figure 5.12	Expected profit of TSS model per scenario	82
Figure 5.13	Number of binary variables of TSS model and PPT model . .	82
Figure 5.14	Computational time changes per number of scenarios	83
Figure 6.1	Offshore pipeline network damage assessment over a planning horizon	91
Figure 6.2	Flowchart of MAUV model optimization	92
Figure 6.3	An illustrative example of offshore pipeline network	96
Figure 6.4	An illustrative example of maximum number of AUVs passing a node	100

Figure 6.5	An example of AUV specification	103
Figure 6.6	Offshore pipeline network in Gulf of Mexico	104
Figure 6.7	Offshore pipeline damage assessment target area	105
Figure 6.8	Offshore pipeline network topology	106
Figure 6.9	Determining AUV pre-positioning locations considering maximum target coverage of AUVs and its technical endurance under weather disruptions	107
Figure 6.10	Generated paths of 30 AUVs for damage assessment	108
Figure 6.11	Triangular relations of damage assessment time, AUV prepositioning setup cost, and operating cost in accordance with AUV maximum maneuvering time	110
Figure 6.12	Convergence	111

List of Tables

Table 4.1	LNG cargo carriers	42
Table 4.2	Shipping distance between terminals	42
Table 4.3	Demands in the planning horizon	43
Table 4.4	Other parameters	43
Table 4.5	Sensitivity analysis instances	47
Table 5.1	LNG transportation network characteristics	75
Table 5.2	Monthly dust storm days (1990-1999)	75
Table 6.1	Comparison of MAUV-ph1 and its deterministic counterparts	105
Table 6.2	AUV maximum coverage range and MAUV ph-1 solutions	109
Table 6.3	Four combinations of computational options	109

Chapter 1

Introduction

1.1 Background

Through the history of mankind, global supplies and passengers have transported by sea. World seaborne trade has been increasing in proportion to the upward trend of the world merchandise trade as shown in **Figure 1.1**. Oil and gas garnered 28 percent share of the world seaborne trade in 2014 in **Figure 1.2** [1]. Therefore, it is very important task to analyze potential risks which prevents safe maritime transportation and its supporting activities, and to develop solutions to overcome the challenges from the perspective of energy security.

There are various potential risks in maritime environment including such as human-error, natural disaster (e.g. hurricane, earthquake, tsunami, and storm), terrorism, fire and explosion. The most frequent and continuous causative factor in maritime-based activities is extreme weather events. Due to the bad weather, if ships are forbidden to sail, and energy production-inventory, and shipping related onshore/offshore infrastructures are destroyed, then it not only negatively influence on stable energy supply to global customer, but also can cause environmental contamination in cases of oil spills or gas leaks.

In order to control these potential risks, three steps of risk mitigation procedures can be considered: 1) disaster (emergency) preparedness, 2) response, 3) recovery and restoration [7]. From the perspective of disaster (emergency) preparedness, ships and fixed onshore/offshore installation can be constructed in order to properly endure against any disruptions. If an installation is robust enough, on the other hand, it may

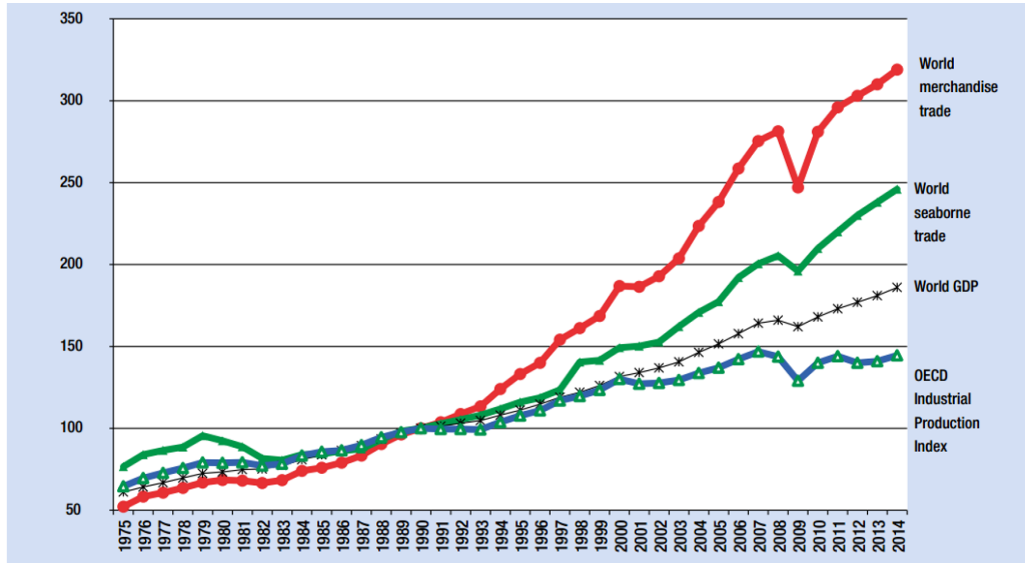


Figure 1.1: World GDP, merchandise trade and seaborne shipments (1975-2014) [1]

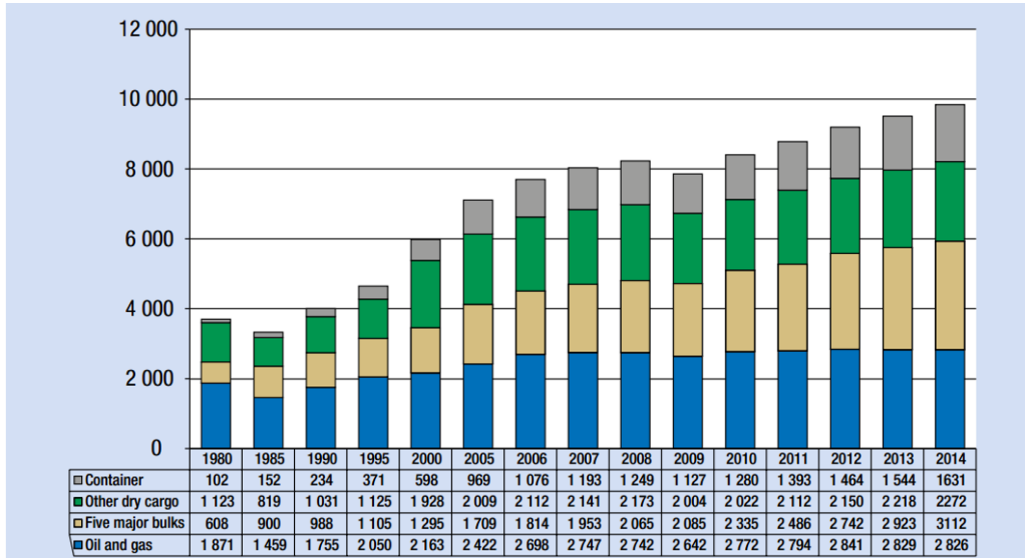


Figure 1.2: International seaborne trade (millions of tons loaded) [1]

increases initial setup cost. Crisis management procedures or emergency response systems can be upgraded to enhance emergency response capability. In general, recovery and restoration is considered as a consequence management if a disruptive situation is out of control in real time.

This study puts emphasis on risk mitigation in LNG production-inventory planning, LNG shipping, and damages on offshore supporting facilities while considering all three steps of risk mitigation procedures.

1.1.1 LNG Value Chain

Natural gas is becoming an important energy source worldwide which accounts for more than 1/5 of the global energy trade. The areas of application for natural gas are in industrial sectors, as well as residential and commercial sectors. Following recent advances in drilling techniques, the market has seen a significant increase in production from unconventional gas resources which were previously not economically efficient. Therefore, prices have dropped to levels that are very competitive with other fossil fuels. As natural gas is also favored among the fossil fuels with regard to environmental concerns, expectations are that growth in demand and supply will continue [8].

Natural gas can be transported to customers either through pipelines or by a fleet of LNG cargo ships [9]. The trade of natural gas through pipeline is convenient and economical up to 2,500 kilometers. However, as shipping distance increases above this maximum distance, maritime transportation of natural gas becomes more economically efficient [10].

In the last decade, there has been a remarkable upward trend in the LNG industry globally shown in **Figure 1.3** [11, 12]. The Global LNG industry is expected to make up 40 %of the world energy consumption by 2016 not only because LNG is highlighted as a cleaner and more efficient energy source when compared to other

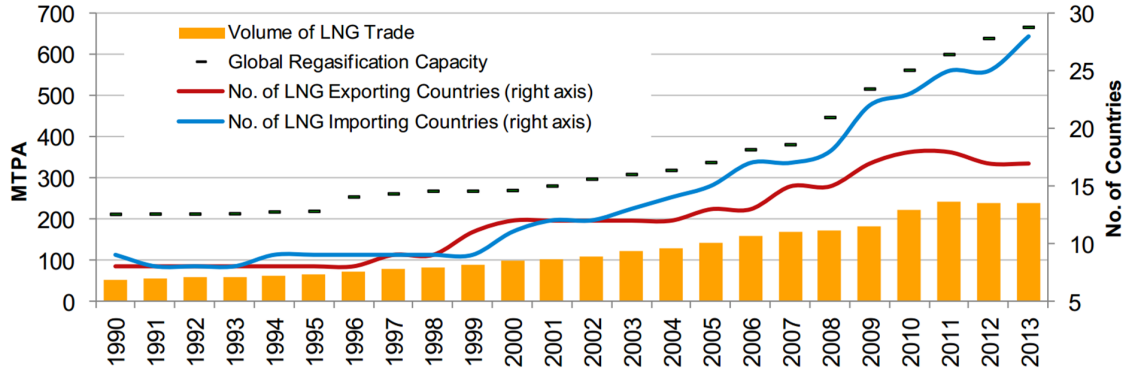


Figure 1.3: LNG trade volumes (1990-2013)

fossil fuels, but also because North America raises shale gas production and Asian demand increases steadily [13, 14].

The majority of LNG has been traded by long term sale and purchase contracts which spans 20-30 years ensuring a stable supply and demand. Most LNG ships have been tied to specific contracts and shuttled between given liquefaction terminals and regasification terminals. In recent years, however, it has been observed that the portion of short-term contracts and spot demand is rapidly increasing in the LNG market, this trend is depicted in **Figure 1.4** [2]. The spot market introduces more flexibility, which in turn means high fleet utilization of LNG cargo ships. The changing demand pattern is directly causing the LNG supply strategy to be more flexible.

The LNG value chain is composed of five phases as seen in **Figure 1.5** [3]. Once natural gas is produced and stored, at a temperature of -160°C , it is loaded into a vessel in liquid form to minimize the volume to $1/600$ of its gaseous state for marine transportation. When an LNG vessel arrives at a regasification terminal, LNG must be transformed back to its original gaseous state for ground transportation [15]. This study covers the first three phases from 'gas production' to 'unloading.' Within this scope, suppliers can optimize their production inventory schedules while making ship routing decisions for a specific time horizon that satisfies the terms and conditions of

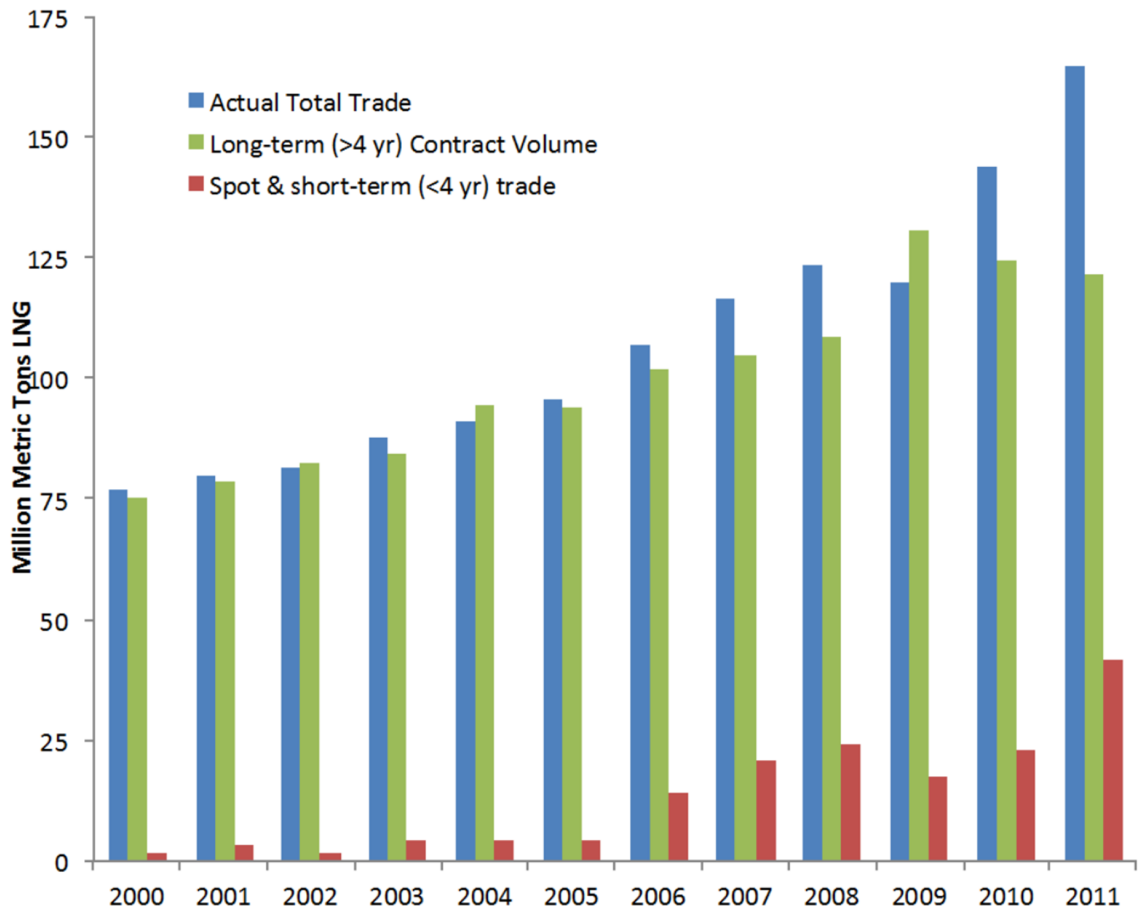


Figure 1.4: Total, contracted and spot & short-term LNG trade [2]

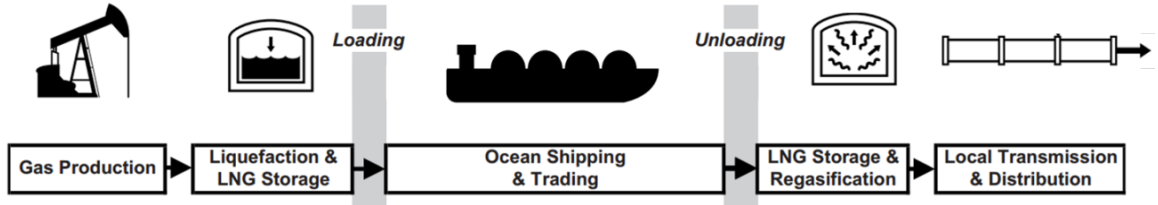


Figure 1.5: LNG value chain [3]

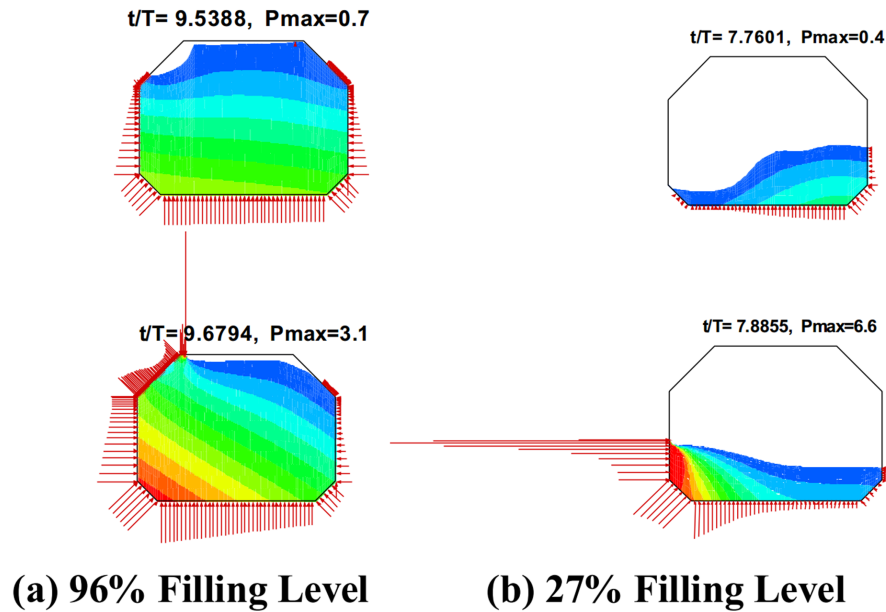


Figure 1.6: Instantaneous pressure distribution at the moment of sloshing impacts in high and low-filling level conditions[4]

their contracts.

LNG vessels usually sail in the fully loaded condition or with minimum filling of LNG to cool down the tank temperature. Otherwise, partly loaded vessels can make an adverse sloshing impact to the containment system and vessel structure as illustrated in **Figure 1.6** [4].

Thanks to recent advances in ship design technology, newly constructed LNG vessels can voyage without completely filling the tanks [16, 17]. Consequently, LNG transportation strategies are transforming to cope with the changing business environment. The next generation of LNG shipping model may need to satisfy multiple customers with different contract durations utilizing various types of LNG vessels

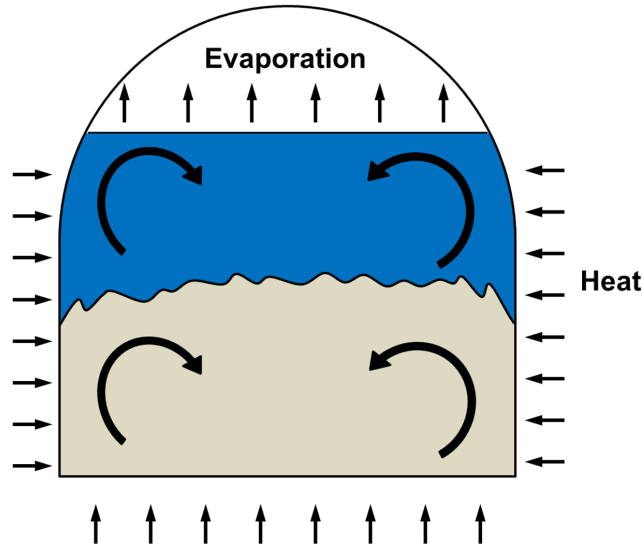


Figure 1.7: LNG stratification inside tank

with different technological constraints and cargo capacities.

There are many inherent uncertainties in the LNG value chain network which can lead to significant differences between the planned supply schedule and the actual delivery to customers.

Uncertain weather conditions and geo-political volatility (e.g. Japanese tsunami in 2011, Russian military intervention in Ukraine in 2014-2015) have disrupted stable supply of traditional energy sources. Hence LNG trade is steadily growing as an alternative energy source.

Maritime LNG transportation takes from a few days to a few weeks in general. The transportation time can fluctuate due to uncertain marine weather conditions. The weather variations also influence the laden LNG cargo by constantly changing the internal tank environment (e.g. temperature, density and pressure). Therefore it is hard to estimate the amount of natural gas that evaporates during the voyage seen in **Figure 1.7** [18].

Another disruption factor in LNG trade is extreme weather condition such as hurricane, dust storm, and fog. For example, dust storms impact the world's largest

LNG production facilities in Ras Laffan, Qatar. Dust storms occur in southwest of Iran near the Persian Gulf which cause a negative impact on LNG production and activities in the region [19]. The topography within the region contributes to the frequency and intensity of dust and sand storms in this area. The natural funneling of large air masses by the high mountains in Turkey and Iran combined with the heights in Saudi Arabia, help funnel air across the Mediterranean into the Persian Gulf [20, 21]. Dust storm can last from a few hours to a few days and its' hourly mean speed is 17 knot or above. The storm disturbs LNG loading operations in the phase of transition from a storage to an LNG cargo vessel which takes about 24-36 hours. Dust storm severely disrupt LNG loading operations. The strong winds cause the LNG loading arms and berthed cargo vessels to shake loading. Loading under this conditions could lead to a gas leak, and also can quickly reduce visibility to 1/4 of a mile or less. In extreme cases, leaked gas can cause a 'rapid phase transition' fire and explosion, or injure people through direct contact due to its extremely low temperature. Therefore, from a safe LNG supply viewpoint, on-going LNG cargo loading must be strictly prohibited during a storm period and all scheduled loading must be postponed until the storm passes to prevent any accidents.

1.1.2 Offshore Pipeline Damage Assessment

Oil and gas products transportation by pipeline system has many benefits comparing with shipping by trucks or cargo ships. As the pipeline networks usually avoid densely populated area, it secures safer and reliable environment. Once pipeline networks are setup as permanent infrastructure, maintenance cost is lower than others measures over the long run, and transit loss of pipeline shipping is negligible as well. Any states of products - in liquid, gaseous, or slurry form - can be transported by pipelines without limitations.

Pipeline systems can be categorized as onshore and offshore pipelines. Cross

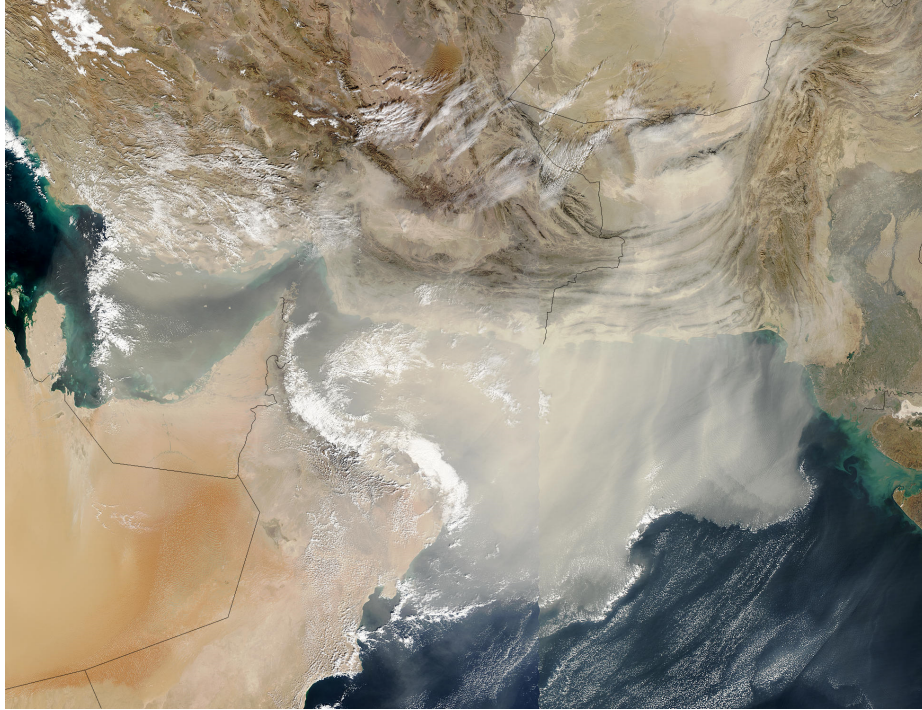


Figure 1.8: A dust storm in the Persian Gulf [5]

country trunk pipelines, spur lines, and gathering and distribution lines are classified as onshore pipelines. Trunk lines, infield pipelines, intra-field pipelines, offshore terminals, and effluent outfalls are offshore pipelines. The focus of this research is offshore pipeline system.

Offshore pipelines system is mainly composed of main pipeline, risers, laterals, pipeline end manifolds, shore approaches and terminal facilities, and electrical and instrumentation system.

There are six stages of offshore pipeline installation: conceptual study, feasibility study, basic engineering, detailed engineering, construction, and testing and commissioning. Especially, when designing a pipeline network, six routing factors must be carefully considered: pipeline length, sensitive locations, obstructions, installation limitations, crossings, and drilling and rig movement.

In the Gulf of Mexico, majority of the pipeline systems setup after 1970th have been designed to sustain storms for 100 years. However, despite of the storm-resistant

design, after experiencing years of hurricanes, it was observed that pipelines were damaged by various reasons [22].

According to the Saffir-Simpson hurricane scale in **Figure 1.9**, hurricane is categorized as five levels. This scale helps to estimate potential damages on property along the coast from a hurricane landfall [6]. The strength of storm surge is highly depends on the slope of the continental shelf and the shape of the coastline and wind velocity are key factors to determine the scale of hurricane.

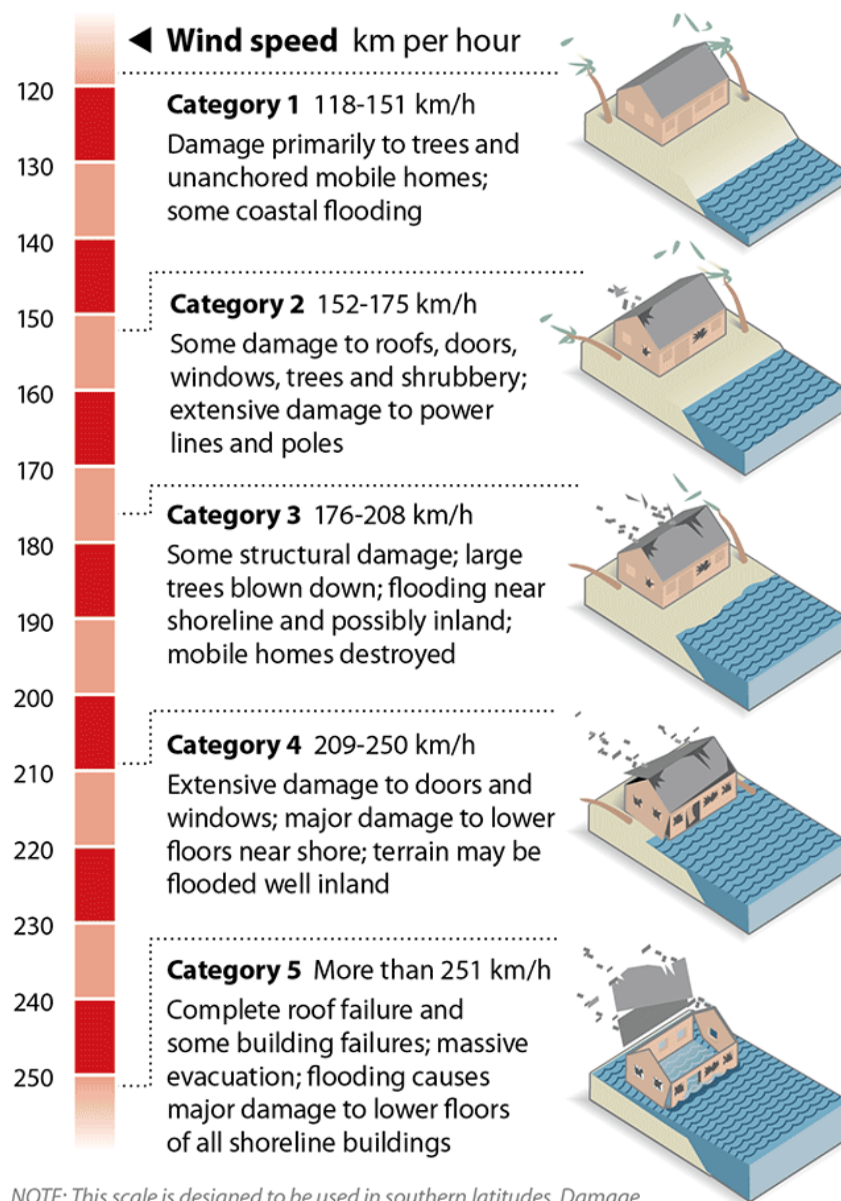
For example, in 2005, Hurricanes Katrina and Rita had significantly disrupted production capability of the oil and gas industry along the Gulf of Mexico. When hurricane Katrina entered the outer continental shelf (OCS), the strength was in category 5, and hurricane Rita was a category 4.

After the two major hurricanes, 10% of the nation's consumption was shut-in because of production problems in the Gulf of Mexico, which are mainly due to critical infrastructure damages. As the United States relies on the oil and gas supply from the Gulf of Mexico, its impact to the economy has increased as well [23].

It has been reported that more than 600 offshore pipeline damages. Most of the pipeline damages were found near platform interfaces, and estimated that caused by the movement of pipelines that are near shore and in shallow water. In general, it is difficult to identify how and what might have caused pipeline damages. We can only assume the cause of damages in accordance with previous studies such as failure of installation fixture, strong impact forces such as extreme hydrodynamic loading and mud slide, inadequate design of the riser support clamps, or drifting vessels and its anchor dragging during an extreme weather [22, 24].

In order to find causal factors of the damages, it is essential to develop proper procedures and techniques for subsea pipeline damage assessment. We may consider to deploy multiple sensors or unmanned underwater vehicles (UUVs) [25].

UUV is usually categorized as remotely operated vehicle (ROV), autonomous



NOTE: This scale is designed to be used in southern latitudes. Damage may be different for Canada as storm surge values are highly dependent on the slope of the continental shelf and the shape of the coastline in the landfall region.

Figure 1.9: Saffir-Simpson hurricane scale [6]

underwater vehicles (AUV), and remotely towed vehicles (ROTV). Especially, AUV is a maritime vessel that can travel underwater without an operator on its own power source. AUV is used for surveillance and reconnaissance, mine countermeasures, anti-submarine warfare, mapping of the ocean floor, testing water samples, polar ice research, and pipeline inspection. As AUV has its own power source and does not require operator's involvement, AUV is replacing ROV. AUV products are divided into three categories: 200 meters + depth of water (30% of the market), up to 200 meters depth of water (40%), up to 30 meters of water (30%) [26].

1.2 Optimization Problems

1.2.1 LNG Production-Inventory Planning and Vessel Routing Problem

In LNG business, production-inventory planning and LNG carrier routing problem involves the integration of two logistics components: production control & inventory management and cargo vessel route planning. Accordingly, the problem is formulated as an inventory routing problem so that suppliers can plan a production-inventory schedule and a routing schedule for a fleet of cargo ships within a time horizon based on the given terms and conditions of contracts.

As LNG carrier construction technology advances, ships are having a larger cargo capacity, and relaxing the rules for loading or unloading conditions. In the mean time, various types of contracts - short-term, spot, and long-term contract - have to be satisfied by properly assigning LNG ships. Therefore, it is also an important consideration in LNG supply problem. Similar to other perishable goods, a certain amount of LNG in a cargo tank evaporates as time goes. Considering this phenomenon, initial loading amount also has to be predetermined.

There are several decisions variables to find an optimal plan. The main variables

typically considered are the amount of LNG cargo delivering to each customer, assignments of vessels to each established path, the daily production & inventory level in a given time horizon based upon the vessel routing schedule, and expected cargo arrival time at customers' side. Once a production schedule and routing decisions are determined, the departure time and the arrival time of an assigned vessel at each terminal can also be obtained.

The impact of extreme weather in LNG value chain is very significant as explained in the previous section. If a disruption delays or put forwards an LNG career departure time, then related production-inventory schedule also influenced. For example, if LNG career departure is changing to an earlier schedule, then the produced LNG may not enough to satisfy the demand. On the other hand, if the cargo ship has to departure in a later date, then as the stored LNG cargo in a ground facility needs to be kept in the storage in an extended time period. Therefore, in order to mitigate expected disruptions, weather forecast information can be utilized for initial production-inventory planning and adjustment of the plan to minimize the potential impacts to the supply operations.

1.2.2 AUV-aided Offshore Pipeline Damage Assessment Problem

Offshore pipelines damage assessment problem using multiple AUVs are categorized two steps. In order to collect data to know what and how an extreme weather influence to the pipeline network, pre-deployment of AUVs can be considered before the beginning of an extreme event, and AUVs pre-deployment locations and timing needs to be determined. From the pre-positioned locations, every targeted areas must be covered considering maximum operating capacity of deploying AUVs. Well before the beginning of an extreme weather, its forecast accuracy would be low. However, as the time gets closer to the beginning of the extreme weather, the accuracy will

be enhanced in spite of that the AUVs and supporting ships are exposing to a high risk environment. The key consideration in AUV pre-positioning problem is how to mitigate risks which is random by utilizing uncertain weather information.

Efficient path generation algorithm for AUV is very important as it maneuvers in a designated target area without operator's intervention. Once AUV begins to operate underwater, it is difficult to communicate with supporting ship due to the low bandwidth channels undersea. Therefore, AUV has to maneuver based on pre-programmed route information and obstacle avoidance algorithm to search out an optimal or sub-optimal path between an initial position and the desired target under specific constraint conditions.

As one of the key research topics for AUVs, path planning is a necessary and fundamental element of AUVs and makes the vehicle fully autonomous and reliable. Its goal is to plan a sequence of suitable paths subjected to some optimization criteria that allows the vehicle to complete its task objectives by reaching the specified destination point from the starting location. No autonomous vehicle or robot can successfully operate in a constrained environment without a systematic mechanism for planning its motion path. Path planning is one of the key techniques of AUVs' intelligent control system. Assuming the underwater environment is known, the main idea of the path planning is to keep the AUV following connected pipelines maneuvering from the source position to the destination position according to some optimization criteria.

1.2.3 Contributions

Contributions of this dissertation is highlighted as follows:

- In Chapter 3, a new mathematical model for LNG carrier routing and production-inventory scheduling in the form of an inventory routing problem (IRP) is proposed which can cover overall contract patterns including long-term, short-term



Figure 1.10: The scope of the study

and spot demand. A fleet of LNG carriers with partial loading and unloading capabilities is exploited to serve multiple customers in a single route. This LNG IRP is basis of stochastic extensions of LNG IRPs.

- In Chapter 4 and 5, it is suggested that two different versions of stochastic LNG IRPs based on the proposed new LNG IRP model. The first one considers randomly evaporating gas losses during transport. The second model is formulated by considering the random impact of uncertain weather condition to LNG loading operations. Specifically, the production inventory constraints is reinforced to be more practical since an extreme weather affects not only routing decisions but also production and inventory schedules. In the first stochastic model, boil-off-rate (BOR) is considered as a random element [27]. However, in the second one, BOR is set as a constant to highlight the impact of weather disruptions as the random element in the model. This is a reasonable assumption because the weather disruption are much higher than the impact of uncertain BOR in the latter one. Probing-based preprocessing techniques are developed on to the proposed LNG IRP model. These techniques utilize the relationship between time windows and the amount of BOG generated in each path. Since the LNG IRP is a highly complex two-stage stochastic mixed integer program, this approach reduces the size of problems and enables faster convergence. LNG IRPs are reformulated by replacing the MTZ sub-tour elimination constraints to the proposed logical inequality to enhance the computational performance [28]. A decision maker's preference (DMP) model is proposed which reflects a decision maker's risk preference as a primary consideration rather than maximizing expected profit. This model is formulated as a parametric optimization model by setting the preference as a ratio to allow a decision maker to adjust their level of preference on risk.

- In Chapter 6, a new offshore pipeline damage assessment concept and procedure is developed to minimize overall inspection time and cost. The proposed approach begins by positioning a certain number of AUVs in pre-determined nodes over the weather impact zone before an expected event. After the extreme event, pre-placed AUVs maneuver over the network following the optimal scanning paths. A two-phased mathematical optimization model is proposed for multi-AUV pre-positioning and routing (MAUV). In phase 1 (MAUV-ph1), the optimum AUV positions are found. The MAUV-ph1 is formulated as a two-stage stochastic integer program, where the first stage decision determines each AUV position and the second stage augments additional AUV positions based on weather forecast. In phase 2 (MAUV-ph2), AUV scanning paths are generated while minimizing AUV operating cost and inspection completion time. Four Computational techniques have been suggested, including constraints reformulation, probing-based pre-processing techniques, logical inequality, and Lagrangian method, to enhance the computational performance.

1.2.4 List of Publications

Journal Publications

- J. Cho, G. Lim, B. Taofeek and S. B. a. H. Parsaei, "Liquefied natural gas ship route planning model considering market trend change," *Transactions on maritime science*, vol. 3, no. 02, pp. 119-130, 2014.
- G. Lim, S. Kim and J. Cho, Y. Gong, A. Khodaei, "Multi-UAV prepositioning and routing for power network damage assessment," (submitted to *IEEE Transactions on Smart Grid*), 2016.
- S. Kim, G. Lim and J. Cho, "Drone-aided Healthcare Services for Patients with

Chronic Diseases in Rural Areas," (submitted to Operations Research for Health Care), 2016.

- Cho, J., J Lim, G., Biobaku, T., Bora, S., and Parsaei, H, "Planning for LNG Inventory Routing under Dust Storm," (working paper).
- S. Bora, G. Lim, T. Biobaku and S. J. Cho, H. Parsaei, "Models and Computational Algorithms for Maritime Risk Analysis: A review," (under revision), Annals of Operations Research, 2015.
- T. Biobaku, G. Lim, J. Cho, S. Bora and H. Parsaei, "An optimal sonar placement approach for detecting underwater threats under budget limitations," Journal of Transportation Security, pp. 1-18, 2015.
- T. Biobaku, G. Lim, J. Cho, S. Bora and H. Parsaei, "Literature survey on underwater threat detection," Transactions on maritime science, vol. 4, no. 01, pp. 14-22, 2015.

Conference Proceedings and Presentations

- J. Cho, G. Lim, T. Biobaku, S. J. Kim and H. Parsaei, "Safety and security management with Unmanned Aerial Vehicle (UAV) in oil and gas industry," in Procedia Manufacturing, Las Vegas, 2015.
- T. Biobaku, J. Cho, G. Lim, S. J. Kim and H. Parsaei, "Liquefied natural gas ship route planning: a risk analysis approach," in Procedia Manufacturing, Las Vegas, 2015.
- J. Cho, G. Lim and S. j. Kim, "A mothership-based UAV routing problem in support of counterfire operations," in INFORMS Annual Conference, Philadelphia, 2015.

- T. Biobaku, G. Lim, J. Cho, S. Bora and H. Parsaei, "Optimal sonar deployment in a maritime environment: A fortification approach," in INFORMS, Philadelphia, 2015.
- J. Cho, G. Lim and S. J. Kim, "Use of unmanned aerial vehicle (UAV) for risk monitoring in oil and gas industry," in IIE Annual Conference, Nashville, 2015.
- J. Cho, G. Lim and S. J. Kim, "Use of Unmanned Aerial Vehicle (UAV) to aid healthcare delivery service," in IIE Annual Conference, Nashville, 2015.
- T. Biobaku, G. Lim, J. Cho, S. Bora and H. Parsaei, "Case studies on maritime incidents: a review," in IIE Annual Conference, Nashville, 2015.
- J. Cho, G. Lim, T. Biobaku, S. Bora and H. Parsaei, "Robust liquefied natural gas shipping problem under Shamal disruptions," in INFORMS Annual Conference, San Francisco, 2014.
- T. Biobaky, G. Lim, J. Cho, S. Bora and H. Parsaei, "Optimal deployment of underwater sonar system," in INFORMS, San Francisco, 2014.
- S. Bora, G. J. Lim, T. O. Biobaku, J. Cho and H. R. Parsaei, "Assessing the resiliency and importance of a supply chain network," in International Conference on Computers & Industrial Engineering, Turkey, 2014.
- J. Cho, G. J. Lim and T. Biobaku, "Liquefied Natural Gas (LNG) inventory routing problem under weather disruptions: a case study of dust storm in Persian Gulf," in THC-IT-2014 Conference & Exhibition, Houston, 2014.
- J. Cho, G. Lim, T. Biobaku, S. Bora and H. Parsaei, "A stochastic approach to liquefied natural gas (LNG) ship route planning model under weather disruptions," in Qatar Foundation Annual Research Conference, Doha, 2014.

- T. Biobaku, G. Lim, J. Cho, S. Bora and H. Parsaei, "Under-water sonar placement," in IIE Annual Conference, Montreal, 2014.

1.3 Organization

This dissertation is organized as follows.

Chapter 2 is a review of the optimization problems two areas: 1) LNG production-inventory scheduling and ship routing, 2) AUV-aided offshore pipeline damage assessment. It also includes a comprehensive overview about environmental uncertainties associated with maritime vehicle routing problems. In Chapter 3, a new deterministic mathematical framework for LNG IRP is presented reflecting technological advances in LNG carrier design and diversifying demand patterns. In Chapter 4, a two-stage stochastic LNG IRP model considering BOG generation uncertainty is introduced. This model is an extension of the proposed deterministic LNG IRP in chapter 3. A deterministic equivalent to a stochastic programming model is derived and solved by Monte Carlo sampling techniques. Experimental results are demonstrated how the proposed stochastic model outperforms the deterministic counterpart by measuring the value of stochastic solution. In Chapter 5, the impact of random extreme weather condition on LNG carrier routing decisions and production-inventory scheduling is analyzed. Based on this analysis, two LNG IRP models are presented. The first one is a two-stage stochastic LNG IRP model for revenue maximization while minimizing disruption cost. Second one is a parametric optimization model to project a decision maker's preference on risks. Chapter 6 discusses multiple AUV deployment and path planning in support of offshore pipeline damage assessment. This problem is constructed as a two-phased mathematical framework: 1) pre-deployment of multiple AUVs for underwater weather impact data collection, 2) its path planning for pipeline damage assessment. In Chapter 7, the dissertation is concluded with a summary of contributions and future researches that can be pursued.

Chapter 2

Literature Review

2.1 LNG Inventory Routing Problem

The IRP is an integration of production-inventory problem and vehicle routing problem (VRP). The very first IRP was formulated as a mixed integer program to manage industrial gases at customer locations [29]. Major applications of IRP are usually in the oil and gas industries because of the maritime shipping environment. From the perspective of ship routing and scheduling, the problems can be categorized into four basic models: 1) network design, 2) fleet deployment, 3) tramp cargo routing and scheduling problem and 4) maritime IRP for a single product [2]. The fourth model is the focal point of this research.

Ship routing and production inventory planning in the LNG business is a representative maritime IRP. While optimizing inventory and production levels within a given time horizon, a fleet of LNG vessels must be properly assigned to a path between a liquefaction terminal and a single or multiple regasification terminals. Since 2009, there has been notable research on LNG IRP. The earliest LNG models proposed were formulated in an arc-flow and a path-flow model considering inventories at a liquefaction and regasification terminals [30]. Some of the LNG value chain optimization models to decide sailing schedule and vessel assignments were studied. These study reflecting variations in seasonal price, price gaps among markets and various contract types [31, 32]. This problem is similar to this study, but it differs as it serves single customer in a route. Traditional LNG demand is mostly identified from well-determined long-term contracts, and so an annual delivery program (ADP) was considered with a limited number of berths, and a heterogeneous fleet of LNG

ships to fulfill a set of long-term contracts [33]. However, this model is unsuitable when considering spot-demand and short-term contracts.

Since LNG IRP is a complex optimization problem under various conditions, there have been many studies on solution techniques. LNG IRP with 800,000 variables and 200,000 constraints has been solved by Lagrangian relaxation technique to near optimality [29]. Three branch-and-price methods were also suggested [34, 35, 36]. A rolling horizon heuristic iteratively solved short planning horizons while sub-problems obtained a good solution iteratively. Two constraint programming models iteratively solved the problems, too [37]. A multi-start local search heuristic [38] and a set of construction and improvement heuristic were also introduced [39] as well as a two-stage decomposition algorithm that iteratively solved a master problem and its sub-problems [40]. There is a heuristic with a local intra-period search and a large inter-period neighborhood search [41] as well as an approximate dynamic programming [42]. As the proposed LNG IRP is the first attempt to include more than one customer in a single journey of a vessel, no identified solution techniques have been developed.

In practice, the LNG IRP is significantly affected by uncertainties. This is also the case for most other marine transportation problems. One of the most difficult challenges is the ability to accurately estimate demands. A simple way to approximate demand is to average recent customers' inventory levels as a constant [29], or to consider the demand as a random element [43]. Even if the demands are known, disruptions from the supplier side can still make a value chain unstable [44]. Other uncertainties are the volatile market prices which influences the production inventory decisions [45] and the unusual commodity characteristics such as random evaporation rate of BOG in LNG transportation which limits accurate estimation of cargo load [27]. In maritime transportation, sailing time is inherently uncertain due to changing weather conditions [46, 47] as well as extreme weather disturbance especially in the

Persian Gulf [48]. However, neither of these studies have considered uncertain internal system dynamics of LNG carriers, but mostly focused on the impact from external environments.

It is particularly recognized that there is limited literature regarding BOG effect in LNG value chain. In an early stage of research, the focus was on discovering the characteristics of BOG in a partially filled tank and developing mathematical models [49]. In addition, the occurrence and the effect of BOG on LNG value chain have been examined dividing the time phases into three categories: loading, unloading and marine transportation [18]. Although the concept of evaporated gas involving LNG inventory routing problem has been studied, BOG was often considered as a constant [48, 47, 34]. The initial literature review reveals that there is a need for more research on the impact of BOG and weather disruptions and the possible solutions. Especially, it has not been identified that any mathematical models consider weather disruptions on the LNG value chain. Because of this, three challenging issues are encountered. First, the existing deterministic LNG IRPs may not generate efficient solutions in response to the random BOG or extreme weather disruptions. Second, if the LNG IRP is approached by a two-stage stochastic programming model, it requires significant computational cost to obtain optimal solutions. Lastly, and in certain cases, if a decision maker wants to be involved in the planning process under risks, it is required to develop a model to project such preference on risks.

2.2 AUV Deployment and Path Planning Problem

Path planning is inherently a routing process to find an optimal path selecting nodes and arcs to complete a given mission. There are two types of path generation techniques: global path generation and local path generation depending on information availability [50]. In this dissertation, global path planning is the focus of the research.

Path generation algorithms for AUVs have been constantly developed and improved in many ways. Artificial potential fields based path generation algorithm was introduced. This algorithm generated an optimal solution with entire network information on two- and three-dimensional problems [51]. D* and A* algorithms have been introduced [52]. In particular, A* considers bathymetry, exclusion zone, obstacle, and ocean current data bases to facilitate planning [53]. A* is practiced in Western Mediterranean Sea by varying operational conditions [54]. The performance of A* is proved by comparing with four other algorithms: breadth first search, depth first search, and Dijkstra's and wall following algorithms. It has been observed that A* and Dijkstra's algorithm outperformed to the others. A continuous form of A* algorithm which is named as FM* is developed [55]. This algorithm generates paths continuously by updating perceived environmental information.

Mathematical optimization based approaches have been developed either in mixed integer linear programming (MILP) or nonlinear programming. Multi-beam forward looking sonar aided real-time obstacle avoidance and path planning algorithm is developed. This is a nonlinear programming model which generates path while minimizing the Euclidean distance to the goal [56]. Genetic algorithm is proposed which minimizes the energy cost considering the variability of the environment. This model generated an optimum path to cross the Sicily channel which has strong current fields and complex [57]. MILP-based path generation algorithm for adaptive sampling is presented. This algorithm aims to maximize the line integral of the uncertainty of field estimate along the generated path. This model considers to optimize multiple AUV paths based on a supporting ship [58]. Sensor-Driven Online Coverage Planning for AUVs is formulated as a multi-objective optimization model [59]. Three-dimensional path planning technique is suggested and solved by multi-objective optimization algorithm. This model considers four criteria: total length of path, margin of safety, smoothness of the planar motion, and gradient of diving [60].

As real-time obstacle avoidance and path generation is an important research area, various algorithms have been developed. In the early stage of the research in real-time path planning and obstacle avoidance is designed to conduct two real-times missions: pre-deployment survey of sea bottom and visual inspection of pipelines [61]. Morse-based boustrophedon decomposition coverage path-planning algorithm for 3D coverage and Stochastic Trajectory Optimization for Motion Planning (STOMP) algorithm is used for real-time path re-planning [62]. Informative path planning is suggested which has used for surface vehicles. This model generates paths while maximizing mutual information [63].

In another approach, two risk-aware path planning techniques - minimum expected risk planner and risk-aware Markov decision process - are proposed from the perspective of safety and reliability of AUV operations [64]. Case-based path planning is presented. This algorithm retrieves a matching route from the DV and modifies it to suit to the current situation. If there is no matching route, then it generates a new routes based on past cases which have similar navigational environments [65]. Hybrid route-path planning model is developed which utilizes task assign-route planning and path planning based on differential evolution and firefly optimization algorithms [66]. Multiple AUVs task assignment and path planning have been studied considering variable ocean current. The goal of this model is to reach all designated target nodes [67]. In many AUV path generation problems, two criteria can be considered to select a preferred path generation algorithm: length of the path and computational time. By properly combining of two criteria in an objective function of a path planning model, an optimal solution can be obtained [68].

There has been an increasing trend of research on unmanned vehicle applications. Considerable body of work on a large number of AUVs has been done including topics such as coordination between multiple unmanned vehicle (UV) operators [69], future position prediction [70], traffic flow optimization [71, 72], and routing

optimizations [73, 74]. Especially, mathematical optimization models for multiple UV task assignment and path planning have studied considering technical specifications and operational constraints including mission types, time limits, and no fly zones [75, 76, 77, 78, 79]. This problem has the structure of multiple vehicles routing problem, and is tried to be solved by either exact or approximation algorithms [80, 81, 82, 27]

Chapter 3

A New Deterministic Framework for LNG IRP

3.1 Introduction

In this chapter, a novel LNG ship routing and production-inventory planning model in the form of IRP is presented which serving geographically dispersed multiple customers using a fleet of heterogeneous vessels. This model can cover any type of contract patterns including long-term, short-term and spot demand. It is exploited that a fleet of heterogeneous LNG carriers with partial loading and unloading capabilities to serve multiple customers in a single route.

The rest of this chapter is organized as follows: Section 3.2 describes the proposed problem. Section 3.3 provides mathematical formulations of the LNG ship routing and scheduling problem in a deterministic form.

3.2 Problem Statement and Model Overview

The general goal of the proposed LNG IRP is to provide an optimal production inventory schedule and transportation plans that satisfy all demands from customers in an LNG supply chain while maintaining the terms and conditions of the contracts. LNG contracts typically include the duration of a contract, frequency of deliveries, the total amount of demand, and expected shipping dates and locations.

This model generates biannual shipping schedule that maximize the profit and meets all customer demands, while ensuring the optimal LNG production and inventory level at the liquefaction terminal in each time period. The shipping plan

includes not only long-term contract but also short-term and spot demand. All operating vessels must initiate a tour from a liquefaction terminal at the depot and complete the tour after unloading cargoes visiting regasification terminals at remote demand locations by designated sea routes.

For the maximization of the expected revenue, an LNG supplier has to consider various aspects such as maximum capacities for production and storage, the total number of LNG vessels per types, and shipping time. This problem considers two types of LNG vessels according to the specifications of cargo tanks. The first vessel type has a strict barred filling limit of LNG cargo which is categorized as a Type I vessel. It has a permissible loading range that is either more than 70 % or less than 10 % of the tank. This exact filling limit is due to the sloshing impact which increases potential risks such as gas leaks and other related accidents [27]. The second vessel type (Type II) is not limited to this filling limit for its cargo. It is flexible to any level of partial loading based on the cargo tank capacity which allows for numerous cargo discharges at multiple regasification terminals in a path [83, 84]. Type I vessels can only serve individual customers unless the additional short-term or spot demand is very small. Type II vessels have no restriction on partial tank filling so that multiple customers can be served by an assigned LNG vessel within the given tank capacity.

Unlike other products, the BOG during marine transportation is proportional to the amount of cargo and shipping distance. Therefore, the loading amount of LNG from a departing regasification terminal must aggregate not only all demands in a path but also estimated BOG during a voyage. In particular, if a Type II vessel is assigned to a path serving more than one customers, the overall sailing time in a voyage may be longer than the travel time of each Type I vessel. As a result, a supplier must consider gas losses during the shipment because the amount of evaporating gas is proportional to the time of voyage.

This problem is formulated as a deterministic LNG IRP considering the constant

rate of BOG. In addition, shipping grace period is considered to give a scheduling flexibility. But, if a shipping delays beyond the grace, then it generates a penalty for the delay which is proportional to the number of delay days.

There are four categories of decision variables involved in the problem: 1) the amount of LNG cargo delivered to each customer, 2) vessel assignment to a path, 3) the daily inventory and production schedule, 4) departure and arrival time of an incoming and outgoing vessel at each regasification terminal.

3.3 Mathematical Formulation

3.3.1 Sets, Elements, Data and Variables

In the context of IRP, the problem can be modeled on a directed network $G(V, A)$. A supplier at a liquefaction terminal $i \in V$ delivers the requested LNG cargo in time period t $D_{j,t}$ to a customer at a regasification terminal $j \in V$ by LNG vessel $k \in K$ through the traverse arc $(i, j) \in A$. A supplier transports a total r number of cargoes to its customers within a given time horizon in accordance to the agreed contracts. The most appropriate LNG vessel $k \in K$ is assigned to transport demand from each customer $j \in V$. Recall from the previous section that there are two types of vessels: Type I vessel $k_1 \in K_1$ and Type II vessel $k_2 \in K_2$. Type I vessels strictly follow the barred cargo fill range α . When an LNG vessel $k \in K$ makes a tour, the sequence of visits is determined by introducing a flow variable u_i for each terminal $i \in V$. To determine the daily production rate x_i^{prd} and inventory level x_i^{str} within a time horizon, a maximum production capacity $\bar{\psi}$ and minimum production rate $\underline{\psi}$ must be considered, and a maximum storage capacity $\bar{\rho}$ and minimum safety stock level $\underline{\rho}$. When a customer $j \in V \setminus \{1\}$ wants to receive an ordered demand in time period t $D_{j,t}$ at the expected target delivery date TM_j^{tot} , a shipping schedule allows for the grace period β . The departure time x_j^{dep} of a vessel from a departing

liquefaction terminal to a regasification terminal $j \in V$ and arrival time x_j^{tot} to a regasification terminal $j \in V$ must be provided.

The deterministic LNG IRP model is presented in this section as a full formulation. The following notations have been used, some of which have already been defined. Then the mathematical formulation is presented with explanations on it:

Sets:

S	Set of LNG terminals;
T	Set of time periods;
K	Set of LNG tankers;
$G(V, A)$	Directed graph nodes $V = \{1, 2, \dots, S = s + \max(s) \cdot (r - 1)$ where r is a sequence of deliveries per terminal } as the set of terminals and $A = \{(i, j) : i, j \in V, i \neq j\}$ as the set of arcs in the planning time horizon;
H	Index of the origin (depot), where $h = 1 + S (t - 1) = \max(s) \cdot (t - 1)$ in the planning time horizon, $H \subseteq V$;
R	Index of Type I LNG tanker, $R \subseteq K$;
K_1	Set of Type I LNG vessels, $K_1 \subseteq K$;
K_2	Set of Type II LNG vessels, $K_2 \subseteq K$, and $K_1 \cap K_2 = \emptyset$.

Data:

$TR_{i,j}$	Estimated travel time from i to j ;
C_k^{vsl}	Daily shipping cost of a vessel type k ;
$D_{j,t}$	Demand at j in time period t ;
R	Unit revenue of LNG per billion cubic meters (bcm) ;
TM_j^{tot}	Expected target delivery date at j ;

CG_k^{vsl}	Cargo capacity of vessel k ;
C^{str}	Unit storage cost;
C^{prd}	Unit production cost;
γ	Maximum number of terminals can be visited in a route;
M	Big-M;
α	Barred fill range (%) of Type I LNG vessels α ;
β	Number of days of grace;
ε	Boil-off rate (BOR) (%) $[\underline{\varepsilon}, \bar{\varepsilon}]$;
ρ	Minimum / maximum storage level $[\underline{\rho}, \bar{\rho}]$;

Decision Variables:

$x_{i,j}^{lng}$	Amount of loaded LNG at terminal i heading to terminal j ;
$x_{i,j,k}^{vsl}$	$= \begin{cases} 1, & \text{If vessel } k \text{ operates from terminal } i \text{ to terminal } j; \\ 0, & \text{Otherwise;} \end{cases}$
x_t^{prd}	Production level on date t ;
x_t^{str}	Storage level on date t ;
x_j^{tot}	Vessel arrival date at a regasification terminal j ;
x_j^{del}	Number of days of shipping delays at a regasification terminal j ;
x_j^{dep}	Departure date from a liquefaction terminal to a regasification terminal j ;
u_i	A flow in the vessel after it visits terminal i .

3.3.2 Objective Function

The objective function is defined as

$$\begin{aligned}
\max \quad & R \cdot \left(\sum_{j \in V \setminus \{1\}} \sum_{t \in T} D_{j,t} - \sum_{(i,j) \in A} \varepsilon \cdot TR_{i,j} \cdot x_{i,j}^{lng} \right) \\
& - \sum_{t \in T} C^{prd} \cdot x_t^{prd} \\
& - \sum_{t \in T} C^{str} \cdot x_t^{str} \\
& - \sum_{(i,j) \in A} \sum_{k \in K} C_k^{vsl} \cdot TR_{i,j} \cdot x_{i,j,k}^{vsl}
\end{aligned} \tag{3.1}$$

to maximizes the overall revenue considering all cost factors in the supply chain. The first term maximizes profit by subtracting the cost of evaporated gas in accordance with BOR, duration of shipping and the amount of LNG in a cargo tank. The second and third term minimize production and storage cost. These values are dependent not only on the production level and storage level but also on the amount of BOG and ship routes decisions indirectly from the first term. The fourth term is to minimize overall vessel operating cost based on daily shipping cost of each vessels and ship duration from a previous terminal to next destination.

3.3.3 Constraints

The proposed model considers multiple time periods in a planning horizon. However, it is formulated as single time period model by re-indexing the terminal index with time period index. So, the index of terminals implies what terminal is served in which time period. For indexing purpose, all redundant indices of liquefaction terminals in the model are nullified by constraints (3.2) and (3.3):

$$\sum_{k \in K} x_{s,s+|S|(t-1),k}^{vsl} = 0, \quad \forall s \in S, t \in T \setminus \{1\} \tag{3.2}$$

and

$$\sum_{k \in K} x_{s+|S|(t-1),s,k}^{vsl} = 0, \quad \forall s \in S, t \in T \setminus \{1\}. \quad (3.3)$$

When a route decision is made, a vessel assignment also has to be determined simultaneously. Once a vessel is assigned to a path, the vessel must complete the tour without being replaced by other vessels returning to the origin. Therefore, flow of a vessel from a previous terminal to a following one is described as

$$x_{i,j,k}^{vsl} \leq \sum_{k \in K} x_{i,j,k}^{vsl} \leq |S| - (|S| - 1) \cdot x_{i,j,k}^{vsl}, \quad \forall (i, j) \in A, k \in K. \quad (3.4)$$

When a ship is assigned to a route, the amount of laden LNG cargo must be less than the tank capacity of a vessel. This condition is defined as

$$x_{i,j}^{lng} \leq \sum_{k \in K} CG_k^{vsl} \cdot x_{i,j}^{lng}, \quad \forall (i, j) \in A. \quad (3.5)$$

The number of operating vessels also must be less than the number of vessels in a fleet and is expressed as

$$\sum_{(i,j) \in A} x_{i,j,k}^{vsl} \leq |K|, \quad \forall k \in K. \quad (3.6)$$

All departing vessels must return to the original liquefaction terminal once they finish all planned shipping and is defined as

$$\sum_{j \in V} \sum_{k \in K} x_{h,j,k}^{vsl} = \sum_{i \in V} \sum_{k \in K} x_{i,h,k}^{vsl}, \quad \forall h \in V. \quad (3.7)$$

Constraints (3.8) and (3.9) establish the condition that a customer receives a shipment by one designated vessel in each time period:

$$\sum_{j \in V} \sum_{k \in K} x_{i,j,k}^{vsl} \leq 1, \quad \forall i \in V \setminus \{1\} \quad (3.8)$$

and

$$\sum_{i \in V} \sum_{k \in K} x_{i,j,k}^{vsl} \leq 1, \quad \forall j \in V \setminus \{1\}. \quad (3.9)$$

As stated above, all outgoing vessels from a depot must return to the same location, and should not terminate the tour while making any sub-tours. For each routing decision, MTZ sub-tour elimination constraints filter any possible sub-tours and is defined as

$$u_i - u_j + \gamma \cdot \sum_{k \in K} x_{i,j,k}^{vsl} \leq \gamma - 1, \quad \forall (i, j) \in A. \quad (3.10)$$

The relation between the amount of LNG loading to a cargo tank and the demands in each time period is denoted as

$$\sum_{i \in V} (1 - \varepsilon \cdot TR_{i,j}) \cdot x_{i,j}^{lng} - \sum_{t \in T} D_{j,t} = \sum_{l \in V} x_{j,l}^{lng}, \quad \forall j \in V \setminus \{1\}, \quad (3.11)$$

Particularly, as evaporated gas losses are expected during transportation, an additional amount of LNG is considered in the constraints.

Once a laden LNG vessel unloads all cargoes at each regasification terminal, the returning vessel must be empty in practice. So, constraints (3.12),

$$\sum_{i \in V} x_{i,h}^{lng} = 0, \quad \forall h \in V, \quad (3.12)$$

set the cargo level of laden LNG vessel returning to a liquefaction terminal as ‘0’.

Based on LNG contract terms, a specific amount of LNG cargoes have to be delivered to customers at the expected time on regasification terminals allowing a few days of grace period. Accumulated sailing time of an operating vessel is described as

$$x_j^{tot} \geq x_i^{tot} + TR_{i,j} - M \cdot (1 - x_{i,j,k}^{vsl}), \quad \forall (i, j) \in A, k \in K \quad (3.13)$$

and

$$x_j^{dep} \geq x_i^{tot} + TR_{i,j} - M \cdot (1 - x_{i,1,k}^{vsl}), \quad \forall (i, j) \in A, k \in K. \quad (3.14)$$

Time window is obtained by backward calculation from an expected delivery date on a target customer and defined as

$$|x_j^{tot} - TM_j^{tot}| \leq 0.5 \cdot \beta, \quad \forall j \in A. \quad (3.15)$$

set the time window from an expected delivery date on a target customer.

As type I LNG vessels have strict filling limits on cargo tanks during voyages, the conditions is set as

$$x_{i,j}^{lng} \geq \bar{\alpha} \cdot CG_k^{vsl} \cdot x_{i,j,k}^{vsl}, \quad \forall (i, j) \in A, k \in K_1. \quad (3.16)$$

Planning production inventory levels are determined by the demand in each time period and formulated as

$$x_t^{prd} - x_t^{str} + x_{t-1}^{str} = \sum_{j \in V} D_{j,t}, \quad \forall t \in T. \quad (3.17)$$

Allowed minimum and maximum storage level at the liquefaction terminal is constrained as

$$\underline{\rho} \leq x_t^{str} \leq \bar{\rho}, \quad t \in T. \quad (3.18)$$

Chapter 4

LNG IRP under BOG Uncertainty

4.1 Introduction

The presented deterministic LNG IRP model in the previous chapter is extended to a two-stage stochastic model considering BOG uncertainty. Before a realization of the random BOG, a single production inventory schedule and a vessel routing plan are executed to supply the requested demand. After a realization of random BOG generation during the shipping, the amount of LNG surplus or shortage can be known. Consequently, this model maximizes the revenue particularly minimizing the expected cost in the second stage. The stochastic LNG IRP is approximated to a deterministic equivalent and solved using Monte Carlo sampling techniques. The solutions are evaluated by expected value of perfect information (EVPI) and value of stochastic solution (VSS). The result shows that the proposed model yields more stable solutions over the deterministic model.

The remaining part of this chapter is organized as follows: Section 4.2 describes the proposed problem. Section 4.3 provides mathematical formulations of the two-stage stochastic LNG IRP considering random BOG. Then, Section 4.4 presents the computational study with test case description and settings, numerical results and sensitivity analysis. Finally, the chapter is concluded in Section 4.5.

4.2 Problem Description

Since this model is an extension of the proposed deterministic LNG IRP, it follows all notations and specification defined in the previous chapter.

It is analyzed that Type II vessels stop at multiple regasification terminals in a path, the total sailing time may be longer than the schedule of a Type I vessel which serves only one customer per voyage. As a result, this may lead to a relatively large amount of evaporating gas in a tank in proportion to the time on the sea. In the first stage problem, a single production-inventory schedule and LNG vessels routing is obtained before a realization of the random BOG generation. After the realization of the random gas evaporation, the amount of LNG surplus or shortage can be known when discharging the LNG cargo. For example, if 100,000 bcm is required by a customer, 100,500 may be loaded in an LNG carrier ship considering 500 bcm as the estimated BOG. However, after a voyage, if a dischargeable cargo at a destination is 99,900 bcm due to a gas loss, then you have to compensate the customer for the undelivered 100 bcm. On the other hand, if 100,100 bcm is available at the end, then the remaining 100 bcm may not generate any revenue unless the surplus is sold as a spot demand. In this research, it is assumed that the value of the latter case is ‘0’.

4.3 A Stochastic Extension of BOG Impact to LNG IRP

For the reformulation, it is followed that the general notations already defined in the previous chapter, the following are stochastic elements.

Stochastic Elements:

$\omega \in \Omega$	Set of scenarios;
$p_\omega \in P$	The probability mass function in accordance with scenario ω ;
$x_{i,j,\omega}^{lng}$	Amount of loaded LNG at terminal i heading to terminal j in accordance with scenario ω ;

$y_{t,\omega}^+$	Amount of LNG surplus at a regasification terminal on date t in accordance with scenario ω ;
$y_{t,\omega}^-$	Amount of LNG shortage at a regasification terminal on date t in accordance with scenario ω ;
C^{com}	Compensation cost for the amount of LNG shortage at a regasification terminal.

A two-stage stochastic model can be written as [85]

$$\begin{aligned} \max_{x \in X} \quad & c^T x - \mathcal{Q}(x), \\ \text{s.t.} \quad & Ax = b, \end{aligned} \tag{4.1}$$

and the recourse function $\mathcal{Q}(x)$ is translated as

$$\mathcal{Q}(x) = E_\omega Q(x, \omega) = \sum_{(i,j) \in A} \sum_{\omega \in \Omega} p_\omega Q(x, \omega), \tag{4.2}$$

where

$$\begin{aligned} Q(x, \omega) &= \min_{y \in Y} d_\omega^T y, \\ T_\omega x + W_\omega y &= h_\omega, \end{aligned} \tag{4.3}$$

which follows a discrete probability distribution P .

We consider BOG which is randomly generated within a minimum BOR $\underline{\varepsilon}$ and a maximum BOR $\bar{\varepsilon}$ and added to the calculation for the amount of loading LNG in a vessel during a laden voyage.

We denote E_ω as a mathematical expectation, and ω as a scenario with respect to probability space (Ω, P) . In the two-stage LNG routing problem, $Q(x, \omega)$ is the optimal value of BOG (second stage problem). First stage decisions are expressed in

vector x and second-stage decisions are actions represented by y . Accordingly, the objective function of the deterministic model can be reformulated into a stochastic form:

$$\begin{aligned}
& R \cdot \left(\sum_{j \in V \setminus \{1\}} \sum_{t \in T} D_{j,t} - \sum_{(i,j) \in A} \sum_{\omega \in \Omega} p_{\omega} \cdot \varepsilon_{\omega} \cdot TR_{i,j} \cdot x_{i,j,\omega}^{lng} \right) \\
& - \sum_{t \in T} C^{prd} \cdot x_t^{prd} \\
& - \sum_{t \in T} C^{str} \cdot x_t^{str} \\
& - \sum_{(i,j) \in A} \sum_{k \in K} C_k^{vsl} \cdot TR_{i,j} \cdot x_{i,j,k}^{vsl} \\
& - \sum_{t \in T} \sum_{\omega \in \Omega} p_{\omega} \cdot (R + C^{com}) \cdot y_{t,\omega}^{-}.
\end{aligned} \tag{4.4}$$

The relation between the amount of LNG loading to a cargo tank and the demands expressed in constraints (3.11) is replaced by

$$\sum_{i \in V} (1 - \varepsilon_{\omega} \cdot TR_{i,j}) \cdot x_{i,j,\omega}^{lng} - \sum_{t \in T} D_{j,t} = \sum_{l \in V} x_{j,l,\omega}^{lng}, \quad \forall j \in V \setminus \{1\}, \omega \in \Omega. \tag{4.5}$$

The dischargeable amount of LNG at an arriving terminal depends on how much BOG is generated during transport. This mechanism is expressed as

$$\begin{aligned}
& \sum_{i \in V} (1 - \varepsilon_{\omega} \cdot TR_{i,j}) \cdot x_{i,j,\omega}^{lng} - \sum_{t \in T} D_{j,t} \\
& = \sum_{l \in V} x_{j,l,\omega}^{lng} - \sum_{t \in T} (y_{t,\omega}^{-} - y_{t,\omega}^{+}), \quad \forall j \in V \setminus \{1\}, \omega \in \Omega,
\end{aligned} \tag{4.6}$$

by adding or subtracting surplus or shortage from a contract demand. These second stage variables are linked to the fifth term in (4.4).

The stochastic version of LNG IRP model has an infinite number of BOG scenarios. We try to obtain an approximated solution from a deterministic equivalent to

a stochastic model using the Monte Carlo sampling. This allows us to have a decent solution in a reasonable time.

Let $\omega_1, \dots, \omega_n$ be randomly generated samples drawn from P . Following the law of large numbers, for a given vector x , we have

$$|\Omega|^{-1} \cdot \sum_{n \in N} Q(x, \omega_n), \quad (4.7)$$

where $E_\omega Q(x, \omega)$ with probability one.

Therefore $Q(x) = E_\omega Q(x, \omega)$ is represented by the sample mean $\hat{Q}_n(x) = |\Omega|^{-1} \cdot \sum_{n \in N} Q(x, \omega_n)$ and the replacing objective function (4.4) can be rewritten as

$$\begin{aligned} & R \cdot \left(\sum_{j \in V \setminus \{1\}} \sum_{t \in T} D_{j,t} - |\Omega|^{-1} \cdot \sum_{(i,j) \in A} \sum_{\omega \in \Omega} \varepsilon_\omega \cdot TR_{i,j} \cdot x_{i,j,\omega}^{lng} \right) \\ & - \sum_{t \in T} C^{prd} \cdot x_t^{prd} \\ & - \sum_{t \in T} C^{str} \cdot x_t^{str} \\ & - \sum_{(i,j) \in A} \sum_{k \in K} C_k^{vsl} \cdot TR_{i,j} \cdot x_{i,j,k}^{vsl} \\ & - |\Omega|^{-1} \cdot \sum_{t \in T} \sum_{\omega \in \Omega} (R + C^{com}) \cdot y_{t,\omega}^- \end{aligned} \quad (4.8)$$

4.4 Computational Result

4.4.1 Numerical Example

The computational study presented in this section evaluates the deterministic LNG IRP model and two-stage stochastic model under BOG uncertainty by comparing solutions. In this section, the numerical example is described along with the experimental settings to solve the problems. An optimal routing schedule is depicted on a diagram with analysis on routing decisions. And then, the solution differences between the deterministic and the stochastic model are compared by means of Expected Value of Perfect Information (EVPI) and Value of Stochastic Solution (VSS). Further sensitivity analysis is done to investigate how the ratio between Type I and II vessels in a fleet influence to optimal solutions and what are the implied meanings of the composition of vessels.

The LNG IRP has been solved by GAMS/CPLEX [86] setting relative termination tolerance as 3% (optcr=0.03) and time limits as 10 hours (reslim=36000) in GAMS/CPLEX. All following experimental outcomes were optimized on a 3.00 GHz Intel Xeon machine with 400 GB of memory, running CPLEX version 12.6.

We tested the incidence of LNG business in Qatar, the biggest LNG exporter with 5 contracted importers over the world planning a biannual shipping schedule. For the deliveries, the supplier owns a total of 18 LNG vessels including 12 Type I vessels and 6 Type II vessels. The average sailing speed is 19.5 nautical miles per hour (kn). All sea routes are determined and the distances between terminals are given as constants. Each demand is classified as long-term, short-term or spot with expected target delivery dates with 4 days as time window. Overall planning horizon is from D+0 to D+192 days. Daily BOG in a tank ranges 0.1% 0.15% follows a normal distribution, $N(0.00125, 0.000104567^2)$. Inventory level is between 5,000 bcm and 10,000 bcm at the depot. To solve the proposed model, weather scenarios are

generated by Monte Carlo sampling technique.

Table 4.1: LNG cargo carriers

	Tank capacity (bcm)	Daily shipping cost (US \$)	Vessel type
#01	140,000	200,000	II
#02	140,000	195,000	II
#03	140,000	190,000	II
#04	140,000	185,000	II
#05	160,000	195,000	II
#06	160,000	190,000	II
#07	160,000	185,000	I
#08	160,000	180,000	I
#09	180,000	195,000	I
#10	180,000	190,000	I
#11	180,000	185,000	I
#12	180,000	180,000	I
#13	200,000	195,000	I
#14	200,000	190,000	I
#15	200,000	185,000	I
#16	200,000	180,000	I
#17	200,000	175,000	I
#18	216,000	180,000	I

Table 4.2: Shipping distance between terminals

	(unit: knot)				
	Ter.#1	Ter.#2	Ter.#3	Ter.#4	Ter.#5
Depot	9,882	9,770	6,576	6,350	6,233
Ter.#1		533	9,191	5,073	9,940
Ter.#2			9,208	4,891	9,957
Ter.#3				11,513	954
Ter.#4					11,141

4.4.2 Result

Figure 4.1 shows the optimized 6 month routing plan from D+1 to D+192 observing target delivery dates with times windows per each time period. In the schedule, 11 routes are generated and 9 LNG carriers are assigned to the routes.

Table 4.3: Demands in the planning horizon

Time Index	Demand (bcm)	Target date	Contract type
#02	60,000	D+36	spot demand
#03	62,500	D+36	short-term
#04	65,000	D+60	long-term
#05	175,000	D+60	long-term
#06	60,000	D+60	long-term
#08	60,000	D+72	spot demand
#09	62,500	D+72	short-term
#10	65,000	D+72	long-term
#11	175,000	D+120	long-term
#12	60,000	D+120	long-term
#14	60,000	D+108	spot demand
#15	62,500	D+108	short-term
#16	65,000	D+180	long-term
#17	175,000	D+180	long-term
#18	60,000	D+180	long-term

Table 4.4: Other parameters

Item	Data	Unit
Unit Price	105	US \$ / bcm
Storage operating cost	10.5	US \$ / bcm
Production cost	10.5	US \$ / bcm
Maximum storage level	10,000	bcm
Minimum storage level	5000	bcm
BOG level	[0.001, 0.0015]	percent
Filling limit of vessels type #07- #18	0.9	percent
Vessel speed	19.5	knots
Time window (from a target date)	4	days

Among the assigned vessels, there are four Type II vessels serving two demand cargoes in a route, and another seven Type I vessels delivering cargoes to a single customer in a tour.

The measures to evaluate stochastic solutions are EVPI and VSS. EVPI is the difference between Wait and See (WS) and stochastic solutions (RP) which expresses the value of information. WS is defined as a probability-weighted average of deterministic solution assuming any specific scenario realization [85]. In this experiment,

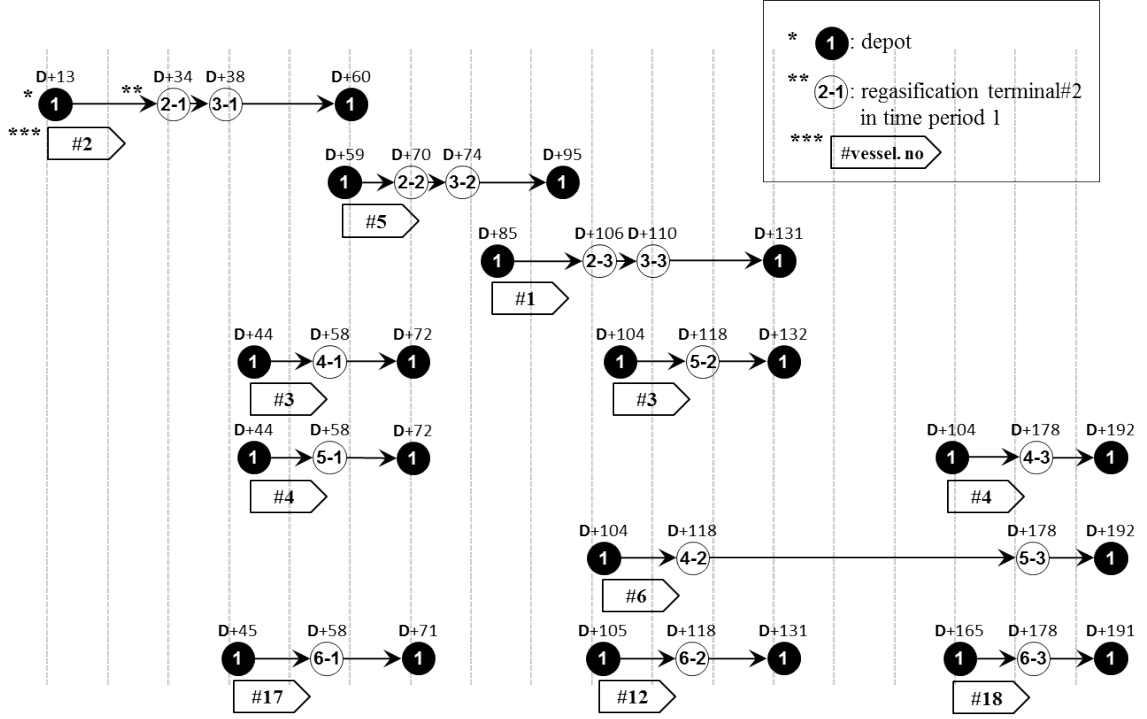


Figure 4.1: LNG ship routing plan from D+1 to D+192

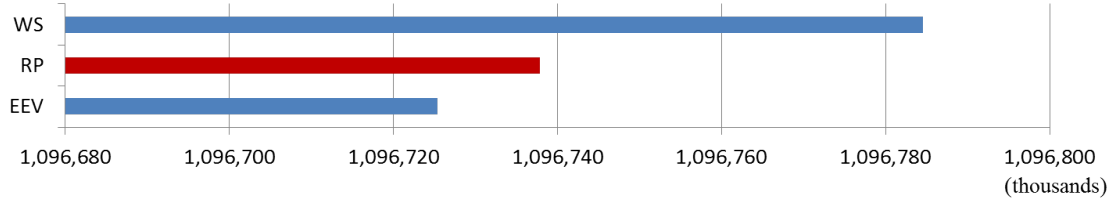


Figure 4.2: Optimal solutions of WS, RP and EEV

we can calculate $EVPI = WS - RP = 1,096,784,497 - 1,096,737,898 = 46,599$. On the other hand, VSS is RP minus EEV in this maximization problem which is the expected result of using mean value problem. In this test problem, $EEV = 1,096,725,454$ and so the value $VSS = RP - EEV = 12,444$ verifying the general relations between the defined measures; $EEV \leq RP \leq WS$ in **Figure 4.2**.

We conducted sensitivity analysis (SA) by varying the number of vessels between Type I and II vessels in a fleet seen in **Figure 4.3**:

(1) SA #1-#5: SA#1 is the instance that all vessels are Type I. SA#5 is the case that all vessels are Type II. SA#2, 3 and 4, examined the sensitivity of adding

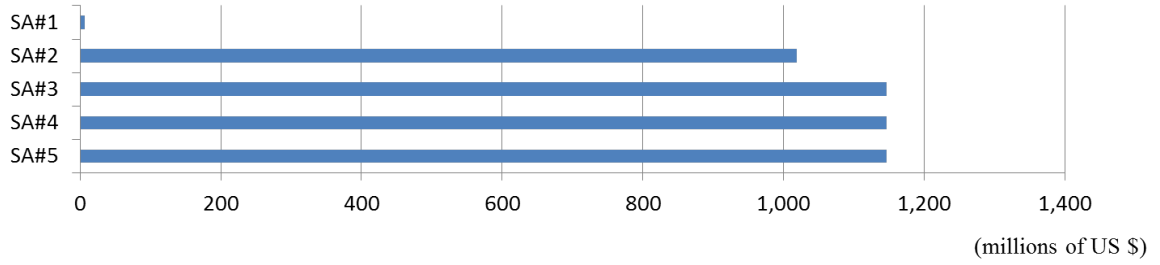


Figure 4.3: Sensitivity analysis: SA#1-5

different numbers of Type II vessels. As a result in Figure 9, it is observed that there is a significant gap between SA#1 and SA#2. This means that removing partial filling cargo restrictions allows delivery to multiple customers if transportation is cost beneficial. In SA#3 and 5, there is no change because additional vessels are not necessary to maximize the profit. So, in term of long-term vessel procurement, decisions to acquire additional vessels may be critical to avoid unnecessary costs.

(2) SA #6-#10: SA #6-#10 analyzes the impact of increasing the number of vessels in a fleet. The fleet of vessels is composed of ships with capacities of 140,000 bcm to 216,000 bcm. **Figure 4.4** shows that increasing profit is roughly proportional to the number of Type II vessels. Hence, it is recommended to replace the current Type I vessels to Type II.

4.5 Conclusion

In this chapter, a new biannual LNG IRP model is proposed, and formulated as a multiple vehicle routing and production-inventory routing problem. Based on this model, further extension of two-stage stochastic model was also presented applying Monte Carlo optimization techniques.

Traditional LNG ship routing and scheduling problem only aims to satisfy long-term contract. However, as short-term and spot demand contracts are rapidly increasing in the LNG market, and also as LNG vessel technology can relax strict

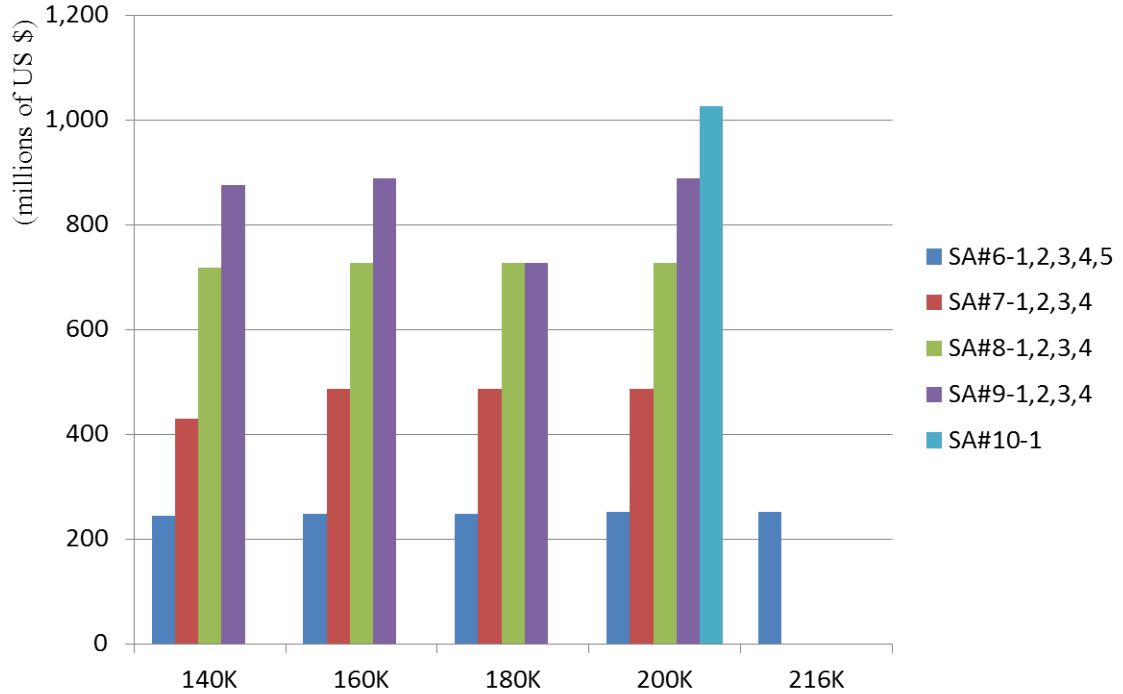


Figure 4.4: Sensitivity analysis #6-#10

restrictions on filling limits of cargo tanks, these changing environmental factors were exactly reflected into the proposed model. The LNG IRP model can generate six months of shipping and production inventory schedule to serve multiple customers in a route assigning appropriate LNG vessels.

In the computational study, the effectiveness of the proposed models was shown within the planning time horizon. By comparing the deterministic LNG IRP and its stochastic version by means of EVPI and VSS, as a result, it is clarified that the stochastic solutions outperform the deterministic one. As verified in the sensitivity analysis, replacing Type I to Type II vessels in a fleet may increase expected profit by reducing the total number of operating vessels.

As stated in the model, BOR is affected by various uncertain interactive factors, and so it needs further research to develop a mathematical model to measure accurate BOR. Even though many other elements are considered as deterministic components, there exist many inherent uncertainties causing severe disruptions in LNG supply

Table 4.5: Sensitivity analysis instances

SA	Objective value	number of Type II vessels				
		140K	160K	180K	200K	216K
#1	7,137,500	0	0	0	0	0
#2	1,018,532,546	1	1	1	1	1
#3	1,146,492,567	2	2	2	2	1
#4	1,146,492,567	3	3	3	4	1
#5	1,146,492,567	4	4	4	5	1
#6-1	244,638,911	1	0	0	0	0
#6-2	248,293,911	0	1	0	0	0
#6-3	248,293,911	0	0	1	0	0
#6-4	252,543,911	0	0	0	1	0
#6-5	252,458,911	0	0	0	0	1
#7-1	430,355,322	2	0	0	0	0
#7-2	487,665,322	0	2	0	0	0
#7-3	487,495,322	0	0	2	0	0
#7-4	487,495,322	0	0	0	2	0
#8-1	718,026,733	3	0	0	0	0
#8-2	726,951,733	0	3	0	0	0
#8-3	726,781,733	0	0	3	0	0
#8-4	726,781,733	0	0	0	3	0
#9-1	875,478,702	4	0	0	0	0
#9-2	888,143,702	0	4	0	0	0
#9-3	726,781,733	0	0	4	0	0
#9-4	887,973,702	0	0	0	4	0
#10-1	1,026,012,546	0	0	0	5	0

chain (i.e., hurricanes, dust storms, Tsunamis, political unrest) causing shipping delays or degradation of LNG facilities. Therefore, it can continue to be extended to the research in these directions.

Chapter 5

LNG IRP under Weather Disruptions

5.1 Introduction

In the last decade, there has been a remarkable upward global trend in the LNG industry [12]. North America has increased the production of shale gas to meet the growing demand internationally, particularly from Asia [13, 87]. Generally, LNG contracts have a 20-30 year duration which guarantees stable supply and demand relations. Natural gas can be transported to customers either through pipelines or by a fleet of LNG vessels. The trade of natural gas through pipeline is convenient and economical up to 2,500 kilometers. However, as shipping distance increases above this maximum, maritime transportation of natural gas in liquid form become more economically efficient [9, 10].

The LNG supply chain is composed of seven phases [3]. Once natural gas is produced, and stored at a temperature of -160°C , it is loaded into a vessel in liquid form to minimize the volume to 1/600 of its gaseous state for marine transportation. When an LNG vessel arrives at a regasification plant at a customer site, LNG must be transformed back to its original gaseous state for ground transportation and distribution [15]. This study covers the phases from gas production to unloading. Within this scope, the problem is formulated as an inventory routing problem (IRP) with which a supplier can optimize their production and inventory schedules while making ship routing decisions for a specific time horizon that satisfies the terms and conditions of their contracts.

There has been an increasing research effort in production-inventory scheduling and ship routing during the last decade, and this research can be categorized into

four basic models: 1) network design, 2) fleet deployment, 3) tramp cargo routing and scheduling problem and 4) maritime IRP for a single product [29, 2]. The fourth model is the focal point of this research.

There has been an increasing trend of research on LNG IRP since 2009. One of the earliest approaches reported in the literature was a mixed integer programming (MIP) model considering LNG cargo ships shuttling from a liquefaction plant to a regasification plant [30]. Other researchers [31, 32] have improved their approach including sailing schedule, terms and conditions of contracts, and various vessel types.

Traditional LNG demand is mostly identified from well-determined long-term contracts, and so an annual delivery program (ADP) was considered to fulfill a set of long-term contracts [33]. However, two conspicuous changes in LNG market have been observed. First, there has been an increasing trend of spot-demand and short-term contracts [43]. Second, recent technological advances in LNG tanker design and construction has enabled more flexible LNG transportation such as a tanker making multiple stops at regasification plants. Therefore this study expands the problem to include any contract types and visiting multiple regasification plants in a journey, which was not considered in previous studies.

There are two major uncertain factors in LNG supply planning. First, an LNG carrier loses a small fraction of gas during the voyage due to random BOG [27]. Therefore, the initial load of LNG to a vessel at the liquefaction plant must consider both the amount of demand to be delivered to the customer and the estimated amount of BOG. Second, sudden changes in weather conditions (i.e., dust storm in the Persian Gulf) can disrupt LNG supply schedule. For example, Qatar (the biggest exporter of LNG in the world in volume) has experienced frequent disruptions in the LNG supply operations caused by dust storms in the Persian Gulf [46, 47, 48].

The literature review reveals that some researchers have considered the BOG impact in LNG supply chain, but no mathematical models have been specifically

developed to consider weather disruptions as an uncertain factor in LNG carrier routing and production-inventory scheduling. Therefore, it is proposed that new mathematical models considering random extreme weather conditions, and computational techniques to solve the models more efficiently. Contributions of this research is highlighted as follows:

- A two-stage stochastic LNG IRP model (TSS) is suggested to consider the impact of random extreme weather conditions on LNG loading operations. Specifically, it is reinforced that the production planning and inventory control constraints knowing that an extreme weather not only affects routing decisions but also production and inventory schedules. In the previous study, boil-off-rate (BOR) was considered as a random element [48]. However, BOR is set as a constant to focus primarily on the impact of an extreme weather as a major disruption element in LNG shipping scheduling. This is a reasonable assumption because the impact of an extreme weather have a substantially higher impact than that of uncertain BOR.
- A decision maker's preference model (DMP) proposed which allows a decision maker to input his/her preference between the shipping delay (caused by a random extreme weather condition) and the expected profit. Because achieving one may come at the expense of the other. It is formulate as a parametric optimization model to reflect a decision maker's preference on risk between the two extreme scenarios: i) scenario #1 - the earliest extreme weather beginning and ii) scenario #2 - the latest extreme weather ending time.
- A probing-based preprocessing technique (PPT) has been developed to solve TSS to speed up convergence. PPT utilizes the relations between the amount of time spent and the amount of BOG generated in each path. Since TSS is a highly complex two-stage stochastic MIP model, this approach reduces the size

of problems and enables the model to be solved faster.

- A benefit of PPT is that it eliminates the need of tour sequencing decisions in path planning. Accordingly, a reinforced PPT (rPPT) has been developed by replacing the Miller-Tucker-Zemlin (MTZ) sub-tour elimination constraint in the TSS with the proposed logical inequality to enhance the computational performance [28].

Demonstrated experimental results shows that the stochastic solutions are superior to deterministic solutions under a disturbance; parametric solutions provided guidelines for a decision maker's involvement in the planning. Furthermore, it was shown that the proposed probing techniques and a logical inequality to the TSS model were computationally efficient.

The rest of this chapter is organized as follows: Section 5.2 describes the proposed problem. Section 5.3 provides mathematical formulations of the LNG IRP in a two-stage stochastic form considering extreme weather disruptions. Then, Section 5.4 presents the computational study with numerical results and sensitivity analysis. Finally, the chapter is concluded in Section 5.5.

5.2 Problem Description

The general goal of the LNG IRP is to provide an optimal production inventory schedule and transportation plans that satisfy all demands from customers in an LNG supply chain considering the terms and conditions of their contracts. LNG contracts typically include the duration of a contract, the frequency of delivery, and the total amount of demand, expected shipping dates and locations, the grace period and any associated penalties for delays. In order to maximize the expected revenue, an LNG supplier has to consider various aspects such as maximum capacities for production and storage, the total number of LNG vessels per type, and shipping schedule.

We consider two types of LNG vessels according to the specifications of cargo tanks. The first vessel type has a strict barred filling limit of LNG cargo which is categorized as Type I. It has a permissible range that is either more than 70 % or less than 10 % of the tank. This exact filling limit is due to the sloshing effect which increases potential risks such as gas leaks and other related safety accidents [48]. The second vessel type (Type II) is not limited to this filling limit for its cargo. It is flexible to any level of partial loading which allows for numerous cargo discharges at multiple regasification plants in a voyage path [83, 84].

Unlike other products, an LNG cargo evaporates gas during marine transport. The amount of evaporated gas is proportional to the amount of LNG cargo on board and shipping distance. Therefore, the loading amount of LNG from a departing liquefaction plant must aggregate the total amount of LNG to be delivered and the estimated BOG loss during a voyage.

An extreme weather such as a dust storm with strong winds in the Persian Gulf can make the LNG loading operations unstable. In general, any extreme weather event can be forecasted about three days in advance and the LNG loading operations takes about 12 hours [88, 89, 90].

There are two kinds of relationships between an extreme weather and an LNG loading schedule as illustrated in **Figure 5.1**. First, if an extreme weather is expected to impact the LNG loading start time, then a planned loading schedule must be altered. Due to the loading delay, an LNG cargo in the ground facilities must remain in storage for an extended period of time until the facility is open again after the weather disruption, which incurs an additional storage cost. Second, if a storm is expected to begin before the end of planned loading operations, then a loading schedule must be adjusted so that the loading can be completed before the beginning of the storm. In this case, the LNG stock level will be lower than the planned amount because the production inventory schedule was originally aimed to meet the LNG stock level at a

later date. Therefore, additional production efforts must be made at a higher cost to meet the demand.

The LNG supply network in this problem includes three routes: initial delivery route, intermediate route and the return route as shown in **Figure 5.2**. An initial delivery route connects a liquefaction plant to a regasification plant while the return route follows the reverse order. An intermediate route links between two regasification plants. Therefore, an intermediate route(s) can be included only if there are at least two regasification plants to visit in a path. When a vessel starts a voyage through an initial delivery route, the departure time from a liquefaction plant can vary depending on the expected arrival time of an extreme weather condition and its estimated duration.

There are seven categories of decision variables involved in the problem: 1) the amount of LNG to be delivered to each customer per carrier, 2) the vessel assignment to a travel path, 3) the daily inventory and production schedule, 4) departure and arrival times of an incoming and outgoing vessel at each regasification plant, 5) the number of delay days, 6) the amount of additional LNG production anticipating an LNG inventory shortage and 7) the amount of excessive LNG or shortage after the realization of a random weather disruption.

5.3 Mathematical Formulation

Based on the problem discussed in Section II, LNG IRP is formulated as a two-stage stochastic MIP model. Additional details on modeling and solution techniques are provided in this section.

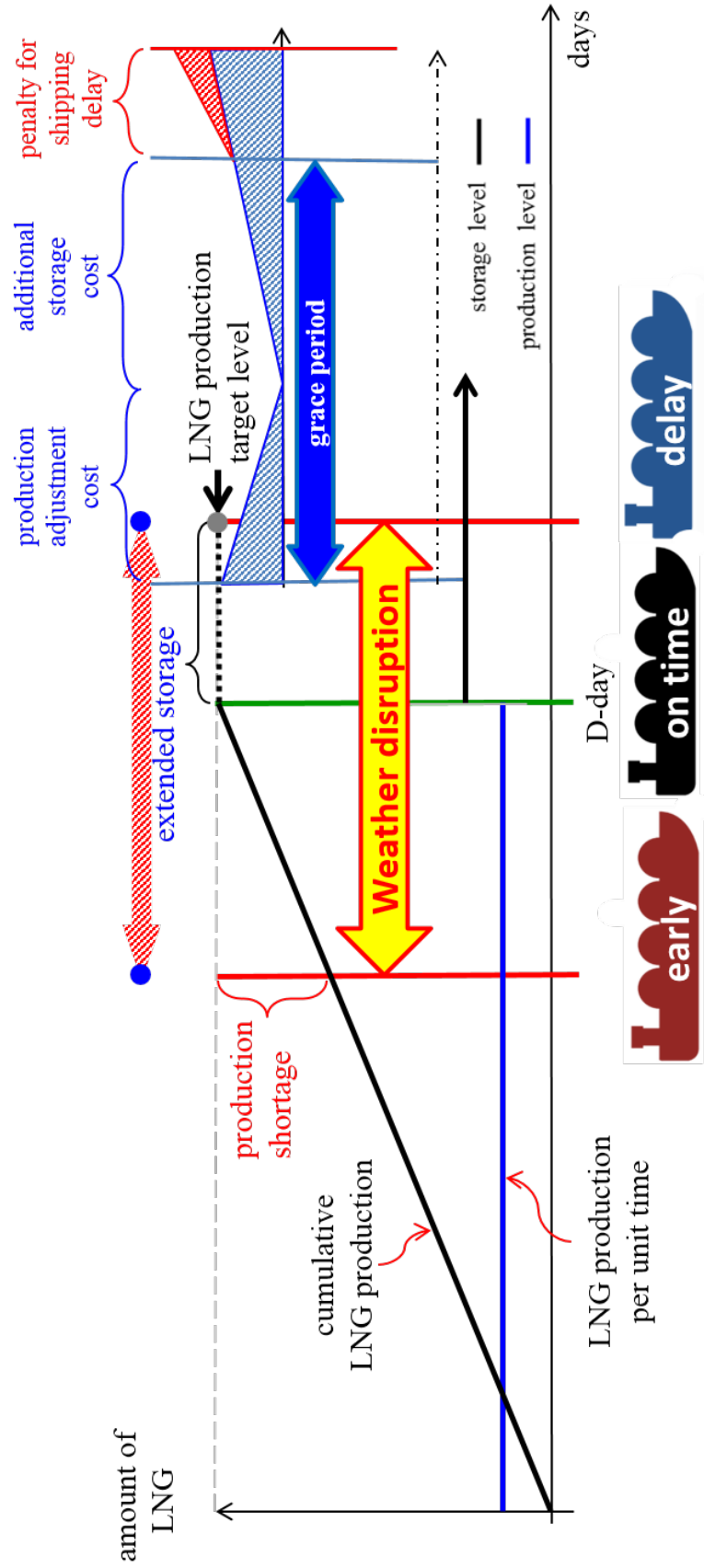


Figure 5.1: A random extreme weather impacts to LNG production & storage plan and vessel departure time

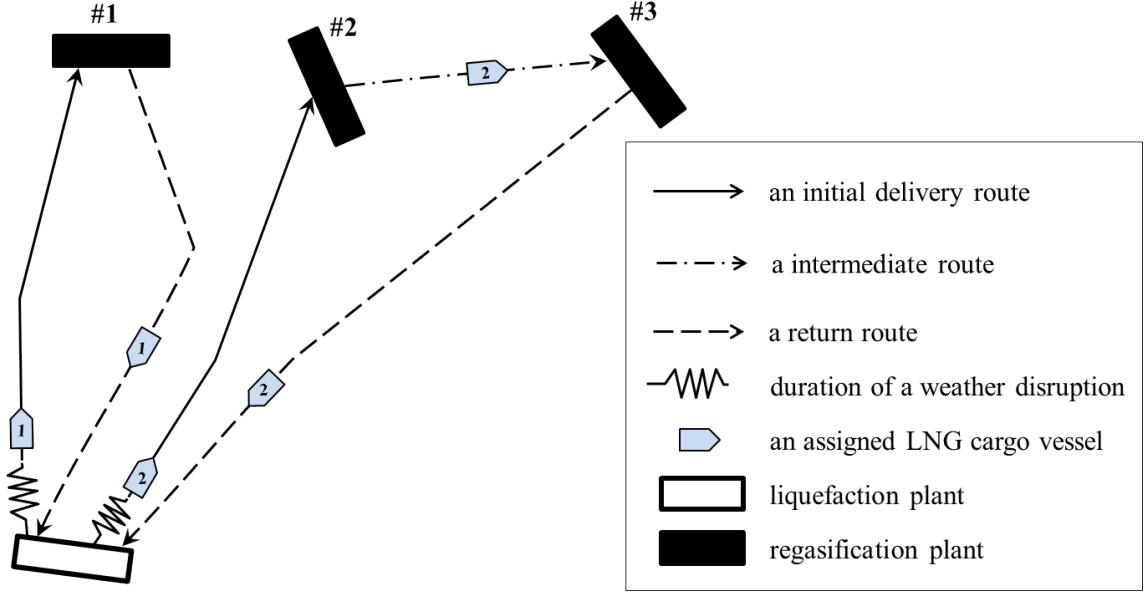


Figure 5.2: Three types of transportation routes connecting terminals

5.3.1 Sets, Elements, Data and Variables

In the context of IRP, the problem can be modeled on a directed network $G(V, A)$. A supplier at a liquefaction plant $i \in V_1$ delivers requested amount of LNG D_j to a customer at a regasification plant $j \in V_2$ by LNG vessel $k \in K$ through the traverse arc $(i, j) \in A$. A path a_n is composed of the initial delivery route A_1 , intermediate route A_2 and return route A_3 . A supplier transports a total $|r_s|$ number of cargoes to its customers within a given time horizon in accordance to their contracts. The most appropriate LNG vessel $k \in K$ is assigned to transport LNG through path a_n . Recall that there are two types of vessels: Type I vessels $k_1 \in K_1$ and Type II vessels $k_2 \in K_2$ where $K = \{K_1 \cup K_2\}$ and $K_1 \cap K_2 = \emptyset$. Type I vessels have to strictly follow the barred cargo fill range $[\underline{\alpha}, \bar{\alpha}]$. When an LNG vessel $k \in K$ makes a tour following a path a_n , the sequence of visits is determined by introducing a flow variable u_i for each plant $i \in V$. Daily production level x_t^{prd} and inventory level x_t^{str} are determined considering maximum production capacity $\bar{\psi}$ and minimum production level $\underline{\psi}$, and maximum storage capacity $\bar{\rho}$ and minimum safety stock level

$\underline{\rho}$ respectively. LNG volume D_j ordered by a customer $j \in V_2$ can be delivered between the expected target delivery date TM_j^{tot} and $TM_j^{tot} + \beta$ considering days of grace. If a cargo is delivered beyond this point, then it generates a penalty μ_j which is proportional to the number of delay days (NDD) $y_{j,\omega}^{del}$ up to TW days. The random extreme weather timing $\xi_{j,\omega,ds}$ influencing a voyage from a liquefaction plant to a regasification plant $j \in V_2$ is represented by the sample $\omega \in \Omega$ and probability mass function p_ω . Scheduling a vessel departure time from a liquefaction plant is subject to an expected vessel arrival time at a destination $y_{j,\omega}^{tot}$, travel time $TR_{i,j}$ and extreme weather timing $\xi_{j,\omega,ds}$ at the point of departure. Therefore a vessel departure time from a depot $\tau_{j,\omega,ds}$ can be obtained by the calculation of $TM_j^{tot} - (TR_{i_0,j} + \xi_{j,\omega,ds})$. BOG is generated at the constant rate ε and added to the calculation for the amount of loading LNG in a vessel during a laden voyage. It is defined that notation for the sets, input data and decision variables used in the mathematical model.

Sets:

S	Set of LNG terminals;
T	Set of dates;
K	Set of LNG vessels;
ds	An indicator of the beginning (1) or ending (2) of an extreme weather, $ds = \{1, 2\}$;
$G(V, A)$	Directed graph nodes $V = \{1, 2, \dots, i = s + S \cdot (r_s - 1)$ where r_s is a delivery sequence number per plant} as the set of plants and $A = \{(i, j) : i, j \in V, i \neq j\}$ as the set of arcs in the planning time horizon;

V_1	Set of liquefaction plants where $V_1 = \{1, 1 + S , 1 + 2 \cdot S , \dots, i_0 = 1 + S \cdot (r_s - 1)\}$ in the planning horizon $V_1 \subseteq V$;
V_2	Set of regasification plants in the planning time horizon where $V_2 \subseteq V$ and $V_1 \cap V_2 = \emptyset$;
A_1	Set of initial delivery routes where $A_1 = \{(i, j) : i \in V_1, j \in V_2\}$ as the set of arcs from a liquefaction plant to a regasification plant where $A_1 \subseteq A$;
A_2	Set of initial intermediate routes where $A_2 = \{(i, j) : i, j \in V_2, i \neq j\}$ as the set of arcs between regasification plants where $A_2 \subseteq A$;
A_3	Set of return routes where $A_3 = \{(i, j) : i \in V_2, j \in V_1\}$ as the set of arcs from a regasification plant to a liquefaction plant where $A_1 \subseteq A$ and $A_1 \cap A_2 \cap A_3 = \emptyset$;
K_1	Set of Type I LNG vessels, $K_1 \subseteq K$;
K_2	Set of Type II LNG vessels, $K_2 \subseteq K$, and $K_1 \cap K_2 = \emptyset$;
a_n	Set of paths where $a_n \in A$.

Data:

$TR_{i,j}$	Estimated travel time from i to j ;
TM_j^{tot}	Expected cargo arrival date at j ;
TW	Time window - maximum NDD from an expected cargo arrival date;
CG_k^{vsl}	Cargo capacity of vessel k ;
D_j	Demand at plant j ;
R	Unit revenue of LNG per billion cubic meters (bcm);
C_k^{vsl}	Daily shipping cost of a vessel k ;
C^{str}	Daily storage cost per bcm ;
C^{prd}	Daily production cost per bcm ;
C^{ap}	Daily contingency production cost per bcm ;

μ_j	Penalty for shipping delay to j ;
γ	Maximum number of plants can be visited in a path;
M	Big-M;
α	Barred fill range (%) of Type I LNG vessels $[\underline{\alpha}, \bar{\alpha}]$;
β	Number of days of grace;
ε	Daily boil-off rate;
ρ	Minimum / maximum storage level $[\underline{\rho}, \bar{\rho}]$;
ψ	Minimum / maximum production level $[\underline{\psi}, \bar{\psi}]$.

Random Elements:

$\omega \in \Omega$	A sample point and sample space of extreme weather variations;
p_ω	The probability mass function of extreme weather variations;
$\xi_{j,\omega,ds}$	An extreme weather beginning time ($ds = 1$) or ending time ($ds = 2$) which impacts to an LNG loading time heading to a regasification plant j in accordance with scenario ω ;
$\tau_{j,\omega,ds}$	Departure date from a liquefaction plant to a regasification plant j in accordance with scenario ω where $\tau_{j,\omega,ds} = TM_j^{tot} - (TR_{i_0,j} + \xi_{j,\omega,ds})$.

Decision Variables:

$x_{i,j}^{lng}$	Amount of LNG cargo from i to j ;
$x_{i,j,k}^{vsl}$	$= \begin{cases} 1, & \text{If vessel } k \text{ maneuvers from } i \text{ to } j; \\ 0, & \text{Otherwise;} \end{cases}$
$x_{i,j,k,ds}$	$= \begin{cases} 1, & \text{If vessel } k \text{ departs at days } ds; \\ 0, & \text{Otherwise;} \end{cases}$

x_t^{prd}	Production level on date t ;
x_t^{str}	Storage level on date t ;
$y_{j,\omega}^{tot}$	Vessel arrival date at a regasification plant j in accordance with scenario ω ;
$y_{j,\omega}^{del}$	NDD at a regasification plant j in accordance with scenario ω ;
$y_{t,\omega}^+$	Amount of excessive LNG on date t in accordance with scenario ω ;
$y_{t,\omega}^-$	Amount of LNG shortage on date t in accordance with scenario ω ;
u_i	A flow in the vessel after it visits plant i .

5.3.2 A Two-Stage Stochastic Approach to LNG IRP

Solving TSS can be computationally challenging due to the existence of uncertain parameters. The realization of uncertain parameters has to be considered in computation. The uncertainty can be assumed to follow a continuous probability distribution. However, one has to deal with a nonlinearity of the model, which leads to a substantial burden in computation. Alternatively, the problem can be solved by a discrete approximation of the continuous variable, in which a set of scenarios are often generated to represent the random events. A drawback is that it can still be computationally expensive if the model requires a large number of scenarios to accurately capture the distribution. However, if the scenario set is small then this is tractable, and the model can be solved with deterministic problem solution techniques without loss of optimality [91]. As the set of set of scenarios Ω are considered being discrete and finite, a deterministic equivalent problem (DEP) form of a two-stage stochastic LNG IRP is formulated as follows.

The objective function is defined as

$$\begin{aligned}
\text{maximize } R \cdot & \left(\sum_{j \in V_2} \sum_{t \in T} D_{j,t} - \sum_{(i,j) \in A} \varepsilon \cdot TR_{i,j} \cdot x_{i,j}^{lng} \right) \\
& - \sum_{(i,j) \in A} \sum_{k \in K} C_k^{vsl} \cdot TR_{i,j} \cdot x_{i,j,k}^{vsl} - \sum_{t \in T} (C^{prd} \cdot x_t^{prd} + C^{str} \cdot x_t^{str}) \\
& - |\Omega|^{-1} \cdot \sum_{t \in T} \sum_{\omega \in \Omega} (C^{ap} \cdot y_{t,\omega}^- + C^{str} \cdot y_{t,\omega}^+) - |\Omega|^{-1} \cdot \sum_{j \in V_2} \sum_{\omega \in \Omega} \mu_j \cdot y_{j,\omega}^{del},
\end{aligned} \tag{5.1}$$

with five terms. The first term is the lump sum profits for exporting LNG minus the boil-off loss. The second term is the vessel operating costs in proportion to the shipping distance. The third term is the production and inventory cost. The fourth term is the expected cost for additional LNG productions or extended inventories after the realization of an extreme weather. The last term is the expected penalty for shipping delays beyond the grace period.

The constraints are divided into three groups. The first group consists of constraint (5.2) to (5.11), their purpose is to make multiple vessel routing decisions while meeting demands from costumers. The second group consists of constraint (5.12) to (5.14), their purpose is to determine the voyage schedule under weather disruptions. The remaining constraint deal with production inventory planning.

To construct a path and make connections between two routes in the path, the condition is described as

$$x_{i,j,k}^{vsl} \leq \sum_{l \in V} x_{j,l,k}^{vsl} \leq |S| - (|S| - 1) \cdot x_{i,j,k}^{vsl}, \quad \forall i, j \in V, k \in K. \tag{5.2}$$

LNG cargo capacity should be greater than or equal to the sum of loading cargo and BOG, and is defined as

$$x_{i,j}^{lng} \leq \sum_{k \in K} CG_k^{vsl} \cdot x_{i,j,k}^{vsl}, \quad \forall (i, j) \in A. \tag{5.3}$$

Total number of assigning vessels which are bounded by the fleet size and is expressed as

$$\sum_{(i,j) \in A_1} x_{i,j,k}^{vsl} \leq |K|, \quad \forall k \in K. \quad (5.4)$$

Flow of an operating LNG carrier in a path is balanced by the following three constraints:

$$\sum_{(i,j) \in A_1} \sum_{k \in K} x_{i,j,k}^{vsl} = \sum_{(i,j) \in A_3} \sum_{k \in K} x_{j,i,k}^{vsl}. \quad (5.5)$$

$$\sum_{j \in V} \sum_{k \in K} x_{i,j,k}^{vsl} \leq 1, \quad \forall i \in V_2, \quad (5.6)$$

and

$$\sum_{i \in V} \sum_{k \in K} x_{i,j,k}^{vsl} \leq 1, \quad \forall j \in V_2. \quad (5.7)$$

MTZ sub-tour elimination constraint is denoted as

$$u_i - u_j + \gamma \cdot \sum_{k \in K} x_{i,j,k}^{vsl} \leq \gamma - 1, \quad \forall (i,j) \in A_2. \quad (5.8)$$

LNG cargo unloading level is determined considering BOG generation which is proportional to the travel distance of a ship and is expressed as

$$\sum_{i \in V} (1 - \varepsilon \cdot TR_{i,j}) \cdot x_{i,j}^{lng} - D_j = \sum_{l \in V} x_{j,l}^{lng}, \quad \forall j \in V_2. \quad (5.9)$$

Barred fill range of Type I vessel is specified by two constraints:

$$x_{i,j}^{lng} \geq \bar{\alpha} \cdot CG_k^{vsl} \cdot x_{i,j,k}^{vsl}, \quad \forall (i,j) \in A, k \in K_1 \quad (5.10)$$

and

$$x_{i,j}^{lng} \geq \underline{\alpha} \cdot CG_k^{vsl} \cdot x_{i,j,k}^{vsl}, \quad \forall (i,j) \in A_3, k \in K_1. \quad (5.11)$$

A vessel departure time should be either before or after the occurrence of a weather disruption, and is described as

$$\sum_{k \in K} x_{i,j,k}^{vsl} = \sum_{k \in K} x_{i,j,k,ds}, \quad \forall (i, j) \in A_1, ds \in DS. \quad (5.12)$$

Determination of the arrival and departure times of an LNG vessel at each regasification plant is defined as

$$\left| (\tau_{j,\omega,ds} + TR_{i,j}) \cdot \sum_{k \in K} x_{i,j,k,ds} - y_{j,\omega}^{tot} \right| \leq M \cdot \left(1 - \sum_{k \in K} x_{i,j,k}^{vsl} \right), \quad (5.13)$$

$$\forall (i, j) \in A_1, \omega \in \Omega, ds \in DS$$

and

$$\left| TR_{i,j} \cdot \sum_{k \in K} x_{i,j,k}^{vsl} - y_{j,\omega}^{tot} + y_{i,\omega}^{tot} \right| \leq M \cdot \left(1 - \sum_{k \in K} x_{i,j,k}^{vsl} \right), \quad (5.14)$$

$$\forall (i, j) \in A_2, \omega \in \Omega.$$

Shipping time window considering a grace period is defined as

$$TM_j^{tot} - TW \leq TM_j^{tot} + \beta + y_{j,\omega}^{del}, \quad \forall j \in V_2, \omega \in \Omega \quad (5.15)$$

and

$$\beta + y_{j,\omega}^{del} \leq TW, \quad \forall j \in V_2, \omega \in \Omega. \quad (5.16)$$

For example, if a vessel is delayed beyond the time window, then a penalty is charged

accordingly. Considering production and storage capacity, production-inventory scheduling scheme is defined as

$$\underline{\rho} \leq x_t^{str} \leq \bar{\rho}, \quad \forall t \in T, \quad (5.17)$$

$$\underline{\psi} \leq x_t^{prd} \leq \bar{\psi}, \quad \forall t \in T, \quad (5.18)$$

and

$$x_t^{str} - x_{t-1}^{str} = x_t^{prd} + y_{t,\omega}^+ - y_{t,\omega}^- - \sum_{a_n \in A} \sum_{k \in K} LD_{a_n, t', \omega, ds} \cdot x_{a_n, k, ds}^{vsl}, \quad (5.19)$$

$$\forall t, t', ds \in T, \omega \in \Omega, ds \in DS.$$

These constraints ensure that the ordered amount of LNG will be ready on or before the loading date to a cargo. In this problem, a random extreme weather variation is considered in lead time estimation in addition to travel times. For example, if an extreme weather delays a planned LNG loading operation for a certain length of time, then production inventory schedule and an LNG vessel departure time should be synchronized with the adjusted LNG loading schedule. For the time synchronization, the following procedures are proposed in the preprocessing stage.

Time Synchronization Elements:

$t'_{\omega, ds}$	Departure date from a liquefaction plant in accordance with ω ;
t''	Arrival date at the last regasification plant in a path;
$j_{a_n}^m$	m^{th} regasification plant in path a_n where $m \in V_2, j : (\cdot, j) \in a_n$;
$D_{a_n}^m$	Demand from m^{th} regasification plant in path a_n ;
$TR_{a_n}^m$	Trevel time from $(m - 1)^{th}$ to m^{th} plant in path a_n where $\sum_{(i,j) \in A} TR_{i,j} \in a_n$;

$LD_{a_n, t'_{\omega, ds}}$ The total amount of LNG to be loaded for path a_n in accordance with ω .

First, the departure date from a liquefaction terminal $t'_{\omega, ds}$ of an LNG vessel from a liquefaction plant needs to be determined. Let us assume that an LNG vessel is to serve m regasification plants in path a_n . The departure date can be estimated by subtracting the total travel days $\sum_{m \in V_2} TR_{a_n}^m$ and the storm duration $\xi_{j_{a_n}^1, \omega, ds}$ from the expected cargo arrival date t'' at the m^{th} regasification plant as

$$t'_{\omega, ds} = t'' - \left(\xi_{j_{a_n}^1, \omega, ds} + \sum_{m \in V_2} TR_{a_n}^m \right), \forall a_n \in A, t'_{\omega, ds}, t'' \in T, \omega \in \Omega, ds \in DS. \quad (5.20)$$

Second, the amount of LNG $LD_{a_n, t'_{\omega, ds}}$ to be loaded for a vessel at date $t'_{\omega, ds}$ from a liquefaction plant is estimated by

$$LD_{a_n, t'_{\omega, ds}} = \sum_{m \in V_2} D_{a_n}^m + BOG_{a_n}$$

$$\text{where } BOG_{a_n} = \varepsilon \cdot \sum_{m \in V_2} TR_{a_n}^m \cdot \left(\sum_{m \in V_2} D_{a_n}^m - \sum_{cr=1}^{|m|} \sum_{m=cr}^{|m|} D_{a_n}^m \right). \quad (5.21)$$

$$\forall a_n \in A, t'_{\omega, ds} \in T, ds \in DS.$$

Basically, $LD_{a_n, t'_{\omega, ds}}$ includes the sum of demands and the estimated evaporated loss BOG_{a_n} during the voyage on a path a_n . The total amount of BOG in a path BOG_{a_n} depends on a daily BOR ε , total travel time $\sum_{m \in V_2} TR_{a_n}^m$ and the amount of LNG on board in each route $\sum_{m \in V_2} D_{a_n}^m - \sum_{cr=1}^{|m|} \sum_{m=cr}^{|m|} D_{a_n}^m$ as seen in equation (21). Therefore, one thing to note here is that BOG losses may vary depending on the travel sequence on a path, which can change the combination of travel days and LNG on board. This property is utilized to eliminate inferior routing options using this preprocessing technique, which is explained in detail in Section 5.3.4. The following **Proposition 5.1** provides a basis for BOG-based probing technique.

Proposition 5.1. For any path a_{n1} and a_{n2} ($a_{n1} \neq a_{n2}$) with same set of regasification terminals, if $LD_{a_{n1},t',\omega} \geq LD_{a_{n2},t',\omega}$ then $BOG_{a_{n1}} \geq BOG_{a_{n2}}$.

5.3.3 Generalization of Production-Inventory Constraints

In the previous section, a production-inventory control constraint (5.19) and time synchronization scheme are presented which include maximum two customers in a single journey of an LNG carrier. If both constraint (5.19) and time synchronization scheme are integrated into a single constraint in the model, then it makes the model as a nonlinear mixed integer programming model which is difficult to solve. Therefore, this section presents a new constraints set which makes the LNG IRP model as an MILP.

With this constraints set, it is possible to solve the problem in the case of more than two customers in a path.

Let us assume that time index t is discrete, and there is no weather disruption impact to a production-inventory control constraint which is in a deterministic form such as

$$x_t^{str} = x_{t-1}^{str} + x_t^{prd} - \sum_{j \in V_2} LD_{j,t}, \forall t \in T. \quad (5.22)$$

To determine the amount of LNG cargo $\sum_{j \in V_2} LD_{j,t}$, which is loading to an LNG vessel at time t two factors needs to be considered: i) LNG cargo loading time before the beginning of a weather disruption which is random, ii) LNG volume to be produced and stored which is loading to an LNG carrier heading to a terminal j . Let's define that LNG carrier loading time which is heading to a terminal j as $ST_{t,j} \in \{0, 1\}$. Total number of variables $ST_{t,j} \in \{0, 1\}, \forall t \in T, j \in J$ in the model is

$$numberofdays(|t|) \times numberofregasificationterminals(|j|). \quad (5.23)$$

In order to synchronize the time index t in variable $ST_{t,j} \in \{0, 1\}$ and the LNG carrier departure time, the relation is formulated as

$$(TM_j^{tot} - TR_{i_0,j}) \sum_{k \in K} \sum_{ds \in DS} x_{i_0,j,k,ds}^{vsl} = \sum_{t \in T} c_t ST_{j,t} \quad \forall j \in V_2, c_t = \{1, 2, 3, \dots, t\}. \quad (5.24)$$

LNG carrier departure timing is expressed in the left-hand side (LHS). If a route from a liquefaction terminal i_0 to a regasification terminal j is selected, then travel time between the two terminals $TR_{i_0,j}$ are subtracted from an expected arrival time of a vessel at terminal j TM_j^{tot} . The LHS is equal to the right-hand side (RHS) value which is composed of c_t and $ST_{j,t}$. To transform the time index t to a constant value, constant c_t is introduced which is equal to the index t . For example, if an LNG carrier is heading to a regasification terminal 2 as an initial destination from a liquefaction terminal, then the cargo arrival time at terminal j $TM_j^{tot} = 20$, and shipping days between two terminals $TR_{i_0,j} = 10$. Therefore an LNG carrier departure time is at day 10. In order to synchronize the value in the LHS to the RHS, $\sum_{t \in T} c_t ST_{j,t}$ must be 10 where $c_{10} = 10$ and $ST_{2,10} = 1$.

LNG carrier departure timing is indicated by

$$\sum_{t \in T} ST_{j,t} \leq 1, \forall j \in V_2. \quad (5.25)$$

If j is an initial destination in a path of an LNG carrier which is from a liquefaction plant, then $\sum_{t \in T} ST_{t,j} = 1$. Otherwise 0.

When $\sum_{t \in T} ST_{t,j} = 1$, cargo level in an LNG carrier $x_{i_0,j}^{lng}$ is equal to the LNG production target level $\sum_{t \in T} LD_{j,t}, \forall j \in V_2$. If j is not an initial destination in a path, $x_{i_0,j}^{lng} = \sum_{t \in T} LD_{j,t} = 0$. The condition is expressed as

$$x_{i_0,j}^{lng} = \sum_{t \in T} LD_{j,t}, \forall j \in V_2. \quad (5.26)$$

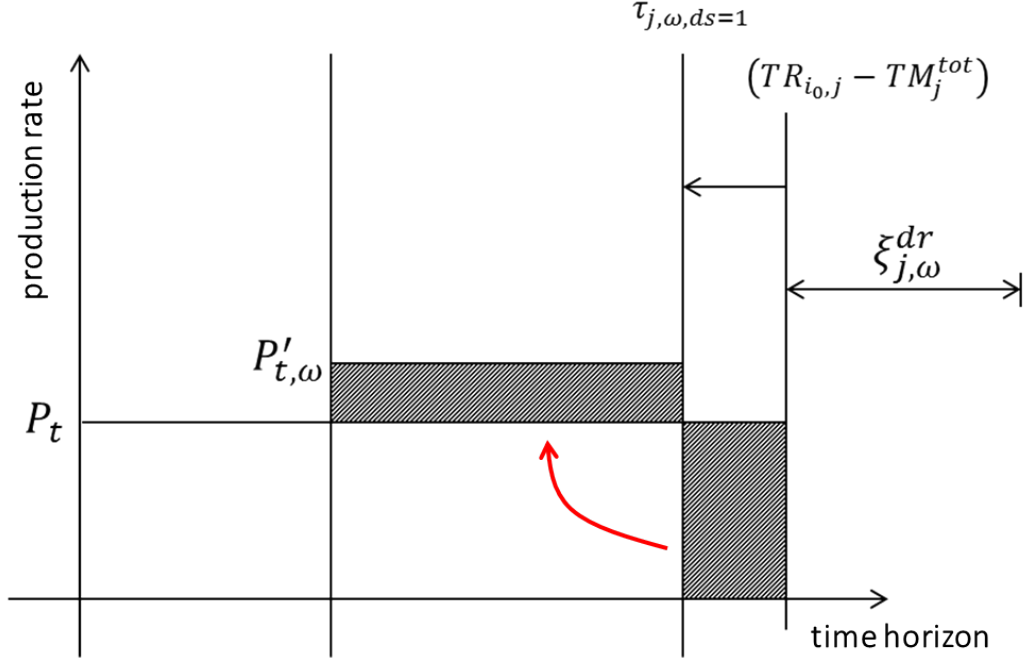


Figure 5.3: Two-stage production-inventory planning strategy

So far, a deterministic production-inventory control constraints set (DPIC) has been explained. The ultimate goal of the proposed mathematical model is to mitigate the impact of random weather disruption in production-inventory planning and LNG carrier routing scheduling problem.

LNG carrier departure time $(TM_j^{tot} - TR_{i_0,j})$ is influenced by random weather disruption timing $\xi_{j,\omega,ds}$. Time t is also replaced to \tilde{t} which is random. Constraint (5.24) is extended to

$$\tilde{\tau}_{j,ds} \sum_{k \in K} \sum_{ds \in DS} x_{i_0,j,k,ds}^{vsl} = \sum_{\tilde{t} \in T} c_{\tilde{t}} ST_{j,\tilde{t}} \forall j \in V_2, \quad c_t = \{1, 2, 3, \dots, t\}, \quad (5.27)$$

$$\text{where } \tilde{\tau}_{j,ds} = (TM_j^{tot} - TR_{i_0,j}) - \tilde{\xi}_{j,ds}.$$

The random value of $\tilde{\tau}_{j,ds}$ needs to be synchronized with the index \tilde{t} . Therefore, constraint (5.28) is approximated by assuming $\tilde{\tau}$ as discrete time point $\tau_{j,\omega,ds}$ with

samples $\omega \in \Omega$ in the following constraint

$$\tau_{j,\omega,ds} \sum_{k \in K} \sum_{ds \in DS} x_{i_0,j,k,ds}^{vsl} = \sum_{t \in T} c_t ST_{j,t,\omega} \forall j \in V_2, \omega \in \Omega, \quad c_t = \{1, 2, 3, \dots, t\}, \quad (5.28)$$

$$\text{where } \tau_{j,\omega,ds} = (TM_j^{tot} - TR_{i_0,j}) - \xi_{j,\omega,ds}.$$

In the same way, a deterministic production-inventory constraint (5.22) is extended as

$$x_{\tilde{t}}^{str} = x_{\tilde{t}-1}^{str} + x_{\tilde{t}}^{prd} + x_{\tilde{t}}^{prd+} - x_{\tilde{t}}^{prd-} - \sum_{j \in V_2} LD_{j,\tilde{t}}, \forall \tilde{t} \in T \quad (5.29)$$

by introducing a second-stage production adjustment variable $x_{\tilde{t}}^{prd+}, x_{\tilde{t}}^{prd-}$ considering random realization of an extreme weather. Its deterministic equivalent constraint is shown as

$$x_{t,\omega}^{str} = x_{t-1,\omega}^{str} + x_t^{prd} + x_{t,\omega}^{prd+} - x_{t,\omega}^{prd-} - \sum_{j \in V_2} LD_{j,t,\omega}, \forall t \in T, \omega \in \Omega. \quad (5.30)$$

Deterministic equivalent form of a stochastic time indicator constraint is formulated as

$$\sum_{t \in T} ST_{j,t,\omega} \leq 1, \forall j \in V_2, \omega \in \Omega. \quad (5.31)$$

For example, $ST_{2,10,1}$ means that a LNG cargo for customer 2 is produced or stored at day 10 according to a weather scenario #1. In the same way, constraint (5.26) is also extended as

$$x_{i_0,j}^{lng} = \sum_{t \in T} LD_{j,t,\omega}, \forall j \in V_2, \omega \in \Omega. \quad (5.32)$$

5.3.4 Decision Maker's Preference Model (DMP)

The TSS model is formulated to maximize the mathematical expectation of profits while minimizing second-stage costs resulted by random weather disruptions. In this section, DMP model is proposed to take a decision maker's preference into account in the planning. Suppose an LNG supplier wants to put more emphasis on 'on-time delivery' rather than 'profit maximization.' Then the priority should be to minimize the NDD caused by a weather disruption. This implies that the overall LNG shipment preparation must be done well before the beginning of any possible storm disruptions. With this in mind, a parametric optimization model is proposed in which the decision maker decides how much risk he/she is willing to take in shipment delay over making optimal profit considering a potential disruption. As shown in **Figure 5.4**, two extreme weather scenarios are considered for the construction of proposed DMP model: i) scenario #1 - the earliest beginning time of an extreme weather $\underline{\xi}_j$ and ii) scenario #2 - the latest ending time of an extreme weather $\overline{\xi}_j$. The number of extreme weather days in the DMP model ξ_j^{pref} is obtained by

$$\xi_j^{pref} = \lceil \lambda \cdot \underline{\xi}_j + (1 - \lambda) \cdot \overline{\xi}_j \rceil, \quad \forall j \in V_2, \omega \in \Omega \quad (5.33)$$

as a convex combination of the two extreme scenarios reflecting a decision maker's preference by a weight parameter λ ($0 \leq \lambda \leq 1$). A risk-averse decision maker may take a large value of λ (closer to 1) to secure a longer shipment preparation time. Then the number of weather disrupted days considered in the DMP is getting closer to scenario #1. As a result, 1) inventory schedule, 2) production schedule and 3) a vessel departure time from a liquefaction plant moves toward the left-hand side in the timeline in **Figure 5.4**. Otherwise, all shipment preparation schedules move toward the right-hand side getting closer to scenario #2.

The decision maker's preference also influences the timing of extreme weathers

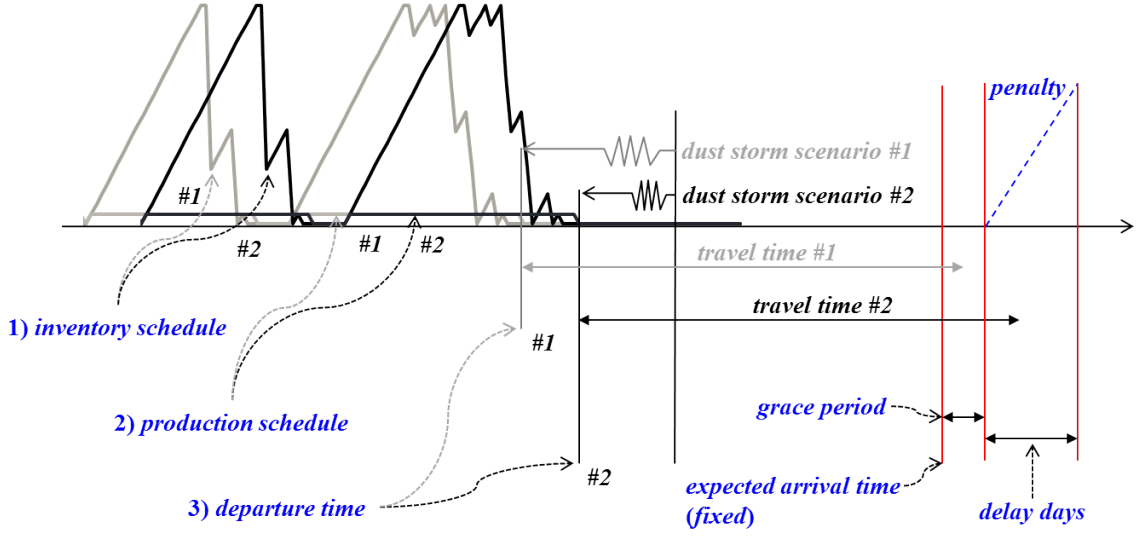


Figure 5.4: An illustrative example of DMP solutions with two extreme weather scenarios: 1) inventory schedule, 2) production schedule and 3) departure time of an LNG vessel

in the daily inventory and production schedule in constraints (5.19). Accordingly, time-synchronization elements in the pre-processing stage expressed in (5.20) is also replaced by

$$t' = t'' - \xi_{j_{a_n}}^{pref} - \sum_{m \in V_2} TR_{a_n}^m, \quad \forall a_n \in A, t', t'' \in T. \quad (5.34)$$

As stated above, the expected objective value (i.e., revenue) of the DMP model is lower than the expectation of the TSS model by considering decision maker's preference on risks. The relations between the expected value of the TSS model EV_{TSS} and the expected result of the DMP model EV_{DMP} can be established by the following **Proposition 5.2**.

Proposition 5.2 $EV_{TSS} \geq EV_{DMP}$.

Proof. Defining that $z(x(\xi_{j,\omega}), \xi_{j,\omega})$ as the objective function of LNG IRP associated with one particular extreme weather duration $\xi_{j,\omega}$. Let $x^*(\xi_{j,\omega})$ and $EV_{TSS} =$

$E_{\xi_{j,\omega}} z(x^*(\xi_{j,\omega}), \xi_{j,\omega})$ be an optimal solution and the expected value of the TSS model, respectively. Let us represent the expected result of the DMP model $EV_{DMP} = z(x(\xi_j^{pref}), \xi_{j,\omega})$ by replacing all random extreme weather durations $\xi_{j,\omega}$ by a deterministic parameter ξ_j^{pref} . For every realization, $\xi_{j,\omega}$, we have the relation $z(x^*(\xi_{j,\omega}), \xi_{j,\omega}) \geq z(x(\xi_j^{pref}), \xi_{j,\omega})$. Taking the expectation of both sides yields the inequality.

5.3.5 Computational Considerations

In this section, two computational techniques are discussed to improve computational performance supposing that an LNG vessel serves less than two regasification plants $\{i, j\} \in V_2$ in a path (assuming $\gamma = 2$). The first approach is a probing-based preprocessing technique which reduces the number of binary variables in the model. This technique eliminates both infeasible and inferior routing options in terms of time window and potential BOG losses in a path. The second one is a logical inequality which replaces MTZ sub-tour elimination constraint. Five routing cases considered in this model are listed in Figure 4.

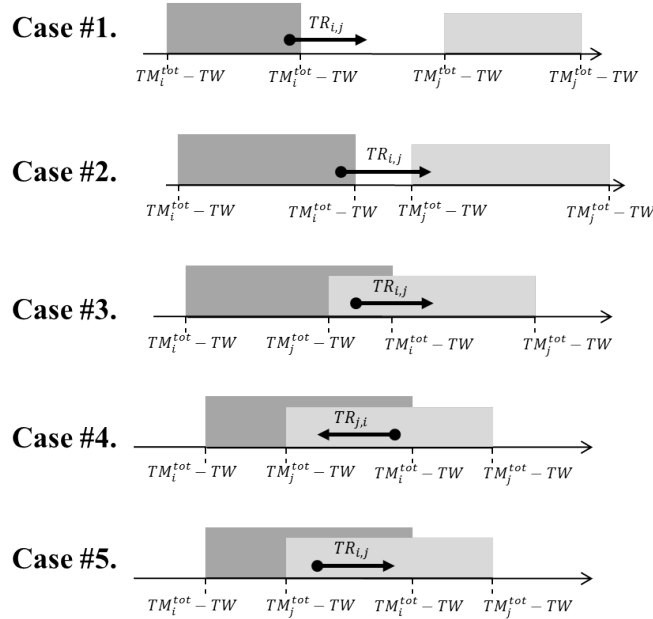


Figure 5.5: Five routing cases

In Case#1, the time gap between two plants are greater than the estimated travel time $TR_{i,j}$. Therefore, this routing option is excluded from the model because it makes unnecessary vessel idle time offshore to meet the scheduled port entry time. The time window gap in Case#2 is less than or equal to the estimated travel time from plant i to plant j . Thus an LNG vessel can travel from plant i to j , but not in the reverse direction. Case#3 shows that two time windows are overlapped and the length of the nested time period is less than or equal to the travel time between two plants. Thus, a vessel also can travel from plant i to j but not in the reverse. In Case#4 and Case#5, the overlapped time duration is greater than or equal to the travel days between two plants. Therefore, an assigned vessel can travel to both directions. However, recalling equation (5.21), it is possible to eliminate one of the two routing options by comparing the amount of BOGs.

We have a simple illustrative example in **Figure 5.6**. If a vessel travels following sequence (A), $i_0 \rightarrow i \rightarrow j \rightarrow i_0$, then $BOG_{(A)} = 0.00125(\%) \cdot \{3,000 \cdot (60,000 + 150,000) + 6,000 \cdot 150,000\} = 19,125(m^3)$, where daily BOR ε is 0.00125(%). If it follows sequence (B), $BOG_{(B)} = 0.00125(\%) \cdot \{7,000 \cdot (60,000 + 150,000) + 6,000 \cdot 60,000\} = 22,875(m^3)$. As a result, it is shown that a routing option (B) is inferior to (A) and should be excluded from a routing option in the optimization model. **Algorithm 1** below provides an overview of the PPT procedure. **Algorithm 1** provides an overview of the proposed probing procedure.

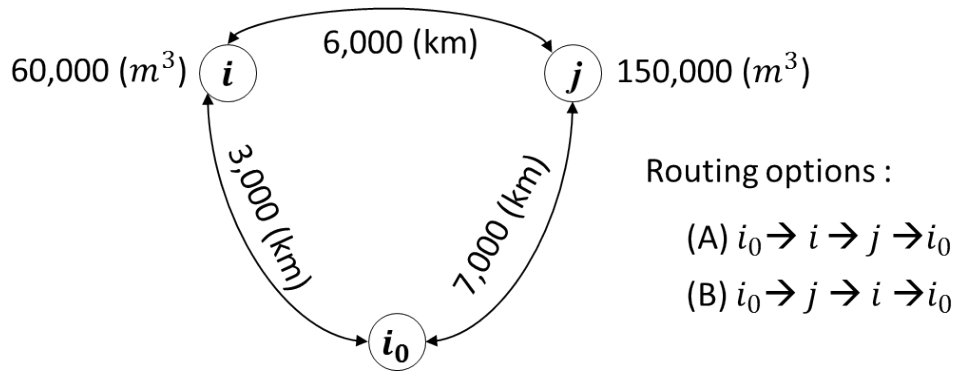


Figure 5.6: An illustrative example of routing options serving two regasification plants

Algorithm 1 Probing procedures: fixing binary variables to either 0 or 1

```

1: for  $(i, j) \in A_2, k \in K$  do
2:   if  $(TM_i^{tot} + TW \leq TM_j^{tot} - TW)$  then
3:     if  $(TM_j^{tot} - TM_i^{tot} - 2 \cdot TW \geq TR_{i,j})$  then
4:        $\sum_{k \in K} x_{i,j,k}^{vsl} = 0$ 
5:        $\sum_{k \in K} x_{j,i,k}^{vsl} = 0$ 
6:     else  $(TM_j^{tot} - TM_i^{tot} - 2 \cdot TW < TR_{i,j})$  then
7:        $\sum_{k \in K} x_{j,i,k}^{vsl} = 0$ 
8:     end if
9:   else if  $(TM_j^{tot} - TM_i^{tot} - 2 \cdot TW \leq TR_{i,j})$  then
10:     $\sum_{k \in K} x_{j,i,k}^{vsl} = 0$ 
11:   else if  $(BOG_{i,j} \leq BOG_{j,i})$  then
12:     $\sum_{k \in K} x_{j,i,k}^{vsl} = 0$ 
13:   else  $\sum_{k \in K} x_{i,j,k}^{vsl} = 0$ 
14:   end if
15:   end if
16: end if
17: end for
  
```

The key advantage of the proposed technique is that there is no need of sequencing process stated by constraint (5.8) because only one routing option is available after the PPT procedure is applied. Thus, a logical inequality

$$2 \sum_{k \in K} x_{i,j,k}^{vsl} \leq \sum_{k \in K} x_{j,i_0,k}^{vsl} + \sum_{k \in K} x_{i_0,i,k}^{vsl}, \quad \forall (i, j) \in A_2 \quad (5.35)$$

can replace constraint (5.8) in the TSS model when when LNG carriers are allowed to serve one or two customers in a path. The resulting model is named as reinforced PPT (rPPT). The logical operation is shown in **Remark 3.2**.

Remark 3.2. Suppose that an assigned LNG vessel departs from a liquefaction plant i_0 and visits two regasification plants i and j in sequence via path $a_n: i_0 \rightarrow i \rightarrow j \rightarrow i_0$ which is the only routing option. Then, $\sum_{k \in K} x_{i,j,k}^{vsl}$ must be equal to 1. If a vessel does not serve i and j together in a path, then $\sum_{k \in K} x_{i,j,k}^{vsl} = 0$.

For the reformulation of production-inventory constraint, in the previous section, a new binary variable $ST_{j,t,\omega}$ is introduced. Maximum number of additional binary

variables is $|j| \times |t| \times |\omega|$. In order to reduce the solution space, probing-based preprocessing algorithm is designed. If a regasification plant becomes an initial destination in a path, then an expected departure time of an LNG carrier can be calculated based on travel time from an origin to the destination. As random weather beginning time put forwards some day, then it needs to be synchronized with $ST_{j,t,\omega}$. Other than the weather disruption period including forecast time period, $ST_{j,t,\omega}$ can be nullified. The procedure is shown in **Algorithm 2**.

Algorithm 2 Probing-based preprocessing: fixing $ST_{j,t,\omega}$ variables to either 0 or 1

```

1: for  $i \in V_2, t \in T, \omega \in \Omega$  do
2:    $sd_{j,t+1} = sd_{j,t} + D_{j,y}$ 
3:   if ( $sd_{j,t+1} > 0$ ) then
4:      $ST_{j,t+ftp,\omega} = 0 : ftp$  (forecast time period)
5:   end if
6: end for

```

5.4 Computational Result

This section presents the computational results of the proposed models. First, an illustrative example and experimental setting details are described. After then, the results is discussed demonstrating computational outcomes and quality of solutions. Particularly, the solutions of DMP model is analyzed to show how decision maker's risk preference is influencing to the planning decisions. Computational performance is evaluated as well. The proposed models are simulated based on the given data below. The major characteristics of this case study are tabulated in **Table 5.1**.

As the impact of a dust storm in the Persian Gulf is considered as a random element, we analyze 10 years' worth of data from 1990 to 1999 provided by Doha International Airport in Qatar. It is identified that dust storms were usually intensive between April and September [92]. Historical data revealed that the variation of dust

Table 5.1: LNG transportation network characteristics

	Data	Unit
Time horizon	D+1 to D+200	days
Total shipping requests	15	times
LNG vessels (Type I / II)	5 / 10	ships
Storage level	[10,220K]	bcm
Production level	[10,10K]	bcm
BOR	0.00125	(%) per day
Barred filling range	<70	(%)
Grace periods	+10	days
Maximum shipping delays	+10	days

storms closely follows the Johnson SB distribution [93]. Hence, random dust storm scenarios are generated accordingly.

Table 5.2: Monthly dust storm days (1990-1999)

	'90	'91	'92	'93	'94	'95	'96	'97	'98	'99	μ_{month}	σ_{month}
JAN	3	0	2	1	2	1	0	0	1	0	1	1.1
FEB	4	6	4	5	6	1	0	5	2	2	3.5	4.5
MAR	7	4	7	6	5	2	4	2	5	6	4.8	3.3
APR	4	9	3	5	2	2	11	5	4	4	4.9	8.5
MAY	9	14	6	9	9	4	1	2	4	10	6.8	16.6
JUN	11	8	11	11	14	10	6	5	7	5	8.8	9.3
JUL	8	7	13	5	14	10	1	12	5	3	7.8	19.3
AUG	6	2	6	2	1	1	0	10	0	1	2.9	11
SEP	1	4	2	0	2	2	1	1	1	3	1.7	1.34
OCT	1	2	1	0	1	1	1	1	1	1	1	0.22
NOV	2	2	3	3	2	4	1	1	0	3	2.1	1.43
DEC	0	1	1	0	3	0	1	1	0	0	0.7	0.9
μ_{year}	4.67	4.92	4.92	3.92	5.08	3.17	2.25	3.75	2.5	3.17		

Johnson SB distributions:

Parameters:

- γ shape parameter $\rightarrow -0.18191$
- δ shape parameter ($\delta > 0$) $\rightarrow 0.4341$
- λ scale parameter ($\lambda > 0$) $\rightarrow 8.3591$
- δ location parameter $\rightarrow 1.837$

Domain:

$$\xi \leq x \leq \xi + \lambda$$

Probability Density Function (PDF):

$$f(x) = \frac{\delta}{\lambda\sqrt{2\pi}z(1-z)} \exp\left(\frac{1}{2}(\gamma + \delta \cdot \ln\left(\frac{z}{1-z}\right))^2\right). \quad (5.36)$$

Cumulative Density Function (CDF):

$$F(x) = \Phi \cdot \left(\gamma + \delta \cdot \ln\left(\frac{z}{1-z}\right) \right) \quad (5.37)$$

where $z \equiv \frac{x - \xi}{\lambda}$, and Φ is the Laplace integral.

CPLEX 12.6 was used to solve the LNG IRP model. However, CPLEX was not able to obtain an optimal solution after 24 hours of computations. Therefore, the solution pools algorithm in CPLEX was used to find a near optimal solution in a fast manner, in which groups of feasible solution candidates are accumulated within a specified gap of optimal solutions. The relative termination tolerance is set at 3% and the time limit is limited up to 24 hours. All following experiments were conducted on a 3.00 GHz Intel Xeon machine with 364 GB of memory.

The computational outcomes are composed of two solution sets. The first set are the routing decisions presented in **Figure 5.8** which include vessel assignments to every path and expected departure and arrival times on plants within the given time horizon.

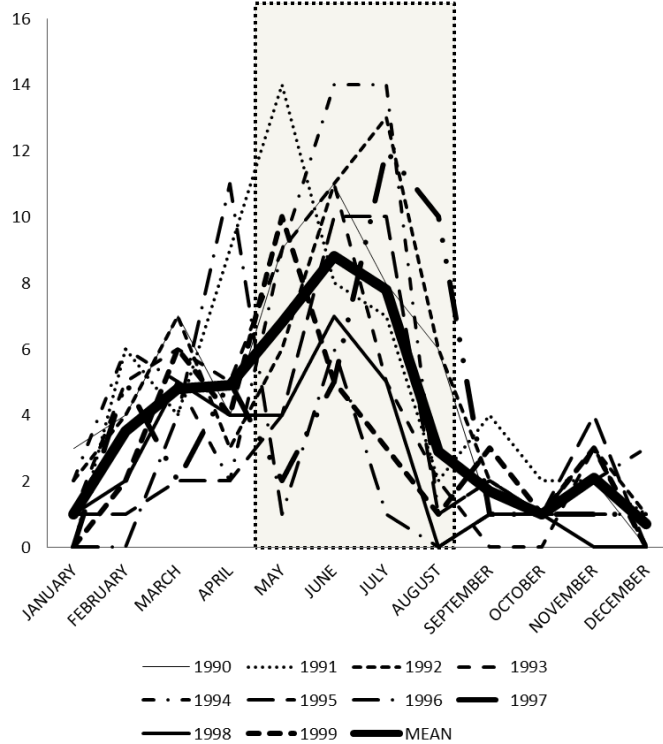


Figure 5.7: Historical records of dust storm in the Persian Gulf (1990-1999)

The second set of the solution is a daily production inventory schedule. The proposed TSS model consists of the first-stage decisions on production inventory schedule and the second-stage decisions on additional production or storage after the realization of disruptions as shown in **Figure 5.9**. In the graph, two things are worth noting here: 1) when dust storms can possibly disrupt LNG operations and 2) how significant the level of disruptions in the time horizon. For instance, when LNG vessel #3 serves plants 16 and 18 and LNG vessel #6 visits plant 5, two vessels are expected to depart from a liquefaction plant from D+106 to D+117. During the period, six different types of LNG shortage scenarios or four types of surplus situations are expected.

While the stochastic model maximizes the expected value of profit, the DMP model reflects a decision maker's preference as a parameter presented in **Figure 5.10**. In this numerical example, when a decision maker is risk averse in order to reduce

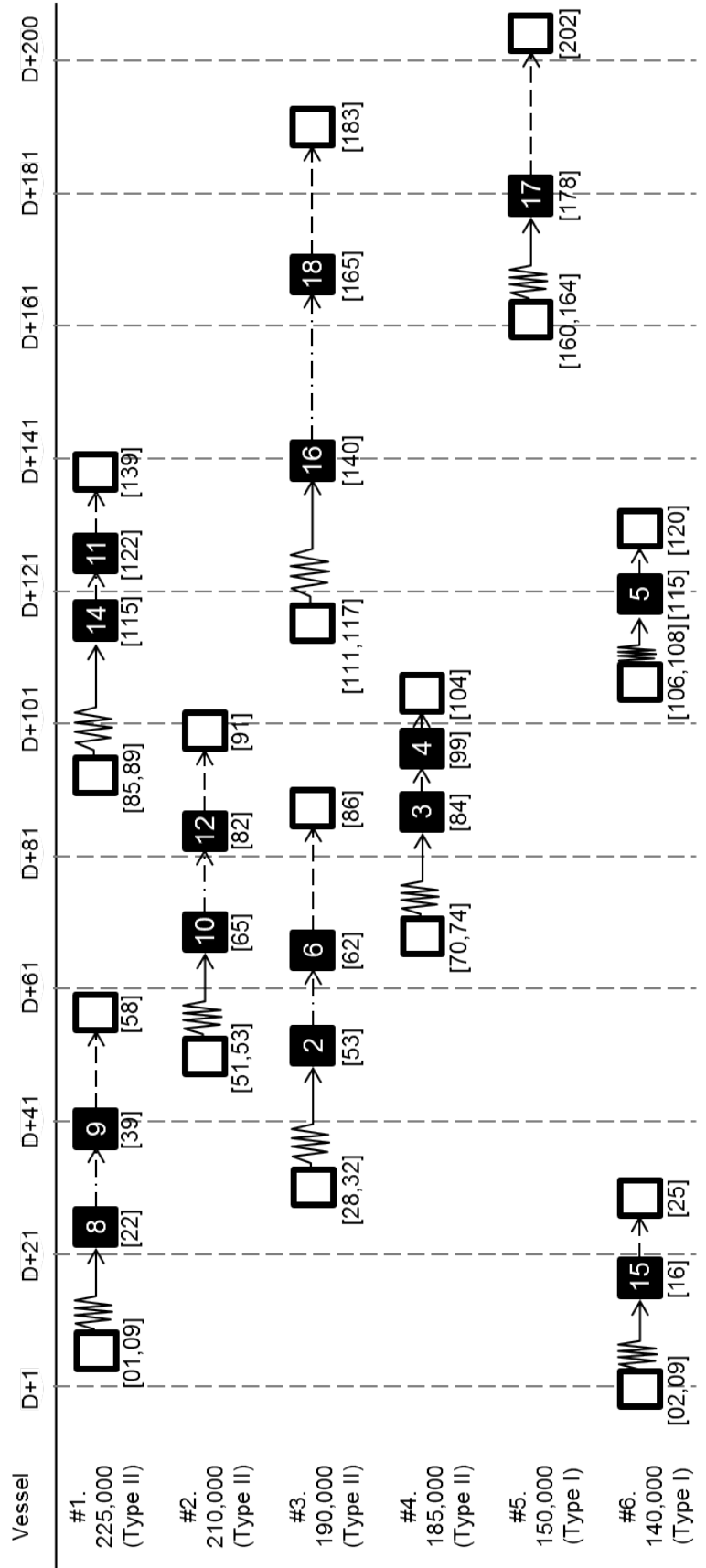


Figure 5.8: A shipping schedule

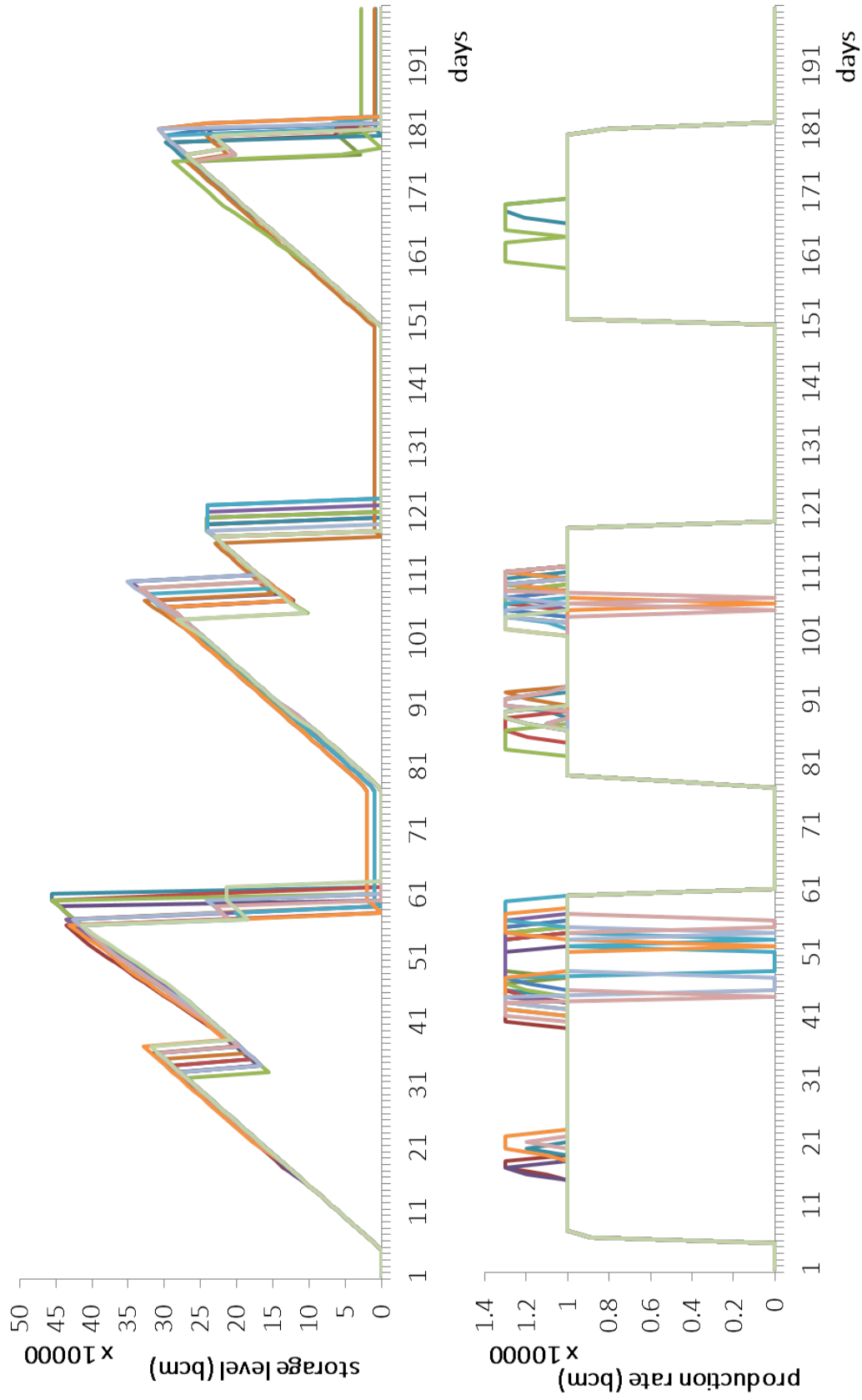


Figure 5.9: Production and inventory schedule considering random weather scenario changes

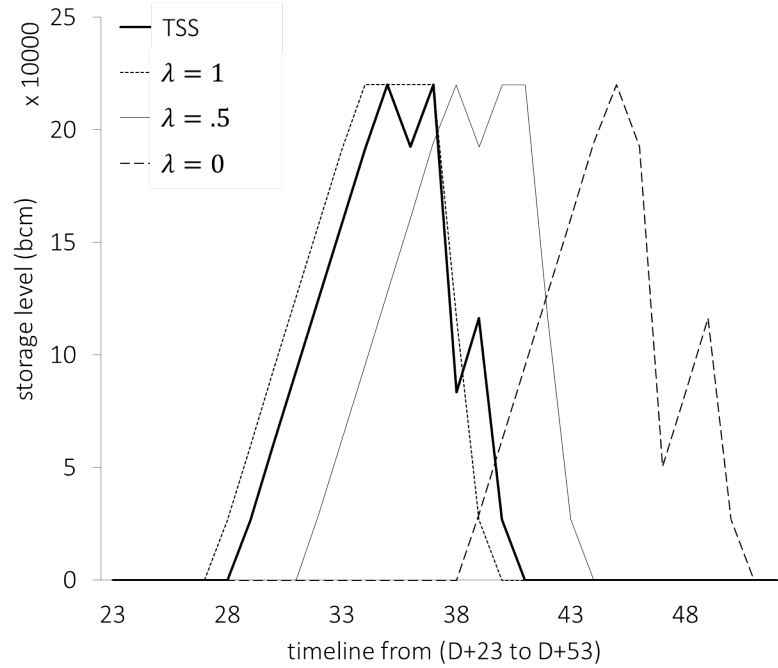


Figure 5.10: Production-inventory schedule by varying the risk preference ratio based on risk preference ratio

NDD ($\lambda \rightarrow 1$), then an ordered LNG stock is ready well before potential dust storm disruptions as the production schedule moves to the left in the graph. Conversely, if a decision maker is risk prone ($\lambda \rightarrow 0$), then the production inventory schedule goes to the right.

Figure 5.11 shows the relationship between the preference ratio and NDD in the DMP model. If $\lambda=0$ (considering the shortest dust storm duration), it is expected to have the least profit because the planned LNG production inventory schedule and a vessel departure time consider the latest ending time of a dust storm which generates the most high value penalty regardless of random dust storm scenarios. When λ becomes 0.1 to 0.5, there is no significant changes in the expected profit but NDD is steadily decreases as λ increases. When λ increases from 0.6 to 1, dust storm scenarios in the early stages influence to the problem generating extended storage costs. There are three remarkable points in this experiment. First, in the worst case ($\lambda = 0$), profit can significantly drop compare to other preference options. Second, when λ is

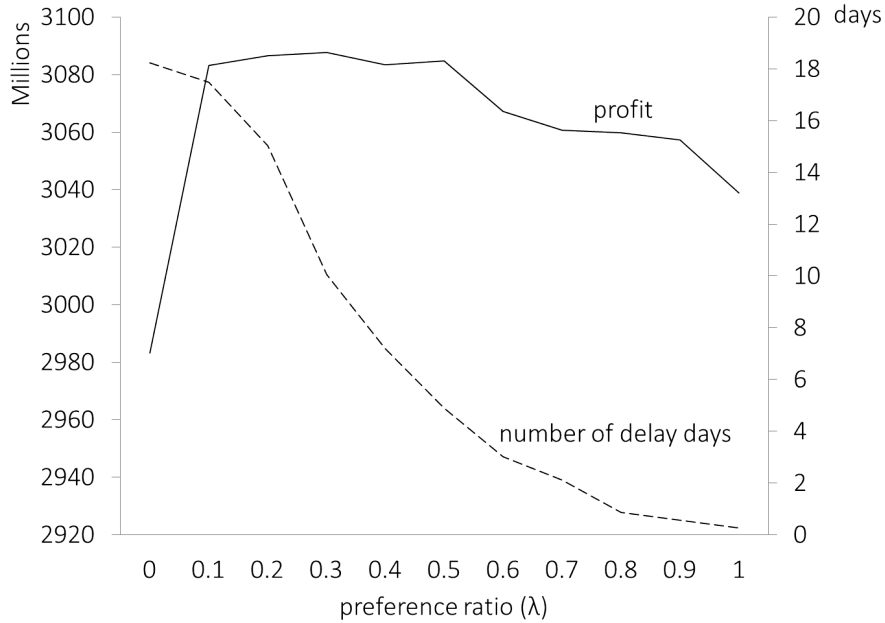


Figure 5.11: Profit and number of delay days changing with preference ratio

in between 0.1 and 0.5, if profits are in an acceptable range, then choosing $\lambda = 0.5$ yields reasonable solution because the NDD are decreasing from 17 to 5 days. As a result, this what-if analysis can help a decision maker to choose a preferred LNG supply operations plan.

A finite number of scenarios are used to solve the deterministic equivalent TSS model. There is a trade-off between the number of scenarios used and the corresponding computation time. As there are more scenarios used in the model, the accuracy of estimating the recourse function improves. However, using more scenarios comes at the cost of longer computation time. Therefore, sensitivity analysis has been conducted by varying the number of scenarios to find where it converges to. As shown in **Figure 5.12**, the objective value (expected profit) is converging to around 3080 million (\$USD) as the scenario size increases.

A probing-based preprocessing technique is applied to the TSS model as shown in **Figure 5.14**. The number of binary variables increases as the size of time window expands. When PPT is applied, the total number of binary variables has reduced

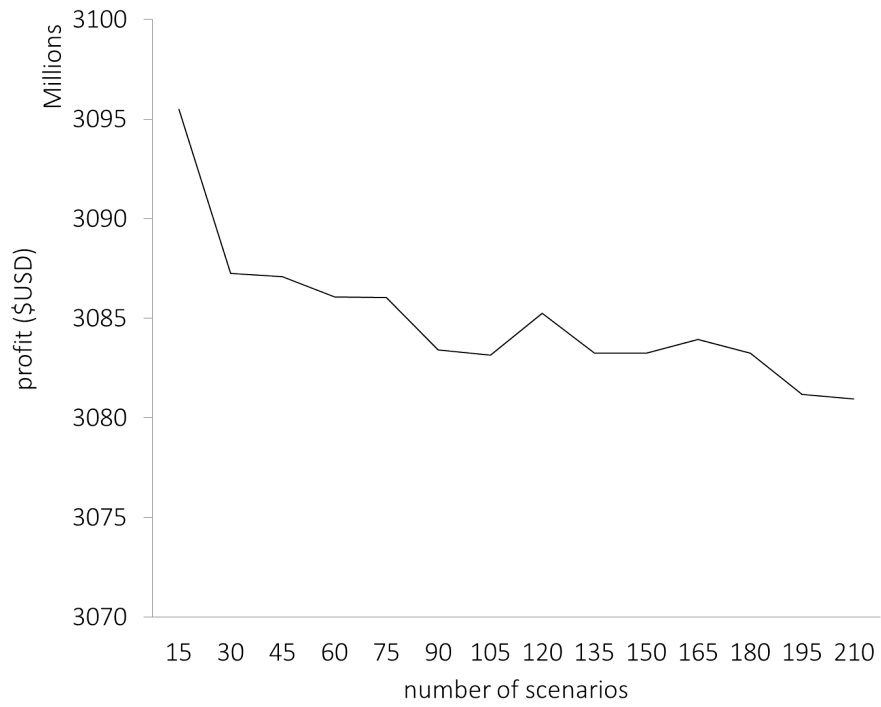


Figure 5.12: Expected profit of TSS model per scenario

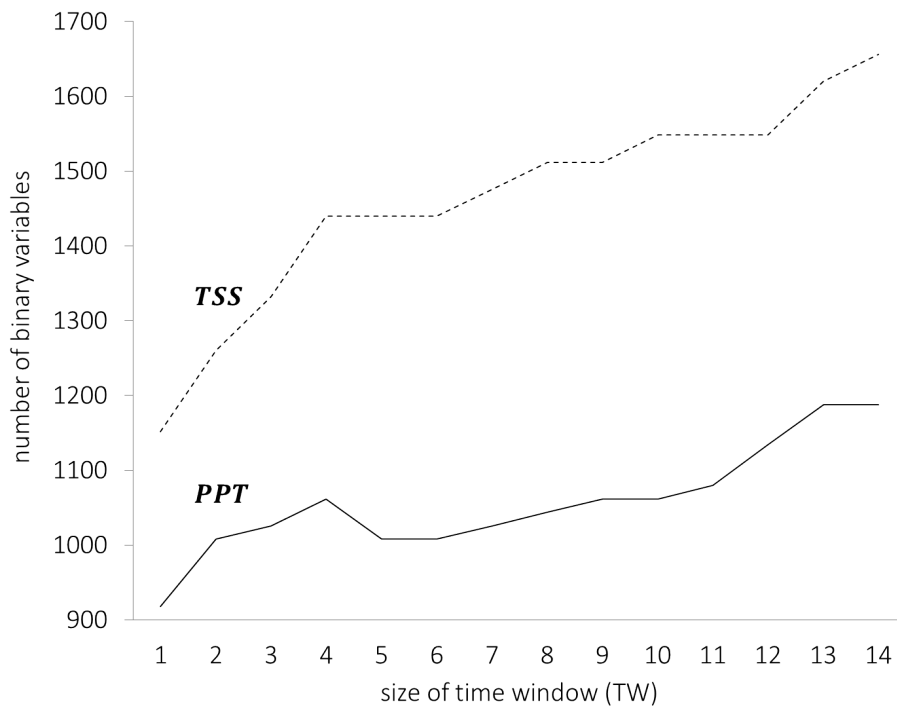


Figure 5.13: Number of binary variables of TSS model and PPT model

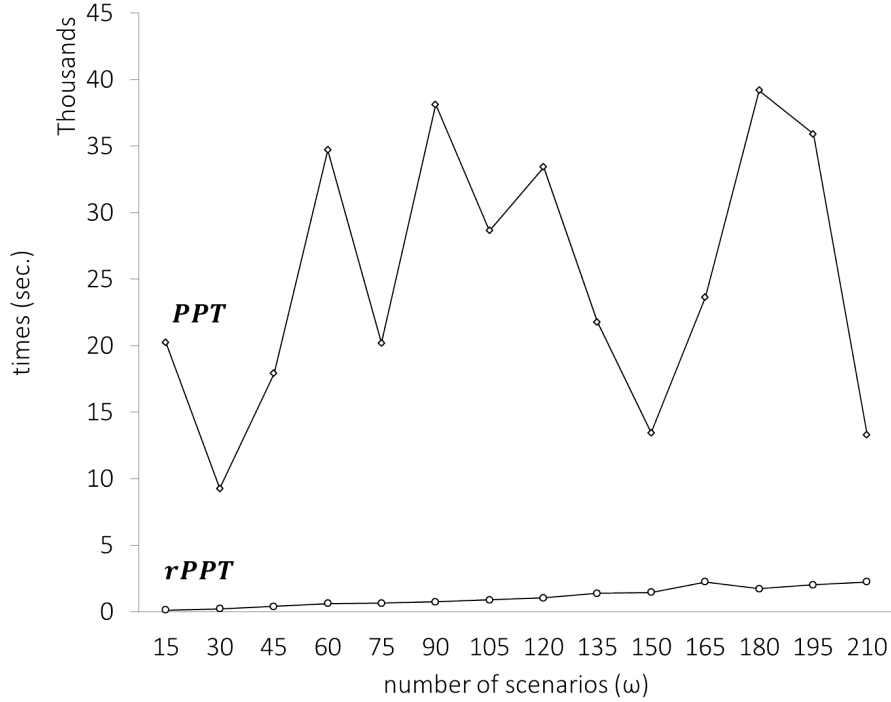


Figure 5.14: Computational time changes per number of scenarios

compared to TSS. For example, when $\beta = 1$, the number of binary variable gap between TSS and PPT is 234 (20.3%); but if β becomes 10, the reduction becomes larger at 486 (30.23%).

Experiments were made to compare computational performance of TSS, PPT and rPPT. Both PPT and rPPT were able to find a solution while the TSS model failed to solve the test problem regardless of the scenario size tried. As Figure 12 shows, there was a positive correlation between computation time and scenario size for rPPT. Furthermore, there was a considerable computational performance gain using rPPT when compared to PPT. This shows a clear advantage of using the proposed logical inequality (rPPT).

5.5 Conclusion

In this chapter, two LNG IRP models are proposed to generate optimal routing decisions and production inventory schedules that satisfy multiple demands in a

path under weather disruptions. The proposed TSS model aimed to maximize the expected profit utilizing weather information derived from historical data. Since the TSS model has a very complex stochastic MIP structure, neither CPLEX solver nor a solution pools algorithm solves the problem. However, the proposed probing-based preprocessing technique was successful at reducing the number of binary variables up to 32% utilizing the time windows relations and BOG amount comparisons. Furthermore, by replacing MTZ constraint by the suggested logical inequality (5.35), it is verified that a very stable and efficient computational performance. The DMP as a parametric model reflects a decision maker's preference such as shipping reliability for weather disruptions. Therefore the DMP also can be considered as a rational decision supporting methodology comparing to the TSS model. By extending this research, we can consider other LNG IRP models with multiple liquefaction plants under various uncertainties that can cooperatively respond to potential disruptions in the supply chain.

Chapter 6

Multiple Autonomous Underwater Vehicle Pre-positioning and Routing for Offshore Pipeline Damage Assessment

6.1 Introduction

In August and September 2005, hurricanes Katrina and Rita overwhelmed southern United States and paralyzed both onshore and offshore oil and gas infrastructures. Damage assessment had been performed focusing on offshore pipeline systems in the Gulf of Mexico in the passage of two Hurricanes. As a result of the damage assessment, more than 600 pipeline damages were reported [24]. It is assessed that the majority of the reported damages occurred at or near platform interfaces, or resulted by the impact of an outside force other than the direct hurricane impact, such as platform failures, riser damages or anchor dragging. The remaining portion of damages was due to loss of cover and movement of pipelines that are near shore and in shallow water. However, due to the incomplete data, it was not easy to determine what the actual root causes of pipeline failures were, and what actual events occurred during the hurricanes.

In order to investigate subsea pipeline networks, divers or unmanned underwater vehicles (UUVs) can acquire damage information. UUV-aided damage assessment is faster and free from safety accidents comparing with divers' inspection [94, 95].

UUV is named in various ways. In US Navy, UUV is named as unmanned undersea vehicle as the military focus is only in the sea. UUV is usually categorized as remotely operated vehicle (ROV), autonomous underwater vehicles (AUV), and remotely towed vehicles (ROTV) [96]. Major focus of this dissertation is AUV. AUV is

vessel that can travel underwater without an operator on its own power source. AUV is used for surveillance and reconnaissance, mine countermeasures, anti-submarine warfare, mapping of the ocean floor, testing water samples, polar ice research, and pipeline inspection. As AUV has its own power source and does not require operator's involvement, AUV is replacing ROV [97]. AUV products are divided into three categories: 200 meters + depth of water (30% of the market), up to 200 meters depth of water (40%), up to 30 meters of water (30%) [26].

In order to overcome complicated hazardous environments and to perform a successful mission in which the AUV travels to the designated targets without operator intervention, it is very important to achieve a high degree of autonomy, reliability and robustness. Particularly, it is critical to develop an efficient path generation algorithm for AUVs.

Path planning is an important task necessary in the application of AUVs, which is to search out an optimal or sub-optimal path between an initial position and the desired target under specific constraint conditions. As one of the key research topics for AUVs, path planning is a necessary and fundamental element of AUVs and makes the vehicle fully autonomous and reliable. Its goal is to plan a sequence of suitable paths subjected to some optimization criteria that allows the vehicle to complete its task objectives by reaching the specified destination point from the starting location.

Path planning is inherently a routing process to find an optimal path selecting nodes and arcs to complete a given mission. There are two types of path generation techniques: global path generation and local path generation depending on information availability [50]. In this dissertation, global path planning is the focus of the research.

Path generation algorithms for AUVs have been constantly developed and improved in many ways. Artificial potential fields based path generation algorithm was

introduced. This algorithm generated an optimal solution with entire network information on two- and three-dimensional problems [51]. D* and A* algorithms have been introduced [52]. In particular, A* considers bathymetry, exclusion zone, obstacle, and ocean current data bases to facilitate planning [53]. A* is practiced in Western Mediterranean Sea by varying operational conditions [54]. The performance of A* is proved by comparing with four other algorithms: breadth first search, depth first search, and Dijkstra's and wall following algorithms. It has been observed that A* and Dijkstra's algorithm outperformed to the others. A continuous form of A* algorithm which is named as FM* is developed [55]. This algorithm generates paths continuously by updating perceived environmental information.

Mathematical optimization based approaches have been developed either in mixed integer linear programming (MILP) or nonlinear programming. Multi-beam forward looking sonar aided real-time obstacle avoidance and path planning algorithm is developed. This is a nonlinear programming model which generates path while minimizing the Euclidean distance to the goal [56]. Genetic algorithm is proposed which minimizes the energy cost considering the variability of the environment. This model generated an optimum path to cross the Sicily channel which has strong current fields and complex [57]. MILP-based path generation algorithm for adaptive sampling is presented. This algorithm aims to maximize the line integral of the uncertainty of field estimate along the generated path. This model considers to optimize multiple AUV paths based on a supporting ship [58]. Sensor-driven online coverage planning for AUVs is formulated as a multi-objective optimization model [59]. Three-dimensional path planning technique is suggested and solved by multi-objective optimization algorithm. This model considers four criteria: total length of path, margin of safety, smoothness of the planar motion, and gradient of diving [60].

As real-time obstacle avoidance and path generation is an important research area, various algorithms have been developed. In the early stage of the research in

real-time path planning and obstacle avoidance is designed to conduct two real-times missions: pre-deployment survey of sea bottom and visual inspection of pipelines [61]. Morse-based boustrophedon decomposition coverage path-planning algorithm for 3D coverage and STOMP algorithm is used for real-time path re-planning [62]. Informative path planning is suggested which has used for surface vehicles. This model generates paths while maximizing mutual information [63].

In another approach, two risk-aware path planning techniques - minimum expected risk planner and risk-aware Markov decision process - are proposed from the perspective of safety and reliability of AUV operations [64]. Case-based path planning is presented. This algorithm retrieves a matching route from the DV and modifies it to suit to the current situation. If there is no matching route, then it generates a new routes based on past cases which have similar navigational environments [65]. Hybrid route-path planning model is developed which utilizes task assign-route planning and path planning based on differential evolution and firefly optimization algorithms [66]. Multiple AUVs task assignment and path planning have been studied considering variable ocean current. The goal of this model is to reach all designated target nodes [67]. In many AUV path generation problems, two criteria can be considered to select a preferred path generation algorithm: length of the path and computational time. By properly combining of two criteria in an objective function of a path planning model, an optimal solution can be obtained [68].

There has been an increasing trend of research on unmanned vehicle applications. Considerable body of work on a large number of AUVs has been done including topics such as coordination between multiple unmanned vehicle (UV) operators [69], future position prediction [70], traffic flow optimization [71, 72], and routing optimizations [73, 74]. Especially, mathematical optimization models for multiple UV task assignment and path planning have studied considering technical specifications and operational constraints including mission types, time limits, and no fly

zones [75, 76, 77, 78, 79]. This problem has the structure of multiple vehicles routing problem, and is tried to be solved by either exact or approximation algorithms [80, 81, 82, 27]

This proposed study in this chapter covers the AUV utilized offshore natural gas pipeline network damage assessment problem. Within this scope, the proposed concept is to utilize multiple AUVs not only to collect data how an extreme weather event influences to subsea pipeline network but also to accelerate the inspection speed considering the random realization of an extreme weather event. The literature review reveals that no mathematical model been specifically developed to employ a fleet of AUVs for offshore pipeline damage assessment considering uncertainty in weather forecast even though a relatively large volume of research has been conducted in the area of a single AUV inspection. Therefore, a new mathematical framework is proposed in this chapter to find optimal pre-positioning locations and paths for multiple AUVs to cover the whole target nodes and edges considering uncertainty in the weather information. The contributions of the research are listed as follow:

- A new offshore pipeline damage assessment concept and procedure is developed to minimize overall inspection time and cost. The proposed approach begins by positioning a certain number of AUVs in pre-determined nodes over the weather impact zone before an expected event. After the extreme event, pre-placed AUVs maneuver over the network in accordance with the optimized scanning paths.
- A two-phase mathematical optimization model is proposed for multi-AUV pre-positioning and routing (MAUV). In phase 1 (MAUV-ph1), the optimum AUV positions are found. The MAUV-ph1 is formulated as a two-stage stochastic integer program, where the first stage decision assigns each AUV position and the second stage augments additional AUV positions in accordance with updated

weather forecast. In phase 2 (MAUV-ph2), AUV scanning paths are generated while minimizing AUV operating cost and inspection completion time.

- Computational techniques have been suggested, including constraints reformulation, probing-based pre-processing techniques, logical inequality, and Lagrangian method, to enhance the computational performance.

The rest of the chapter is organized as follows. Section 6.2 describes the problem of pipeline network damage assessment using multiple AUVs. Section 6.3 presents the mathematical formulations for MAUV and computational considerations. Section 6.4 discusses computational results. The chapter is concluded with discussions of opportunities for extensions of the proposed work in Section 6.5.

6.2 Problem Statement and Model Outline

The MAUV problem objective is to provide optimal positions of AUVs and their associated maneuvering paths for an expedited damage assessment. Operating AUVs must be able to scan all designated target nodes and edges while minimizing completion time and total cost for multiple AUVs mobilization.

Figure 6.1 presents a pipeline network damage assessment planning procedure over a planning horizon. If we consider that AUVs are prepositioned closer to a potential impact area before an extreme event impacts the region, damage assessment can be expedited as pre-deployed AUVs immediately collect and transmit the assessment information as soon as the event is cleared. Consequently, a fast recovery plan can be developed and its implementation will be accelerated. Therefore, the first phase starts by determining AUVs pre-deployment locations among multiple candidates to cover all target facilities while minimizing the number of AUV positions and the associated cost. As new technologies enable more precise forecast of extreme events, a better prediction of the impact due to such an event can be made as the arrival time

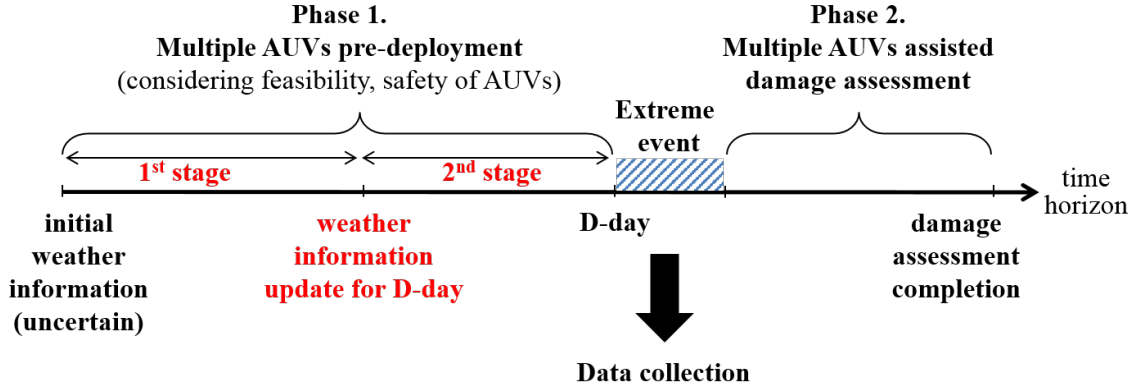


Figure 6.1: Offshore pipeline network damage assessment over a planning horizon

of the event becomes closer. If AUV positions are determined only after accurate event information is available, AUVs can be placed just around the perimeter of the impending event impact area; hence, it can greatly help assess damage soon after the disaster. However, it is likely that there may not be enough time to complete AUV positioning if it delays too long because the limited number of supporting vessels and human resources may not complete AUS pre-deployment activities before the beginning of an extreme weather. On the other hand, if AUV are positioning well in advance, the variance of the forecast error can be high. As a result, some prepositioned AUV locations can be far out of the event impact zone or can be damaged by the harsh weather.

The goal in this research is to address these issues by decomposing the problem into two stages. In the first stage, AUV pre-positioning locations are selected anticipating an arrival of an extreme event. In the second stage, the AUV locations are adjusted, if necessary, when the arrival time of the predicted extreme event becomes closer with updated weather forecast. The second phase determines the optimal number of AUVs to use and generate optimal AUV paths to complete damage assessment in minimal time. It aims to have a condition that no on-site crews are required for the mission. Thus, the objective of MAUV-ph2 is to minimize the AUV operating cost only. For the path planning, every path has to follow five requirements: i) AUV

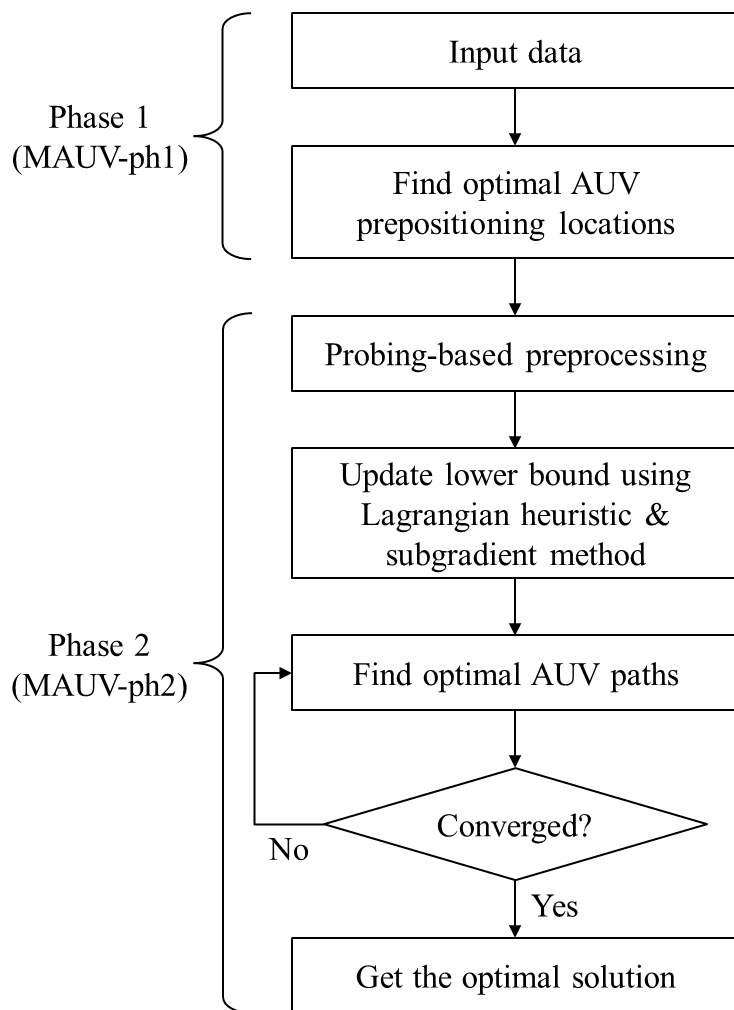


Figure 6.2: Flowchart of MAUV model optimization

traverses directly from depot to any accessible target node; ii) Each target node and edge is scanned only once but can be visited multiple times to pass through; iii) AUV returns either to the original position or any other depot locations, iv) Every indexed AUV conducts a single mission, and v) AUV returns to any of AUV positions off the pipeline.

Figure 6.2 depicts the flowchart of the proposed two-phase optimization of MAUV problem. The Phase 1 problem is formulated as a two-stage stochastic integer program whose goal is to determine AUV pre-positioning locations. Input data to the model include AUV maximum operating time, facility durability scale, and extreme weather impact scale which is random. The Phase 2 problem generates AUV

paths for post-disaster damage assessment. Once AUV location information is given to MAUV-ph2, a probing-based preprocessing method eliminates infeasible edges considering AUV maneuvering capacity, and calculates upper bounds for target coverage constraint. A Lagrangian heuristic and a subgradient method [98] are applied to obtain a tight lower bound on the objective value of MAUV-ph2.

6.3 Mathematical Formulation

6.3.1 Sets, Elements, Data and Variables

Sets:

$G(V, E)$	Directed network with nodes V and edges E
V	Set of nodes $V = \{1, 2, 3, \dots, i\}$
V_1	Set of target nodes where $V_1 \subseteq V$
V_2	Set of AUV pre-positioning candidate nodes where $V_2 \subseteq V$ and $V_1 \cap V_2 = \emptyset$
V_{21}	Set of AUV pre-positioning candidate nodes connected to edge(s) in a network where $V_{21} \subseteq V_2$
V_{22}	Set of AUV pre-positioning candidate nodes where $V_{22} \subseteq V_2$ and $V_{21} \cap V_{22} = \emptyset$
V'	Set of selected AUV pre-positioning nodes where $V' \subseteq V_2$
V''	Set of revised target nodes for phase 2 where $V'' = V_1 \cup (V_{21} - V_r)$
E	Set of edges $E = \{\{i, j\} : i, j \in V'', i \neq j\}$
E_1	Set of initial routes from an AUV prepositioned node to a target node $E_1 = \{\{i, j\} : i \in V', j \in V''\}$ where $E_1 \subseteq E$

E_2	Set of intermediate routes from a target node to another target node $E_2 = \{\{i, j\} : i, j \in V''\}$ where $E_2 \subseteq E$ and $E_1 \cap E_2 = \emptyset$
E_3	Set of returning routes from a scanning node to a recovery node $E_3 = \{\{i, j\} : i \in V'', j \in V'\}$ where $E_3 \subseteq E$ and $E_1 \cap E_2 \cap E_3 = \emptyset$ and $E_1 \cup E_2 \cup E_3 = E$
K	Set of AUVs $K = \{1, 2, 3, \dots, k\}$;
Ω	Set of sample scenarios of extreme events $\omega \in \Omega$

Data:

c_i	Unit setup cost for AUV pre-positioning at node $i \in V_2$ in the first stage
c_i^+	Unit setup cost for AUV pre-positioning at node $i \in V_2$ in the second stage
\bar{c}_p	Maximum number of AUV pre-positioning nodes that can be installed in the second stage
$a_{i,j,\omega}$	Weather impact indicator. 1 if an edge $(i, j) \in E$ is included in weather impact zone in accordance with a scenario $\omega \in \Omega$, 0 otherwise.
$d_{i,j}$	Travel time (min.) of AUV over edge $(i, j) \in E$
P_k	Unit operating cost of AUV k
B_k	Maximum operating time (min.) of AUV k
ST_j	Node scanning time at $j \in V''$
N	Maximum number of scanning nodes in a path
y_i	Pre-positioning indicator. 1 if AUV pre-positioning node $i \in V'$ is selected and 0 otherwise

$x_{i,j,k}$	Edge scanning indicator. 1 if AUV k is traversed over an edge $E(i, j)$ and 0 otherwise
h_k	AUV mobilization indicator. 1 if AUV k is mobilized and 0 otherwise

Decision Variables:

$ad_{i,\omega}^+$	Pre-deployment selection indicator. 1 if AUV pre-deployment node i is added in the second stage according to a scenario $\omega \in \Omega$ and 0 otherwise
$drb_{i,j}$	Durability scale [0,1] of pipeline over an edge $(i, j) \in E$
wx_ω	Impact scale [0,1] of an extreme event according to a scenario $\omega \in \Omega$

6.3.2 Phase 1: AUV Pre-positioning (MAUV-ph1)

Phase 1 model decides which AUV pre-positioning locations are to setup so as to assess all target nodes and edges while minimizing the sum of the AUV pre-positioning setup costs and considering weather forecast uncertainty. MAUV-ph1 is formulated as a two-stage stochastic program. MAUV-ph1 formulation is as follows.

The objective function is defined as

$$\min \sum_{i \in V_2} c_i y_i + \mathbb{E}_P \left[\sum_{i \in V_2} c_i^+ ad_{i,\omega}^+ \right] \tag{6.1}$$

to minimize the overall cost for pre-positioning AUVs. The first term is the sum of fixed costs for AUV position setup in the first stage. The second term is the sum of expected cost for additional AUV position setups in the second stage considering uncertain weather information. Due to the stochastic property of weather

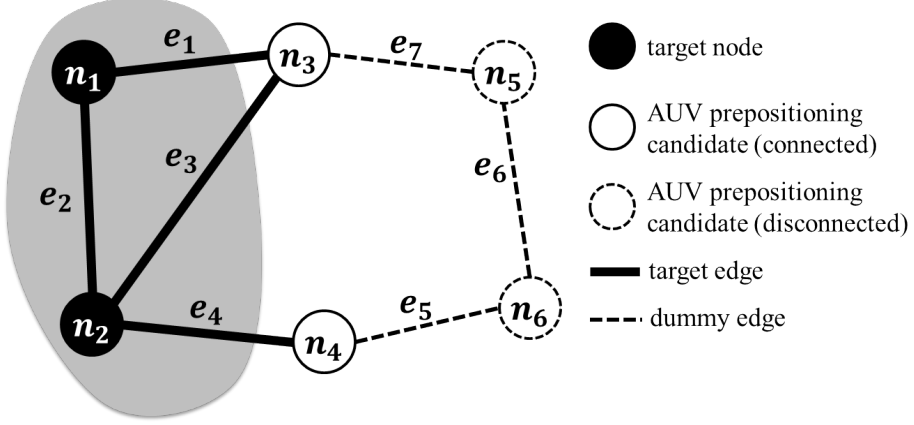


Figure 6.3: An illustrative example of offshore pipeline network

information, solving MAUV-ph1 is computationally challenging. Therefore, scenarios $\omega^1, \dots, \omega^N \sim P$ are generated by Monte Carlo sampling technique and approximated the solution by replacing the expectations that appear in the objective function $\mathbb{E}_P \left[\sum_{i \in V_2} c_i^+ ad_{i,\omega}^+ \right]$ with the corresponding sample average $\frac{1}{|\Omega|} \sum_{i \in V_2} \sum_{\omega \in \Omega} c_i^+ ad_{i,\omega}^+$.

A target edge must be covered by at least one AUV pre-positioning location regardless of the uncertain weather condition, and is constrained as

$$\sum_{i:(i,j) \in E_1} a_{i,j,\omega} (y_i + ad_{i,\omega}^+) \geq 1, \quad \forall j \in V_2, \omega \in \Omega. \quad (6.2)$$

The value of $a_{i,j,\omega}$ in (6.2) is determined based on two criteria: First, every network bus $j \in V_2$ must be covered by at least one AUV. After that the AUV must be able to return to a depot after completing the damage assessment task. This means that the total maneuvering distance from an AUV pre-positioning location $i \in V_1$ to any returning position $l \in V_2$ via a target node $j \in V_2$ should be less than or equal to the maximum maneuvering distance of AUV $k \in K$. Second, uncertain weather conditions need to be considered in addition to the first criterion. For instance, if the impact of the extreme weather wx_ω is higher than the impact of durability of pipeline $drb_{i,j}$ over an edge $(i,j) \in E_1$, then the edge is included in a target network as $a_{i,j,\omega}$ becomes 1, and 0 otherwise. The determination of $a_{i,j,\omega}$ is described in **Algorithm**

3.

Algorithm 3 Determination of $a_{i,j,\omega}$

```

1: for  $(i, j) \in E_1, (j, l) \in E_3, \omega \in \Omega$  do
2:   if  $\{(d_{i,j} + \min\{d_{j,l}\} \leq B_k) \text{ and } (drb_{i,j} \leq wx_\omega)\}$  then
3:      $a_{i,j,\omega} = 1$ 
4:   else
5:      $a_{i,j,\omega} = 0$ 
6:   end if
7: end for

```

Any chosen pre-positioning location is set up either in the first stage or in the second stage and is defined as

$$y_i + ad_{i,\omega}^+ \leq 1, \quad \forall i \in V_1, \omega \in \Omega. \quad (6.3)$$

It limits the maximum number of AUV positions in the second stage considering availability of resources for the tasks and is formulated as

$$\sum_{i \in V_1} ad_{i,\omega}^+ \leq \bar{c}p, \quad \forall \omega \in \Omega. \quad (6.4)$$

After the selection of AUV pre-positioning locations by MAUV-ph1, the remaining nodes are re-labeled as dummy nodes for AUV paths generation in MAUV-ph2. For example, if n_4 is not selected as a pre-positioning location, then a target edge e_4 cannot be scanned by any AUV. Therefore, if there is an unselected element $i \in (V_{21} - V')$, then this point is put as a dummy node in Phase 2. The revised set of target nodes including dummy nodes is defined as $V'' = V_1 \cup (V_{21} - V')$.

6.3.3 Phase 2: AUV Path Generation (MAUV-ph2)

Based on the AUV preposition decision from Phase 1, Phase 2 determines optimal paths for deployed AUVs to assess the target network so as to minimize the sum

of AUV operating costs. AUV $k \in K$ starts and ends assessment from/to locations $i \in V'$ conducting damage assessment through the traverse edge E .

In MAUV-ph2, the objective function is expressed as

$$\min \sum_{k \in K} P_k h_k \quad (6.5)$$

to minimize the sum of AUV operating costs P_k which are proportional to the number of AUVs. AUV allocation for any damage assessment mission is indicated by

$$\sum_{(i,j) \in E_1} x_{i,j,k} \leq h_k, \quad \forall k \in K. \quad (6.6)$$

Each AUV must cover at least one target node in the network and is defined as

$$\sum_{i:(i,j) \in E_1 \setminus E_3} x_{i,j,k} \geq 1, \quad \forall j \in V''. \quad (6.7)$$

Flow conservation of AUVs is controlled by the following two constraints:

$$\sum_{(i,j) \in E_1} x_{i,j,k} = \sum_{(j,i) \in E_3} x_{j,i,k}, \quad \forall k \in K \quad (6.8)$$

and

$$\sum_{i:(i,u) \in E \setminus E_3} x_{i,u,k} = \sum_{j:(u,j) \in E \setminus E_3} x_{u,j,k}, \quad \forall u \in V'', k \in K. \quad (6.9)$$

The total number of AUVs departing from any AUV positions is the same as the number of returning AUVs in (6.8), and flow-in equals flow-out for any target nodes in (6.9). Any target edge E_2 must be assessed at least once by a maneuvering AUV either from i to j or the opposite, and described as

$$\sum_{k \in K} (x_{i,j,k} + x_{j,i,k}) \geq 1, \quad \forall (i,j) \in E_2. \quad (6.10)$$

Every AUV operating path, including maneuvering time over a pipeline and inspection on a specific node, must be bounded by its maximum operating time, and is defined as

$$\sum_{(i,j) \in E} (d_{i,j} + ST_j)x_{i,j,k} \leq B_k, \quad \forall k \in K. \quad (6.11)$$

Sub-tours are eliminated to make a complete operating path using MTZ sub-tour elimination constraints and is formulated as

$$u_i - u_j + (|V''| + 1)x_{i,j,k} \leq |V''|, \quad \forall (i, j) \in E_2, k \in K. \quad (6.12)$$

6.3.4 Computational Considerations

The MAUV-ph2 has a framework of multiple vehicle routing problem which is classified as an NP-hard problem [99]. For the practical large-scale instances, it is very difficult to obtain the optimal solution. Therefore, in this section, four computational techniques are discussed to improve computational performance of MAUV-ph2.

The first technique is to reformulate maneuvering time constraint (6.11) to reduce the number of redundant constraints. The second one is to tighten the solution space using constraint (6.7). In the third approach, a preprocessing algorithm is proposed to fix the values of some binary variables considering operational feasibility under the given technical specifications, and to generate coefficients for the two revised constraints. Lastly, a Lagrangian relaxation method is developed to obtain a tighter dual (i.e., lower) bound on the objective function of MAUV-ph2.

1) Option 1: reformulation of operation time constraint If any AUV is not assigned for damage assessment, then there is no need to check whether the AUV can complete a maneuver within the maximum operation time as stated in constraint (6.11). In this case, the left-hand-side of (6.11) is 0, but the right-hand-side remains at a constant value. Therefore, by replacing B_k to $B_k h_k$ in (6.13), right-hand-side can

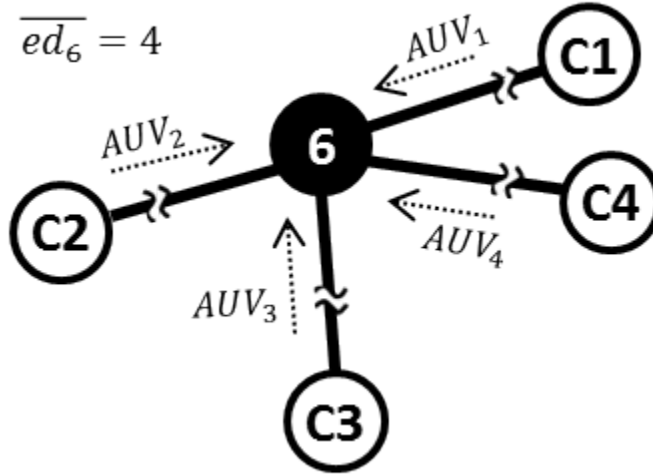


Figure 6.4: An illustrative example of maximum number of AUVs passing a node

only have a positive value only if an AUV is assigned to a task. Otherwise, the value is 0 since h_k is 0. Additionally, as variable h_k indicates whether AUV k is assigned for damage assessment and formulated as

$$\sum_{(i,j) \in E} (d_{i,j} + ST_j)x_{i,j,k} \leq B_k h_k, \forall k \in K. \quad (6.13)$$

Constraint (6.13) substitutes (6.6) which essentially imposes the same constraint.

2) Option 2: upper bound generation for target coverage constraint According to constraint (6.7), a target node must be assessed by at least one AUV, but no upper limit is set on the number of AUVs maneuvering over the node. If we impose an upper bound on the number, it can help reduce solution space; hence it can expedite convergence to find an optimal solution.

Figure 6.4 shows an example in which node 6 is connected with nodes C1, C2, C3 and C4 over four independent edges. If each edge is scanned by multiple independent AUVs toward node 6 and flow-in to any of AUV depots off the network, then a total of four AUVs will maneuver over node 6. Therefore, (6.7) can be reinforced by limiting the number of maximum allowed AUVs on node j \overline{ed}_j as an upper bound

and is formulated as

$$1 \leq \sum_{i:(i,j) \in E \setminus E_3} x_{i,j,k} \leq \overline{ed}_j, \forall j \in V'' \quad (6.14)$$

Upper bound \overline{ed}_j is obtained by **Algorithm 4** discussed in Option 3 below.

3) Option 3: probing-based preprocessing To increase the computation speed of the MAUV-ph2 model, an efficient preprocessing algorithm is developed. First, if the flight distance between two nodes is greater than the maximum operation time of AUV B_k , then the variable $x_{i,j,k}$ will be fixed to 0. Second, the maximum number of AUVs passing over node j \overline{ed}_j is counted which set an upper bound in (6.14). **Algorithm 4** provides an overview of the proposed probing-based preprocessing procedure.

Algorithm 4 A probing-based preprocessing

```

1: Initialize  $\overline{ed}_j$ 
2: for  $(i, j) \in E, k \in K$  do
3:   if  $(d_{i,j} > B_k)$  then: operational feasibility check
4:      $x_{i,j,k} = 0$ 
5:   end if
6:   if  $(d_{i,j} \neq 0)$  then: upper bound for (14)
7:      $\overline{ed}_j = \overline{ed}_j + 1$ 
8:   end if
9: end for

```

4) Option 4: Lagrangian relaxation for lower bound generation A tighter dual (lower) bound on the objective function of MAUV-ph2 can be generated utilizing Lagrangian heuristic approach. In MAUV-ph2 model, the number of sub-tour elimination constraints, i.e., (6.12), is exponential which can consume significant computational resources [100, 101]. Therefore (6.12) is relaxed and added to the objective function (6.5) as

$$L(\lambda) = \min \sum_{k \in K} P_k h_k + \sum_{k \in K} \sum_{(i,j) \in E_2} \lambda_{i,j,k} \{u_i - u_j + (|V''| + 1)x_{i,j,k} - |V''|\} \quad (6.15)$$

subject to (6.6)-(6.12) where $\lambda_k \geq 0$.

The Lagrangian dual problem $L(\lambda)$ provides a lower bound on the objective function of MAUV-ph2 model. From the Lagrangian dual problem, the Lagrangian multiplier is iteratively modified to find the best lower bound by using the subgradient method summarized as follows:

Algorithm 5 Subgradient method

- 1: Initialize upper bound \bar{L} , $\lambda_{i,j,k} \geq 0$, $\theta = 2$
 - 2: repeat
 - 3: $\gamma_{i,j,k} = g(x_{i,j,k})$: **gradient of** $L(\lambda_{i,j,k})$
 - 4: $\frac{t_j = \theta_j (\bar{L} - L(\lambda_{i,j,k}))}{\|\gamma_{i,j,k}\|^2}$: **step size**
 - 5: $\lambda'_{i,j,k} = \lambda_{i,j,k}$
 - 6: $\lambda_{i,j,k} = \max\{0, \lambda_{i,j,k} + t_j \gamma_{i,j,k}\}$
 - 7: until termination condition $\|\lambda'_{i,j,k} - \lambda_{i,j,k}\| < \varepsilon$ is satisfied
-

6.4 Simulation Result

A set of experiments on the proposed MAUV model, composed of two phases of MAUV-ph1 (AUV pre-positioning locations) and MAUV-ph2 (AUV routing decisions), is conducted. In the first part, MAUV-ph1 is validated by using simulated random data with a goal to understand how the model works under extreme events, and compare the results with the solutions from a deterministic model. To simulate uncertain weather condition in MAUV-ph1, the impact scale of an extreme weather $wx_{i,j,\omega}$ is randomly generated, where $wx_{i,j,\omega} \sim U(0.4, 0.9)$. In the second one, MAUV-ph2 is tested with a real offshore pipeline network in the Gulf of Mexico as shown in

Figure 6.6

All experiments were run on a Linux server with Intel Xeon 3.00 GHz processors and 364GB RAM. CPLEX 12.6 was used as the mixed integer programming (MIP) solver. The solution pools algorithm is utilized which accumulates groups of feasible



Max. operating depth: 600 meters (1,500, and 3,000 meter available depends on config.)

Energy: 5.2kWh rechargeable Lithium ion battery

Endurance: 70 hours → about 390 miles

Velocity: 2.6 m/s (5 knots)

Control:

Figure 6.5: An example of AUV specification

solutions to find a near optimal solution [102]. Two algorithm termination criteria are used including the relative termination tolerance gap of 3% and the 12-hour CPU runtime limit.

Figure 6.5 shows the specification of an AUV that are available for damage assessment. Ten instances of MAUV-ph1 model were solved, and evaluated the value of the stochastic solution (VSS) [85] for each of the instances, and compared with solutions from the deterministic counterpart.

Table 6.1 compare the outcomes from the deterministic model and the stochastic programming MAUV-ph1 model by using the VSS. The column “Deterministic Model (total cost)” represents the objective value of a deterministic model. The column “Stochastic Model (total cost)” represents the objective value of MAUV-ph1 model. The VSS equals the total cost of the deterministic model minus the total cost of the stochastic model. As can be seen in column VSS, MAUV-ph1 under stochastic assumption outperforms the deterministic model in all studied cases.

As a result of solving MAUV-ph1, we not only obtain the AUV pre-positioning locations but also identify which pipelines are included in the target area. **Figure 6.8** shows the topology of a offshore pipeline network system example in **Figure 6.6** which is composed of 158 pipeline segments and 72 pipeline joints within the target area

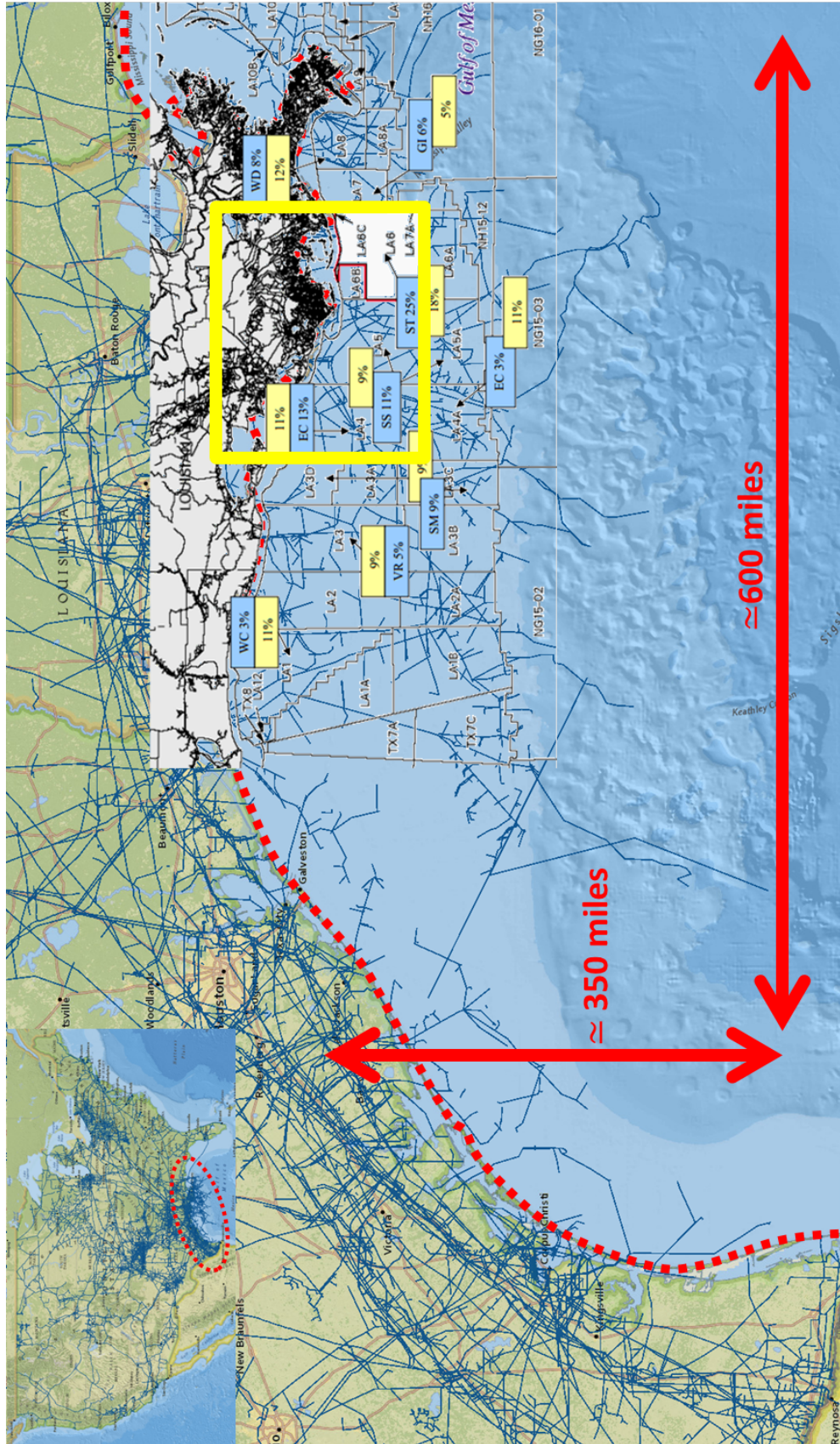


Figure 6.6: Offshore pipeline network in Gulf of Mexico



Figure 6.7: Offshore pipeline damage assessment target area

Table 6.1: Comparison of MAUV-ph1 and its deterministic counterparts

	Case ID	Number of nodes	Deterministic	Stochastic	VSS
#1	20	37	27.67	9.33	
#2	25	44	27.67	16.33	
#3	30	43	30.33	12.67	
#4	35	43	32.00	11.00	
#5	40	44.33	32.67	11.67	
#6	45	47	33.33	13.67	
#7	50	42.67	32.67	10.00	
#8	55	44.00	34.67	9.33	
#9	60	45.33	35.67	9.67	
#10	65	47.33	34.67	12.67	

shaded in grey.

Figure 6.9 and **Figure 6.10** provides a MAUV-ph2 solution set that C1, C2 and C3 are minimum number of AUV positions to cover the target area. Total 30 AUVs are needed to scan the target area, and assigned as the following: 13 AUVs at C1, 9 AUV at C2, and 8 AUVs at C3.

We also conducted sensitivity analysis by varying the maximum range of AUV

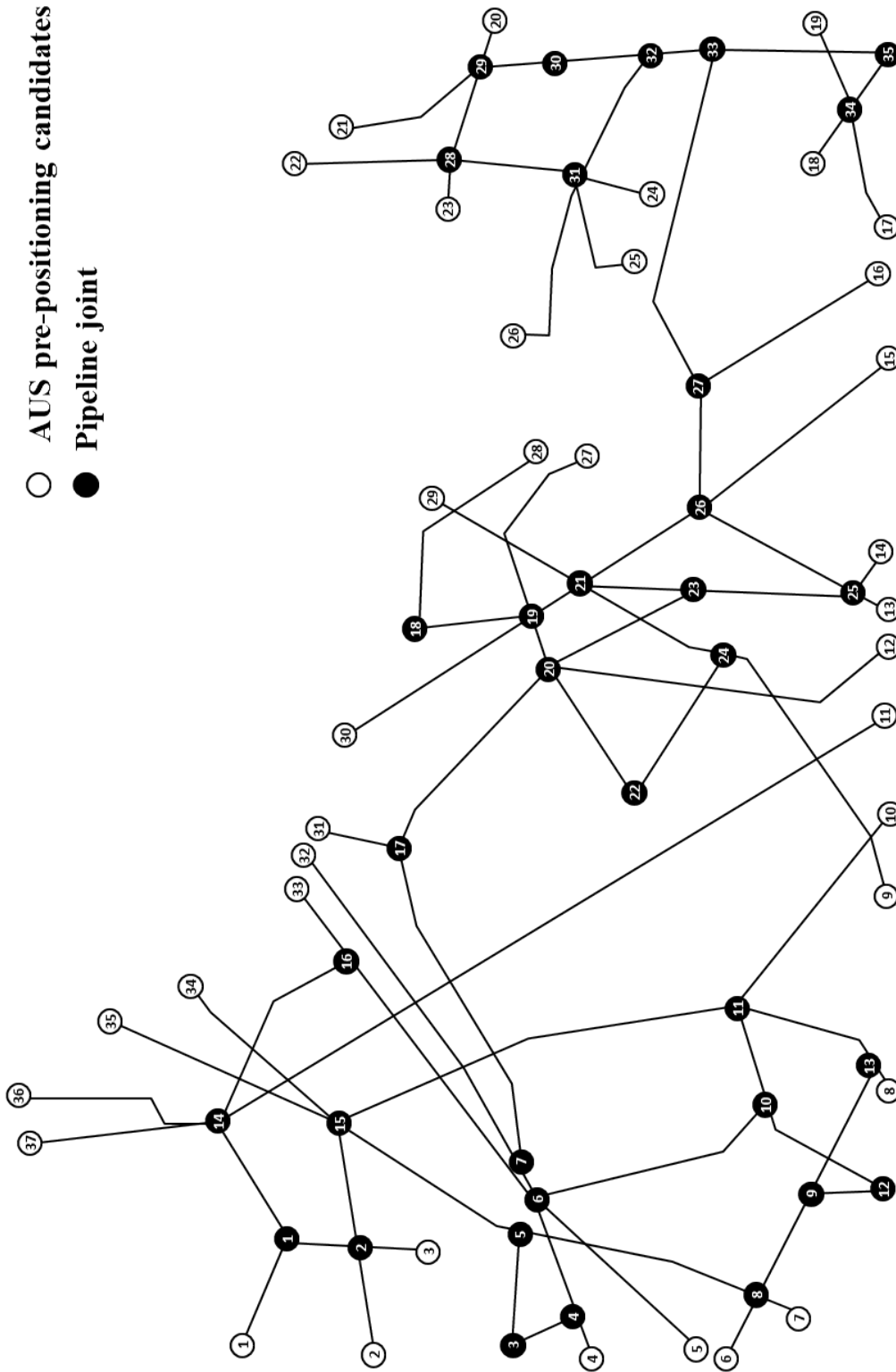


Figure 6.8: Offshore pipeline network topology

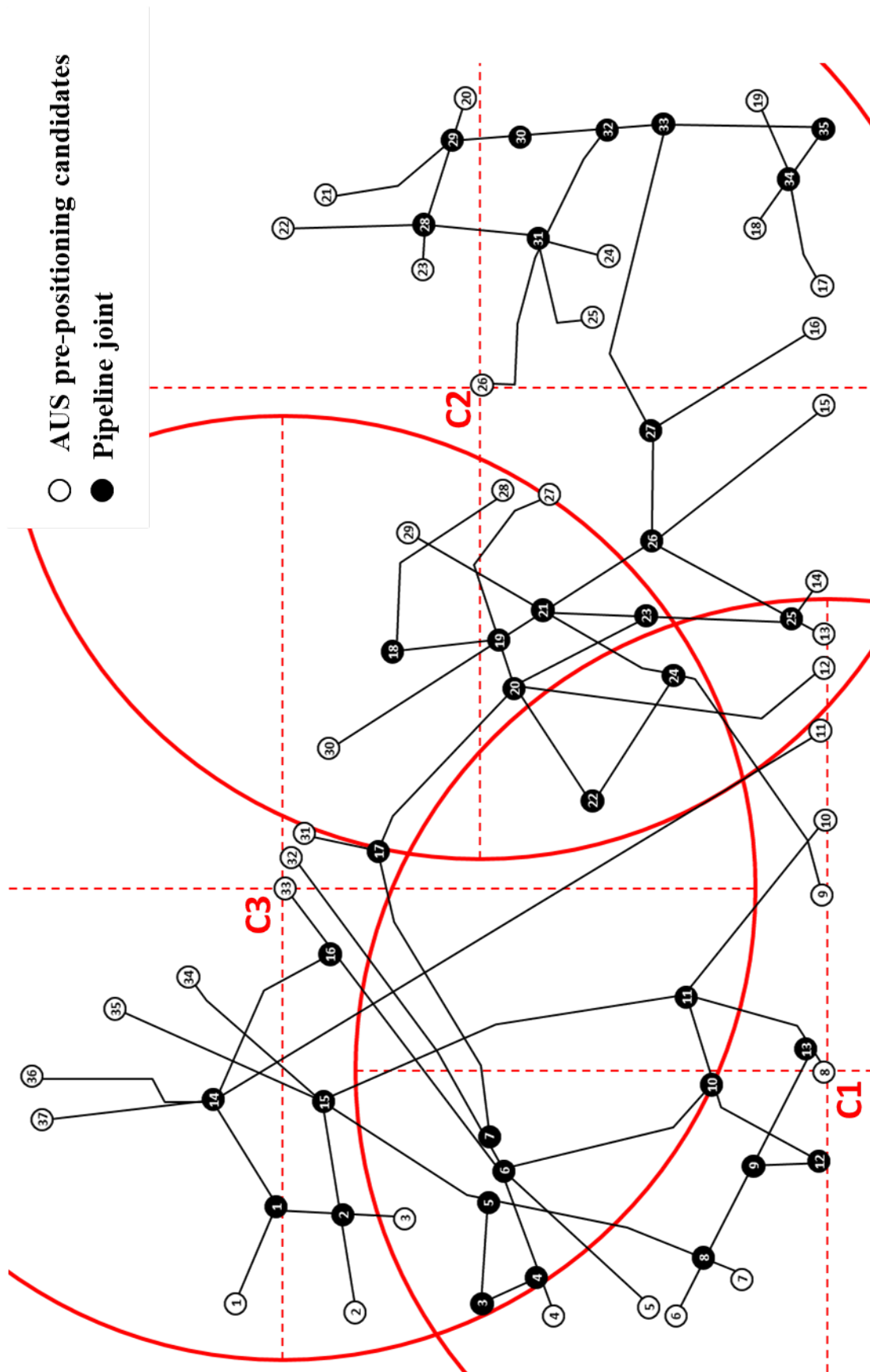


Figure 6.9: Determining AUV pre-positioning locations considering maximum target coverage of AUVs and its technical endurance under weather disruptions

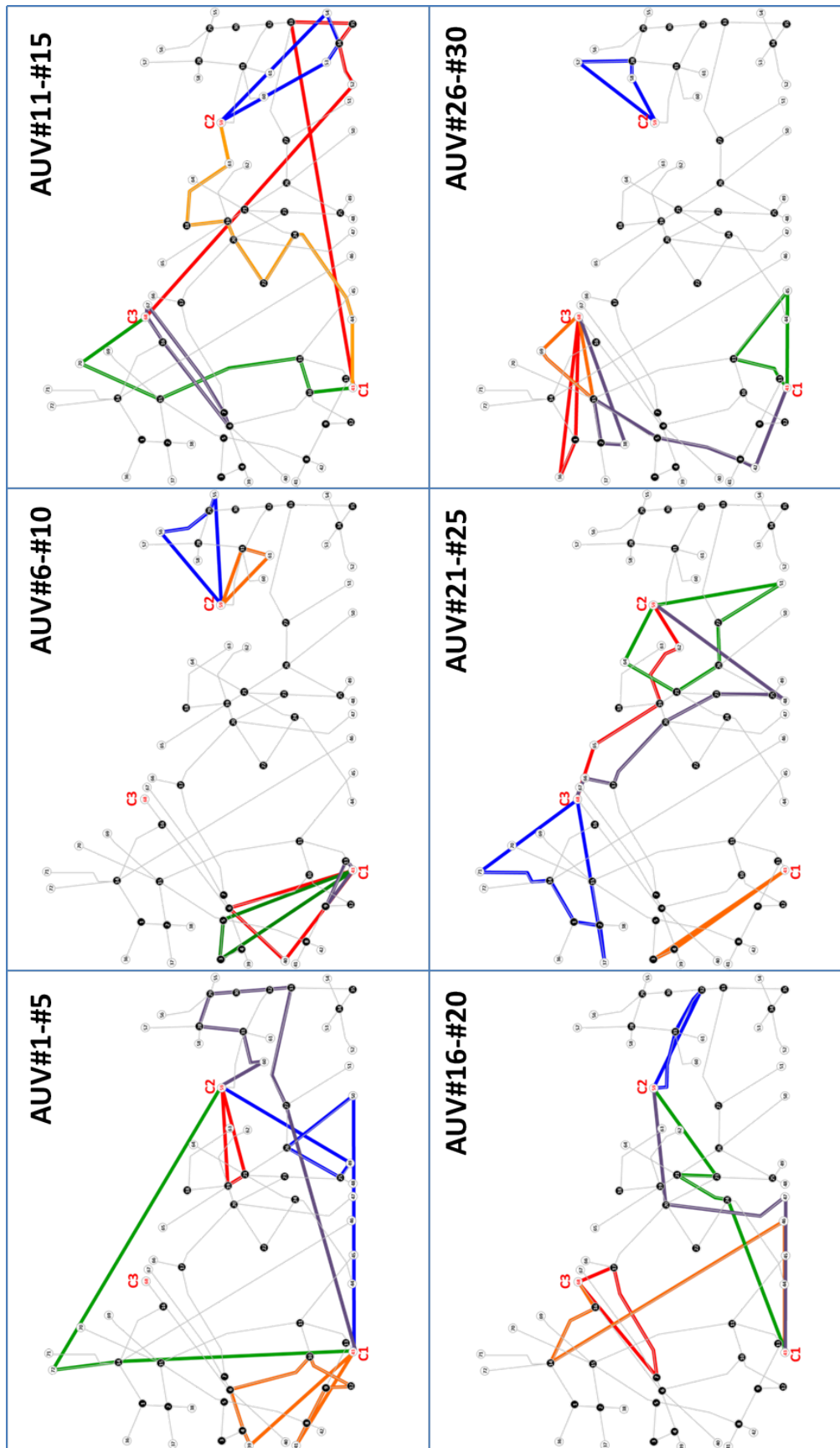


Figure 6.10: Generated paths of 30 AUVs for damage assessment

coverage which affects the result of MAUV-ph1 and consequently the result of MAUV-ph2. It is observed from Table 6.2 that as maximum coverage increases, the number of depots is decreased. In case #4, for example, if an AUV can operate up to 200 hours, then it is possible to cover all target area only from a single depot. As a result, AUV pre-positioning setup cost is minimized but increases overall AUV operating cost in phase 2.

Table 6.2: AUV maximum coverage range and MAUV ph-1 solutions

ID	Max. endurance	AUV depots	AUV types	Total cost	time
#1	25 hrs	C2, C3, C4 (3)	I(6) / II(3)	$C_{dpt}^{\#1} + 255$	33.5 min
#2	50 hrs	C1, C3, C4 (3)	I(3) / II(5)	$C_{dpt}^{\#1} + 250$	33.5 min
#3	100 hrs	C1, C4 (2)	I(5) / II(4)	$C_{dpt}^{\#1} + 265$	33.5 min
#4	200 hrs	C4 (1)	I(5) / II(6)	$C_{dpt}^{\#1} + 335$	34.5 min

* $C_{dpt}^{\#1}$: AUV pre-positioning setup cost of case #no where $C_{dpt}^{\#1} = \sum_{i \in V_2} c_i y_i$

As depicted in **Figure 6.11**, AUV scanning time, pre-positioning setup cost, and operating cost have triangular relations. For example, case#2 has the least AUV operating cost compared with other test cases. Case#4 is the most economical case with regards to AUV pre-positioning setup cost but has the longest scanning time.

Table 6.3: Four combinations of computational options

Case	Option 1	Options 2	Option 3	Option 4
MAUV-ph2	No	No	No	No
MAUV_T1	Yes	No	Yes	Yes
MAUV_T2	Yes	Yes	Yes	Yes

We evaluated performance of computational techniques suggested in section 6.3.4. For the comparison, three combinations of computational options have been used as shown in Table 6.5. MAUV-ph2 is the original MAUV model without any computational techniques. MAUV_T1 considers 1, 3, and 4. MAUV_T2 was solved applying all four options. MAUV-ph2 did not converge within the 12-hour CPU runtime limit. MAUV_T1 could not find an initial feasible solution in nearly 7 hours.

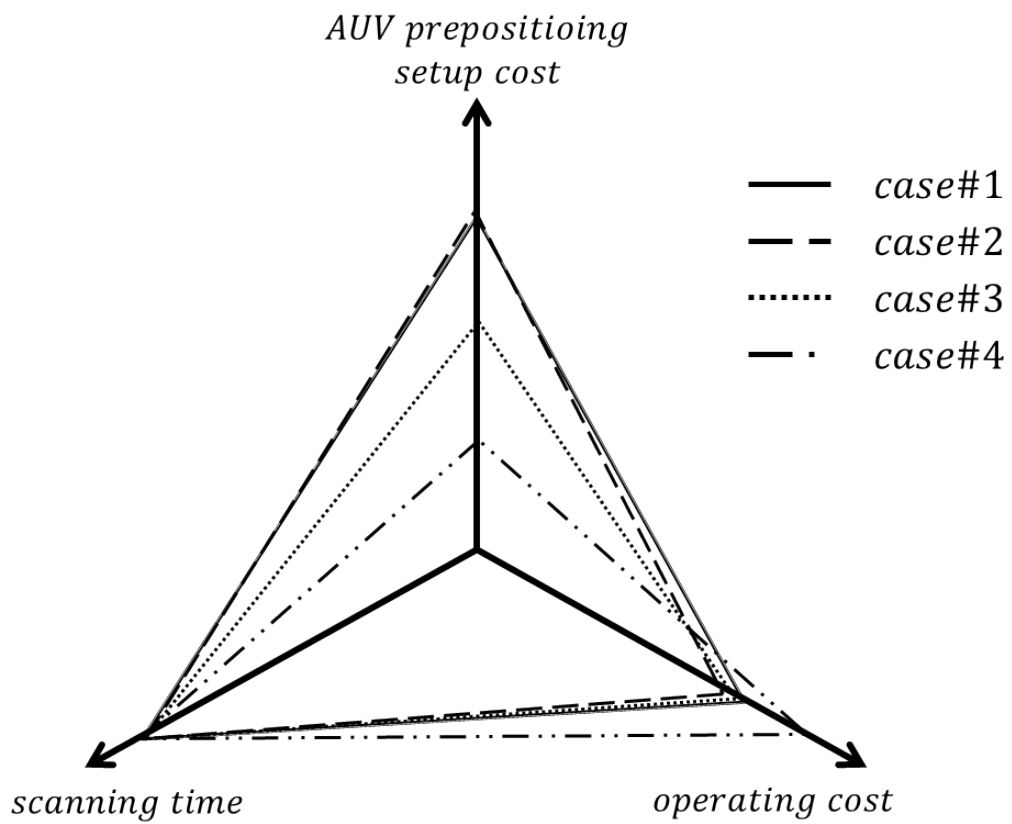


Figure 6.11: Triangular relations of damage assessment time, AUV prepositioning setup cost, and operating cost in accordance with AUV maximum maneuvering time

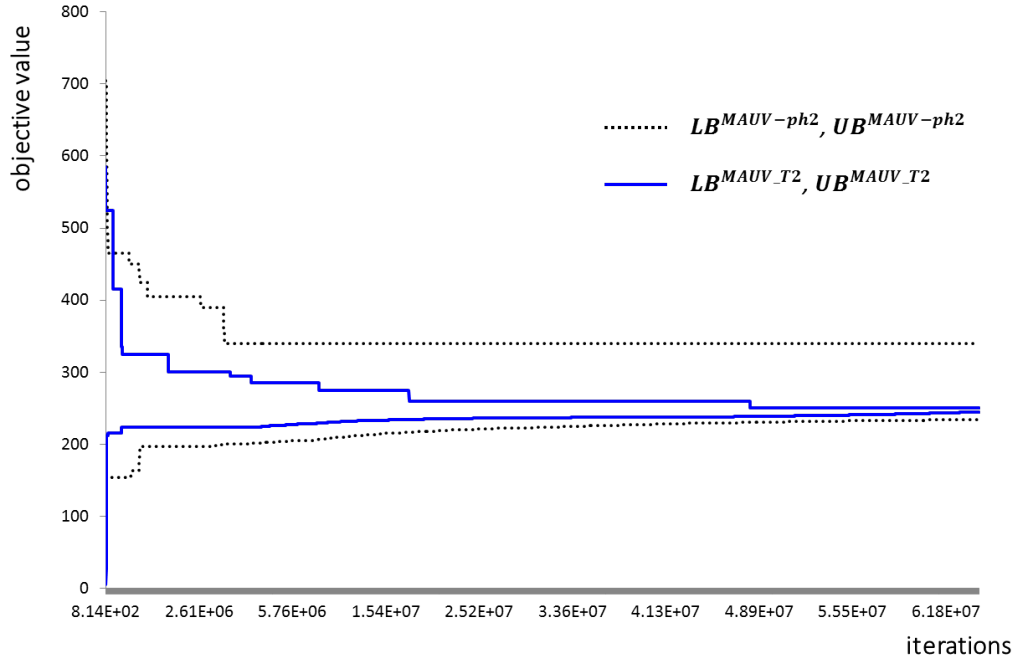


Figure 6.12: Convergence

But then the objective value dropped immediately to the same value of MAUV_T2, and converged after 521 minutes. However, as depicted in Fig. 8, MAUV_T2 converged faster because a tighter upper bound for target coverage constraint was provided to the model in addition to a tighter lower bound on the objective function. This shows that these additional information to the model help expedite convergence of the algorithm.

6.5 Conclusion

A two-phase mathematical optimization model was proposed for offshore natural gas pipeline network damage assessment by using AUVs. As random weather impact is considered to the determination of AUV pre-positioning locations, MAUV-ph1 was formulated as a two-stage stochastic program to cover a target area while minimizing total AUV positions setup cost. Based on the AUV pre-positioning locations from phase I, MAUV-ph2 model further generated AUV paths and required number of

AUVs to complete the damage assessment. As MAUV-ph2 was an NP-hard problem, probing-based preprocessing techniques and a logical inequality are developed, and Lagrangian heuristic is applied to obtain a good lower bound of MAUV-ph2 objective value in a reasonable time. Based on experimental results, it is presented that the superiority of the stochastic solutions compared with deterministic solutions using VSS. By applying four computational techniques, optimal solutions are obtained in a reasonable time. Additionally, in the sensitivity analysis, triangular relations among damage assessment time, AUV pre-positioning setup cost, and operating cost were discovered by varying the service range from each AUV positions.

Chapter 7

Summary and Future Work

This dissertation was directed towards aiding the LNG suppliers overcome the complexity and uncertainty involved in LNG supply projects and offshore pipeline damage assessment.

A new biannual LNG ship routing and scheduling model was proposed in a deterministic setting in Chapter 3. The proposed LNG IRP was extended to a stochastic model considering BOG generation uncertainty while serving geographically dispersed multiple customers using a fleet of heterogeneous vessels in Chapter 4. The research motivations are not only contract trend changes to shorter ones but also technological advances in LNG vessel design. The mutual coincidence of both transitions enables developing a new LNG shipping strategy to keep up with emerging market trend. A deterministic LNG scheduling model was proposed which is formulated as a multiple vehicle routing problem. The model was then extended to a two-stage stochastic model considering BOG generation which is unknown. Since the VRP is typically a combinatorial optimization problem, its stochastic extension is much harder to solve. In order to overcome this computational burden, a Monte Carlo sampling optimization was used to approximate the stochastic model while ensuring good quality of solutions. The solutions were evaluated using expected value of perfect information EVPI and value of stochastic solution VSS.

Chapter 5 investigated LNG inventory planning and ship routing problem with production decision under extreme weather disruptions in LNG business. Once an extreme weather is expected to impact the region of interest, every planned LNG loading operation at a liquefaction plant must be rescheduled. Otherwise, risks under

a disruption drastically increase and it can result in unexpected fires and explosions generating mass casualties and property damages. Two mathematical models were proposed to cope with the potential disruptions. In the first model, LNG inventory routing problem is formulated as a two-stage stochastic mixed integer program to maximize the overall expected revenue while minimizing uncertain impact of dust storms within the established time period. The proposed DMP model differs from the proposed two-stage stochastic LNG IRP in that a decision maker's preference on risks is reflected by a parametric optimization technique. This model enables a decision maker to have a 'what-if analysis' by varying the level of risk preference. To overcome the computational difficulties of the proposed models, two techniques have been proposed. First, a probing-based preprocessing technique was developed to reduce the number of binary variables utilizing the relations among time windows and the amount of boil-off gas in a path. Second, the routing process was further simplified in the model by replacing the sub-tour elimination constraint with a logical inequality. Computational results indicated that the proposed models and techniques are well suited to solve the problem in a reasonable time.

Chapter 6 addressed a two-phase mathematical framework for efficient offshore pipeline damage assessment using AUVs. In the first phase, a two-stage stochastic integer programming optimization model was proposed for damage assessment in which the first stage determines the optimal AUV locations anticipating an arrival of an extreme weather event, and the second stage augments the additional AUV deployment locations, if necessary, when the arrival time of the predicted extreme event becomes closer with updated information. AUV paths to scan the pipeline network are generated in the second phase while minimizing operating costs of the AUVs. Computational techniques are developed to reduce the solution time. Numerical experiments on a test pipeline network showed that the proposed stochastic model outperformed the deterministic counterpart in terms of the total AUV pre-positioning

setup cost. Additional sensitivity analyses exhibit the relationships among damage assessment time, AUV pre-positioning setup cost, and operating cost.

There can be several extensions to the studies presented in this dissertation. The proposed deterministic model, a parametric model and the following two versions of stochastic LNG IRPs were constructed considering changing market trends, technical advances and two crucial uncertainties (BOG and dust storm). As a next step, one can consider safety and security enhancement in LNG supply network. In spite of international collaboration efforts against piracy, pirate attacks are still a serious threat to maritime transportation including global LNG shipping.

There are two potential security challenges in maritime security: 1) terrorism, 2) safety accident prevention & consequence management. First, terror attacks can occur in either onshore or offshore marine activities. Potential attacks can be direct action (e.g., vehicle-borne improvised explosive devices or RPG-7 attacks) or stand-off attacks (e.g., mortar, artillery or rocket fires) in day and night. Second, there are numerous types of safety accidents (e.g., oil spill, gas leak) which require preventive surveillance or early warning. Once an incident is notified, it requires accurate (near) real time information collection capabilities to closely monitor the changing situations.

In response, utilization of security unmanned vehicles (UVs) passing through piracy and disaster or crisis prone areas can be considered. The basic concept is that an LNG cargo vessel becomes a platform for a fleet of security UVs. Therefore, security UVs can provide situational awareness under volatile security situations by taking off and landing at the LNG cargo vessel. The expected outcome of this model is a surveillance and reconnaissance schedule of multiple UVs and an optimal LNG inventory routing schedule as well.

On the perspective of utilizing multiple UVs, this model minimizes the number of operating UVs and idle times of each UV considering regular maintenance constraints. For a practical purpose, various technical specifications and operational limits of

various types of UVs (e.g., maximum operable range, cargo load limit and vision equipment capacity) can be further considered.

If we extend the proposed LNG IRP to a two-echelon LNG IRP model, then, in the first echelon, LNG cargo vessel routes and production inventory plan is optimized while determining an optimal path(s) of security drones in the second echelon. Therefore, extending the proposed LNG IRP to a two-echelon LNG IRP model can be an immediate next step of this study.

The suggested MUAV model mainly focused on weather uncertainty to AUVs pre-positioning and its path generation while minimizing total operation time and cost. In practice, there are numerous other uncertain environmental elements which causing AUVs to be in malfunctioned condition or generating unreliable results resulting from dynamically changing subsea environment. Therefore, as an extension to the proposed model, we can consider various uncertain elements not only in the planning phase but also in the operations phase.

References

- [1] United Nations Conference on Trade and Development. "Review of maritime transport 2015," New York and Geneva: United Nations Secretariat, 2015.
- [2] Marielle Christiansen, Kjetil Fagerholt, Bjørn Nygreen, and David Ronen. "Ship routing and scheduling in the new millennium," *European Journal of Operational Research*, 228(3): 467–483, 2013.
- [3] Michael D. Tusiani and Gordon Shearer. "LNG: a nontechnical guide," PennWell Books, 2007.
- [4] Yung Shin, Jang W. Kim, Hoseong Lee, and Changyu Hwang. "Sloshing impact of LNG cargoes in membrane containment systems in the partially filled condition," In *Proceedings of the 13th International Offshore and Polar Engineering Conference*, volume 3, pages 509–515, 2003.
- [5] Jacques Dexcloitres. "Dust storm over the Arabian sea and the Persian gulf," NASA Visible Earth: A catalog of NASA images and animation of our home planet (accessed 05.11.15). <<http://visibleearth.nasa.gov/>>.
- [6] National Oceanic and Atmospheric Administration / National Weather Service. "The Saffir-Simpson hurricane scale," National Hurricane Center - Tropical Prediction Center, 1999.
- [7] Michael J. Fagel. "Principles of emergency management and emergency operations centers (EOC)," CRC press, 2016.
- [8] Energy Information Administration. "Annual energy outlook 2011 with projections to 2035," Washington D.C.: United States Department of Energy, 2011.

- [9] Peter R. Hartley, George Mitchell, Cynthia Mitchell, and James A. Baker. "The future of long-term LNG contracts," University of Western Australia, Business School, Economics, 2013.
- [10] Peter R. Hartley. "Recent developments in LNG markets," *Technical report*, James A. Baker III Institute for Public Policy, Rice University, 2014.
- [11] International Gas Union. "World LNG report - 2013 edition," IGU (accessed 05.11.15). <<http://www.igu.org/>>.
- [12] Mark Finley. "BP statistical review of world energy," *Technical Report*, 2014.
- [13] National Energy Technology Laboratory. "Liquefied natural gas: understanding the basic facts," U.S. Department of Energy, 2005.
- [14] Margo Thorning. "Setting the record straight on LNG exports: environmental opposition contradicts studies on natural gas realities," *ACCF Center for Policy Research Special Report*, 2014.
- [15] Sydney Thomas and Richard A. Dawe. "Review of ways to transport natural gas energy from countries which do not need the gas for domestic use," *Energy*, 28(14):1461–1477, 2003.
- [16] Joel Tessier. "Operating membrane LNG carriers-partial loading cases for 160,000 m^3 vessels and beyond," In *The 13th International Conference & Exhibition on Liquefied Natural Gas*, Seoul, Korea, May, pages 14–17, 2001.
- [17] Sampo Suvisaari. Delivering LNG in smaller volumes. *Wärtsilä Technical Journal*, 1:21–25, 2012.
- [18] Đorđe Dobrota, Branko Lalić, and Ivan Komar. "Problem of boil-off in LNG supply chain," *Transactions on Maritime Science*, 2(02):91–100, 2013.

- [19] William E. Shenk and Robert J. Curran. "The detection of dust storms over land and water with satellite visible and infrared measurements," *Monthly Weather Review*, 102(12):830–837, 1974.
- [20] H.M. Hasanean. "Middle East meteorology," *Meteorology Department, Faculty of Meteorology, Environment and Arid Land Agriculture, King Abdulaziz University*, 2004.
- [21] Mehdi Samadi, Ali Darvishi Bolorani, Seyed Kazem Alavipanah, Hossein Mo-hamadi, and Mohamad Saeed Najafi. "Global dust detection index (GDDI); a new remotely sensed methodology for dust storms detection," *Journal of Environmental Health Science and Engineering*, 12(1): 20, 2014.
- [22] J.S. Mandke, Y-T Wu, and R.S. Marlow. "Evaluation of Hurricane-Induced Damage to Offshore Pipelines," U.S. Department of the Interior, Minerals Man-agement Service, Engineering and Technology Division, 1995.
- [23] Lawrence C. Kumins and Robert Bamberger. "Oil and gas disruption from hur-ricanes Katrina and Rita," Congressional Research Service, Library of Congress, 2005.
- [24] Det Norske Veritas. "Pipeline damage assessment from hurricanes Katrina and Rita in the Gulf of Mexico," (accessed 03.01.15). <<http://www.boemre.gov/tarprojects/>>.
- [25] Ana M. Cruz and Elisabeth Krausmann. "Damage to offshore oil and gas fa-cilities following hurricanes Katrina and Rita: an overview," *Journal of Loss Prevention in the Process Industries*, 21(6): 620–626, 2008.
- [26] Lukas Brun. "ROV/AUV trends: market and technology," *Marine Technology Reporter*, 5(7): 48–51, 2012.

- [27] Jaeyoung Cho, Gino J. Lim, Taofeek Biobaku, Selim Bora, and Hamid Parsaei. "Liquefied natural gas ship route planning model considering market trend change," *Transactions on Maritime Science*, 3(02): 119–130, 2014.
- [28] Clair E. Miller, Albert W. Tucker, and Richard A. Zemlin. "Integer programming formulation of traveling salesman problems," *Journal of the ACM (JACM)*, 7(4): 326–329, 1960.
- [29] Walter J. Bell, Louis M. Dalberto, Marshall L. Fisher, Arnold J. Greenfield, Ramchandran Jaikumar, Pradeep Kedia, Robert G. Mack, and Paul J. Prutzman. "Improving the distribution of industrial gases with an on-line computerized routing and scheduling optimizer," *Interfaces*, 13(6): 4–23, 1983.
- [30] Roar Grønhaug and Marielle Christiansen. "Supply chain optimization for the liquefied natural gas business," In *Innovations in Distribution Logistics*, pages 195–218. Springer, 2009.
- [31] Henrik Andersson, Marielle Christiansen, and Kjetil Fagerholt. "Transportation planning and inventory management in the LNG supply chain," In *Energy, Natural Resources and Environmental Economics*, pages 427–439. Springer, 2010.
- [32] Marte Fodstad, Kristin Tolstad Uggen, Frode R.ømo, Arnt-Gunnar Lium, Geert Stremersch, and Stéphane Hecq. "LNG scheduler: a rich model for coordinating vessel routing, inventories and trade in the liquefied natural gas supply chain," *Journal of Energy Markets*, 3(4): 31–64, 2010.
- [33] Jørgen Glomvik Rakke, Magnus Stålhane, Christian Rørholt Moe, Marielle Christiansen, Henrik Andersson, Kjetil Fagerholt, and Inge Norstad. "A rolling horizon heuristic for creating a liquefied natural gas annual delivery program," *Transportation Research Part C: Emerging Technologies*, 19(5): 896–911, 2011.

- [34] Roar Grønhaug, Marielle Christiansen, Guy Desaulniers, and Jacques Desrosiers. "A branch-and-price method for a liquefied natural gas inventory routing problem," *Transportation Science*, 44(3): 400–415, 2010.
- [35] Faramroze G. Engineer, Kevin C. Furman, George L. Nemhauser, Martin W.P. Savelsbergh, and Jin-Hwa Song. "A branch-price-and-cut algorithm for single-product maritime inventory routing," *Operations Research*, 60(1): 106–122, 2012.
- [36] Leandro C. Coelho and Gilbert Laporte. "A branch-and-cut algorithm for the multi-product multi-vehicle inventory-routing problem," *International Journal of Production Research*, 51(23-24): 7156–7169, 2013.
- [37] Vikas Goel, M. Slusky, W-J van Hoes, K.C. Furman, and Y. Shao. "Constraint programming for LNG ship scheduling and inventory management," *European Journal of Operational Research*, 241(3): 662–673, 2015.
- [38] Magnus Stålhane, Jørgen Glomvik Rakke, Christian Rørholt Moe, Henrik Andersson, Marielle Christiansen, and Kjetil Fagerholt. "A construction and improvement heuristic for a liquefied natural gas inventory routing problem," *Computers & Industrial Engineering*, 62(1): 245–255, 2012.
- [39] Vikas Goel, Kevin C. Furman, Jin-Hwa Song, and Amr S. El-Bakry. "Large neighborhood search for LNG inventory routing," *Journal of Heuristics*, 18(6): 821–848, 2012.
- [40] Dimitri J. Papageorgiou, Ahmet B. Keha, George L. Nemhauser, and Joel Sokol. "Two-stage decomposition algorithms for single product maritime inventory routing," *INFORMS Journal on Computing*, 26(4): 825–847, 2014.

- [41] Milorad Vidović, Dražen Popović, and Branislava Ratković. "Mixed integer and heuristics model for the inventory routing problem in fuel delivery," *International Journal of Production Economics*, 147: 593–604, 2014.
- [42] Dimitri J. Papageorgiou, Myun-Seok Cheon, George Nemhauser, and Joel Sokol. "Approximate dynamic programming for a class of long-horizon maritime inventory routing problems," *Transportation Science*, 2014.
- [43] Awi Federgruen and Paul Zipkin. "Computational issues in an infinite-horizon, multiechelon inventory model," *Operations Research*, 32(4): 818–836, 1984.
- [44] Atefeh Baghalian, Shabnam Rezapour, and Reza Zanjirani Farahani. "Robust supply chain network design with service level against disruptions and demand uncertainties: a real-life case," *European Journal of Operational Research*, 227(1): 199–215, 2013.
- [45] Oystein Arvesen, Vegard Medbø, S-E Fleten, Asgeir Tomasgard, and Sjur Westgaard. "Linepack storage valuation under price uncertainty," *Energy*, 52: 155–164, 2013.
- [46] Elin E. Halvorsen-Weare, Kjetil Fagerholt, and Mikael R.önqvist. "Vessel routing and scheduling under uncertainty in the liquefied natural gas business," *Computers & Industrial Engineering*, 64(1): 290–301, 2013.
- [47] Chengliang Zhang George Nemhauser Joel Sokol and Myun-Seok Cheon Dimitri Papageorgiou. "Robust inventory routing with flexible time window allocation," (accessed 04.01.15). <<http://www.optimization-online.org/>>.
- [48] Jaeyoung Cho, Gino J. Lim, Taofeek Biobaku, Selim Bora, and Hamid Parsaei. "Liquefied natural gas (LNG) inventory routing problem under weather disruptions: a case study of dust storm in the Persian Gulf," *Texas Hurricane Center for Innovative Technology*, 2014.

- [49] N. Chatterjee and J.M. Geist. "Effects of stratification on boil-off rates in LNG tanks," *Pipeline and Gas Journal*, 199(11), 1972.
- [50] Jean-Claude Latombe. "Robot motion planning," *the Kluwer International Series in Engineering and Computer Science*, 1990.
- [51] Charles W. Warren. "A technique for autonomous underwater vehicle route planning," *IEEE Journal of Oceanic Engineering*, 15(3): 199–204, 1990.
- [52] Joseph Carsten, Dave Ferguson, and Anthony Stentz. "3D field D: improved path planning and replanning in three dimensions," In *2006 IEEE/RSJ International Conference on Intelligent Robots and Systems*, pages 3381–3386. IEEE, 2006.
- [53] Kevin P. Carroll, Stephen R. McClaran, Eric L. Nelson, David M. Barnett, Donald K. Friesen, and G.N. William. "AUV path planning: an A* approach to path planning with consideration of variable vehicle speeds and multiple, overlapping, time-dependent exclusion zones," In *Autonomous Underwater Vehicle Technology, 1992. AUV'92., Proceedings of the 1992 Symposium on*, pages 79–84. IEEE, 1992.
- [54] Bartolomé Garau, Matias Bonet, Alberto Alvarez, Simón Ruiz, and Ananda Pascual. "Path planning for autonomous underwater vehicles in realistic oceanic current fields: Application to gliders in the western Mediterranean sea," *Journal of Maritime Research*, 6(2): 5–22, 2014.
- [55] Clment Petres, Yan Pailhas, Pedro Patron, Yvan Petillot, Jonathan Evans, and David Lane. "Path planning for autonomous underwater vehicles," *IEEE Transactions on Robotics*, 23(2): 331–341, 2007.

- [56] Yvan Petillot, I. Tena Ruiz, and David M. Lane. "Underwater vehicle obstacle avoidance and path planning using a multi-beam forward looking sonar," *IEEE Journal of Oceanic Engineering*, 26(2): 240–251, 2001.
- [57] Alberto Alvarez, Andrea Caiti, and Reiner Onken. "Evolutionary path planning for autonomous underwater vehicles in a variable ocean," *IEEE Journal of Oceanic Engineering*, 29(2): 418–429, 2004.
- [58] Namik Kemal Yilmaz, Constantinos Evangelinos, Nicholas M. Patrikalakis, Pierre F.J. Lermusiaux, Patrick J. Haley, Wayne G. Leslie, Allan R. Robinson, Ding Wang, and Henrik Schmidt. "Path planning methods for adaptive sampling of environmental and acoustical ocean fields," In *OCEANS 2006*, pages 1–6. IEEE, 2006.
- [59] Liam Paull, Sajad Saeedi, Mae Seto, and Howard Li. "Sensor-driven online coverage planning for autonomous underwater vehicles," *IEEE/ASME Transactions on Mechatronics*, 18(6): 1827–1838, 2013.
- [60] Mansour Ataei and Aghil Yousefi-Koma. "Three-dimensional optimal path planning for waypoint guidance of an autonomous underwater vehicle," *Robotics and Autonomous Systems*, 67: 23–32, 2015.
- [61] Gianluca Antonelli, Stefano Chiaverini, Roberto Finotello, and Riccardo Schiavon. "Real-time path planning and obstacle avoidance for RAIS: an autonomous underwater vehicle," *IEEE Journal of Oceanic Engineering*, 26(2): 216–227, 2001.
- [62] Enric Galceran, Ricard Campos, Narcís Palomeras, David Ribas, Marc Carreras, and Pere Ridao. "Coverage path planning with real-time replanning and surface reconstruction for inspection of three-dimensional underwater structures

- using autonomous underwater vehicles," *Journal of Field Robotics*, 32(7): 952–983, 2015.
- [63] Jonathan Binney, Andreas Krause, and Gaurav S. Sukhatme. "Informative path planning for an autonomous underwater vehicle," In *Robotics and automation (ICRA), 2010 IEEE International Conference on*, pages 4791–4796. IEEE, 2010.
- [64] Arvind A. Pereira, Jonathan Binney, Geoffrey A. Hollinger, and Gaurav S. Sukhatme. "Risk-aware path planning for autonomous underwater vehicles using predictive ocean models," *Journal of Field Robotics*, 30(5): 741–762, 2013.
- [65] C. Vasudevan and K. Ganesan. "Case-based path planning for autonomous underwater vehicles," *Autonomous Robots*, 3(2-3): 79–89, 1996.
- [66] Somaiyeh Mahmoud Zadeh, David M.W. Powers, and Amir Mehdi Yazdani. "An efficient hybrid route-path planning model for dynamic task allocation and safe maneuvering of an underwater vehicle in a realistic environment," (accessed 05.08.16). <<http://arxiv.org/abs/1604.07545>>.
- [67] Daqi Zhu, Huan Huang, and Simon X. Yang. "Dynamic task assignment and path planning of multi-AUV system based on an improved self-organizing map and velocity synthesis method in three-dimensional underwater workspace," *IEEE Transactions on Cybernetics*, 43(2): 504–514, 2013.
- [68] K.S. Al-Sultan and M.D.S. Aliyu. "A new potential field-based algorithm for path planning," *Journal of Intelligent and Robotic Systems*, 17(3): 265–282, 1996.
- [69] Ilker Bekmezci, Ozgur Koray Sahingoz, and Şamil Temel. "Flying ad-hoc networks (FANETs): A survey," *Ad Hoc Networks*, 11(3): 1254–1270, 2013.

- [70] Feng Jiang and A. Lee Swindlehurst. "Optimization of UAV heading for the ground-to-air uplink," *IEEE Journal on selected areas in Communications*, 30(5): 993–1005, 2012.
- [71] Alessandro Gardi, Roberto Sabatini, Subramanian Ramasamy, and Trevor Kistan. "Real-time trajectory optimisation models for next generation air traffic management systems," In *Applied Mechanics and Materials*, volume 629, pages 327–332. Trans Tech Publ, 2014.
- [72] Antonio Alonso-Ayuso, Laureano F. Escudero, and F. Javier Martín-Campo. "Collision avoidance in air traffic management: a mixed-integer linear optimization approach," *IEEE Transactions on Intelligent Transportation Systems*, 12(1): 47–57, 2011.
- [73] Yangguang Fu, Mingyue Ding, and Chengping Zhou. "Phase angle-encoded and quantum-behaved particle swarm optimization applied to three-dimensional route planning for UAV," *IEEE Transactions on Systems, Man, and Cybernetics-Part A: Systems and Humans*, 42(2): 511–526, 2012.
- [74] Yangguang Fu, Mingyue Ding, Chengping Zhou, and Hanping Hu. "Route planning for unmanned aerial vehicle (UAV) on the sea using hybrid differential evolution and quantum-behaved particle swarm optimization," *IEEE Transactions on Systems, Man, and Cybernetics: Systems*, 43(6): 1451–1465, 2013.
- [75] Timothy W. McLain and Randal W. Beard. "Coordination variables, coordination functions, and cooperative timing missions," *Journal of Guidance, Control, and Dynamics*, 28(1): 150–161, 2005.
- [76] Han-Lim Choi, Luc Brunet, and Jonathan P. How. "Consensus-based decentralized auctions for robust task allocation," *IEEE transactions on robotics*, 25(4): 912–926, 2009.

- [77] Brett Bethke, Mario Valenti, and Jonathan P. How. "UAV task assignment," *IEEE Robotics & Automation Magazine*, 15(1): 39–44, 2008.
- [78] Mehdi Alighanbari and Jonathan P. How. "A robust approach to the UAV task assignment problem," *International Journal of Robust and Nonlinear Control*, 18(2): 118–134, 2008.
- [79] Jaeyoung Cho, Gino J. Lim, Taofeek Biobaku, Seonjin Kim, and Hamid Parsaei. "Safety and security management with unmanned aerial vehicle (UAV) in oil and gas industry," *Procedia Manufacturing*, 3: 1343–1349, 2015.
- [80] Chi-Guhn Lee, Marina A Epelman, Chelsea C. White, and Yavuz A. Bozer. "A shortest path approach to the multiple-vehicle routing problem with split pickups," *Transportation research part B: Methodological*, 40(4): 265–284, 2006.
- [81] Yupo Chan, William B. Carter, and Michael D. Burnes. "A multiple-depot, multiple-vehicle, location-routing problem with stochastically processed demands," *Computers & Operations Research*, 28(8): 803–826, 2001.
- [82] Russell Bent and Pascal Van Hentenryck. "A two-stage hybrid algorithm for pickup and delivery vehicle routing problems with time windows," *Computers & Operations Research*, 33(4): 875–893, 2006.
- [83] J.F. Kuo, R.B. Campbell, Z. Ding, S.M. Hoie, A.J. Rinehart, R.E. Sandström, T.W. Yung, M.N. Greer, and M.A. Danaczko. "LNG tank sloshing assessment methodology - the new generation," *International Journal of Offshore and Polar Engineering*, 19(4):241, 2009.
- [84] Murray Rudman and Paul W. Cleary. "Modeling sloshing in LNG tanks," In *Seventh International Conference on CFD in the Minerals and Process Industries, Australia*, 2009.

- [85] John R. Birge and Francois Louveaux. *Introduction to stochastic programming*. Springer Science & Business Media, 2011.
- [86] A. Brooke, D. Kendrick, and A. Meeraus. GAMS/CPLEX 12. *User Notes*. GAMS Development Corporation, 2010.
- [87] U.S. Energy Information Administration. Annual energy outlook 2014 with projections to 2040.
- [88] Global Environmental Alert Service. "Forecasting and early warning of dust storms," *United Nations Environment Programme*, 2013.
- [89] Canaport. LNG Ship Loading at the Canaport LNG Terminal. 2013.
- [90] Qatar Petroleum. Port Information and Regulation Guide. 2010.
- [91] Julia L. Higle, James C. Bean, and Robert L. Smith. "Deterministic equivalence in stochastic infinite horizon problems," *Mathematics of Operations Research*, 15(3): 396–407, 1990.
- [92] P. Govinda Rao, Mohammed Al-Sulaiti, and Ali Hamid Al-Mulla. "Winter Shamals in Qatar, Arabian Gulf," *Weather*, 56(12): 444–451, 2001.
- [93] Norman L. Johnson. "Systems of frequency curves generated by methods of translation," *Biometrika*, pages 149–176, 1949.
- [94] Richard Espiner, David Kaye, Graham Goodfellow, and Phil Hopkins. "Inspection & assessment of damaged subsea pipelines: A case study," In *2008 7th International Pipeline Conference*, pages 291–298. American Society of Mechanical Engineers, 2008.
- [95] Dan McLeod, John Jacobson, Mark Hardy, and Carl Embry. "Autonomous inspection using an underwater 3D LIDAR," In *2013 OCEANS-San Diego*, pages 1–8. IEEE, 2013.

- [96] Anders Bjerrum. "Autonomous underwater vehicles for offshore surveys," In *Underwater Technology International: Remote Intervention*. Society of Underwater Technology, 1997.
- [97] Kimon P. Valavanis, Denis Gracanin, Maja Matijasevic, Ramesh Kolluru, and Georgios A. Demetriou. "Control architectures for autonomous underwater vehicles," *IEEE Control Systems*, 17(6): 48–64, 1997.
- [98] Marshall L. Fisher. "The Lagrangian relaxation method for solving integer programming problems," *Management Science*, 27(1): 1–18, 1981.
- [99] Jan Karel Lenstra and AHG Kan. "Complexity of vehicle routing and scheduling problems," *Networks*, 11(2): 221–227, 1981.
- [100] Manfred Padberg and Giovanni Rinaldi. "A branch-and-cut algorithm for the resolution of large-scale symmetric traveling salesman problems," *SIAM review*, 33(1): 60–100, 1991.
- [101] George L. Nemhauser and Laurence A. Wolsey. "Integer programming and combinatorial optimization," *Wiley, Chichester. GL Nemhauser, MWP Savelsbergh, GS Sigismondi (1992). Constraint Classification for Mixed Integer Programming Formulations. COAL Bulletin*, 20: 8–12, 1988.
- [102] IBM ILOG. CPLEX Optimizer. (accessed 05.08.14). <<https://www-01.ibm.com>>.